# PROTEIN PHOSPHATASE REGULATORY PROTEIN 10 COOPERATES WITH NEUROFIBROMIN INACTIVATION IN MYELOID LEUKEMOGENESIS

By

ANGELA HADJIPANAYIS

A DISSERTATION PRESENTED TO THE GRADUATE SCHOOL
OF THE UNIVERSITY OF FLORIDA IN PARTIAL FULFILLMENT
OF THE REQUIREMENTS FOR THE DEGREE OF
DOCTOR OF PHILOSOPHY

UNIVERSITY OF FLORIDA

2008

This work is dedicated to my extended family who never had the opportunity to obtain higher education. To my parents and husband for their loving support and belief in my abilities. To Camilynn I. Brannan whose research expertise led to the discovery of this locus.

ACKNOWLEDGMENTS

First, I would like to thank my mentor Peggy Wallace for her indispensable support over the years, her encouragement, and her advice on how to become a better scientist. Second, I would like to thank my husband for taking a leap of faith in life and moving to Florida with me when he didn't have a job at the time. Third, I would like to thank my parents for their love, support, and advice over the years. Fourth, I would like to thank my other committee members, Dr. Jim Resnick, Dr. Paul Oh, Dr. Stephen Hunger and Dr. Dan Driscoll for their valuable advice on the project. I also would like to thank Dr. Jennifer Embury for the tremendous effort on all the pathology of the mice. In addition, I would like to thank Dr. Kevin Shannon and Dr. Scott Kogan for their leukemia expertise and strategies in modeling leukemia. Lastly, I would like to thank the lab for their help on this project, their jokes, and all their personalities that made the days seem not as long.

TABLE OF CONTENTS

page

LIST OF TABLES

LIST OF FIGURES

LIST OF ABBREVIATIONS

| | |
|---|---|
| AML | Acute Myeloid Leukemia |
| BL | Blood |
| BM | Bone Marrow |
| BSA | Bovine Serum Albumin |
| CMML | Chronic Myelomonocytic Leukemia |
| CML | Chronic Myeloid Leukemia |
| CFU-GM | Colony Forming Unit-Granulocyte/Macrophage |
| Epi1 | Ecotropic Proviral Integration 1 |
| Epi2 | Ecotropic Proviral Integration 2 |
| Epi3 | Ecotropic Proviral Integration 3 |
| GFP | Green Fluorescent PCR |
| GM-CSF | Granulocyte Macrophage Colony Stimulating Factor |
| JMML | Juvenile myelomonocytic leukemia |
| LOH | Loss of Heterozygosity |
| PPP1R10 | serine/threonine phosphatase regulatory protein 10 |
| MDS | Myelodysplastic syndrome |
| MPD | Myeloproliferative disease |
| MPNST | Malignant Peripheral Nerve Sheath Tumor |
| MuLV | Murine Leukemia Virus |
| NF1 | Neurofibromatosis type 1 |
| NF1-JMML | NF1 associated leukemia |
| NS | Noonan Syndrome |
| PCR | Polymerase Chain Reaction |
| PKO | Ppp1r10 mouse line |

| | |
|---|---|
| PP1 | serine/threonine phosphatase 1 |
| PPP1R10 | serine/threonine phosphatase regulatory protein 10 |
| RT-PCR | Reverse Transcription PCR |
| SDS | Sodium Dodecyl Sulfate |

Abstract of Dissertation Presented to the Graduate School
of the University of Florida in Partial Fulfillment of the
Requirements for the Degree of Doctor of Philosophy

# PROTEIN PHOSPHATASE REGULATORY PROTEIN 10 COOPERATES WITH NEUROFIBROMIN INACTIVATION IN MYELOID LEUKEMOGENESIS

By

Angela Hadjipanayis

August 2008

Chair: Peggy Wallace
Major: Medical Sciences-Genetics

Neurofibromatosis (NF1) is an autosomal dominant disease that affects 1 in 4000 people. Patients afflicted with NF1 present a variety of phenotypes, but the hallmark features of the disease are neurofibromas on or under the skin, café au lait spots, and Lisch nodules of the iris. Children with NF1 are at 200 to 500 times greater risk for developing a chronic myeloid leukemia. Often children who are diagnosed with this myeloid leukemia initially are not diagnosed with NF1 until a few years later. Therefore, there are likely more children who are affected by NF1-associated leukemia than are reported in the statistics. The focus of this proposal is to study NF1-associated myeloid leukemia, and to characterize additional genetic events in tumor progression to acute stage using human and mouse model resources.

A viral based mouse model of NF1-associated leukemogenesis identified several common sites of viral integration. I investigated one site (Epi2) to see how the endogenous genes are affected and how this can contribute to myeloid leukemia. The Epi2 locus is on chromosome 6 in humans and chromosome 17 in mice. There are two genes in the Epi2 locus, *PPP1R10* and *MRPS18B*. PPP1R10, whose protein product is PNUTS, is a serine/threonine protein phosphatase regulatory protein, and MRPS18B is a 28S mitochondrial ribosomal protein. Since

both genes are located less than 1kb apart and are transcribed in opposite directions, it was possible that both genes act simultaneously in NF1 leukemogenesis, as oncogenes and/or tumor suppressors. I performed a series of experiments to test some of these hypotheses, and found evidence that *PPP1R10* is a tumor suppressor gene that contributes to development of acute myeloid leukemia.

# CHAPTER 1
# INTRODUCTION

## Neurofibromatosis Type 1 and JMML

Neurofibromatosis type 1(NF1) is an autosomal dominant disease that is characterized by a variety of phenotypes. At the NF consensus conference of 1987, it was decided that the criteria for clinical diagnosis required that a patient have two or more of the following symptoms (Stumpf et al. 1988):

- Six or more café au lait macules on the skin over 5 mm in greatest diameter in prepubertal individuals, and over 15 mm in greatest diameter in postpubertal individuals.
- Two or more neurofibromas of any type or one plexiform neurofibroma (benign Schwann cell tumors).
- Freckling in the axillary (armpit) or inguinal regions (groin).
- Optic glioma. (iris hamartomas).
- A distinctive osseous lesion such as sphenoid dysplasia or thinning of long bone cortex with or without pseudoarthrosis (tibial dysplasia)
- Two or more Lisch nodules
- A first-degree relative (parent, sib, or offspring) with NF1 as defined by the above criteria.

NF1 patients also have an increased risk for other tumors besides those described above. For example, in one review, 12.5 percent of the NF1 cases had tumors in the optic pathway (pilocytic astrocytomas) while 1.0-1.6 percent had tumors at other central nervous system sites (www.ctf.org). For malignancies, 32.76 percent of NF1 individuals had malignant peripheral nerve sheath tumors (MPNSTs) while 1.76-4.2 percent had sarcomas at other sites. Another category is leukemia; 1.7 percent had juvenile myeloid monocytic leukemia (JMML, described further below), while 7.4 percent had myelodysplastic syndrome (MDS). There is also an increased risk for phaeochromocytomas (adrenal tumors), gastrointestinal tumors and non-optic brain tumors.

It is deceiving that NF1 patients with JMML account for a small percentage of the malignancy types observed in NF1 patients. This number is probably higher because JMML patients often get diagnosed with NF1 after their initial diagnosis of leukemia. This is likely due to the fact that JMML has onset very early in childhood, when most kids have not yet met diagnostic criteria for NF1 (Pinkel et al. 2008). Typically, in children without NF1, lymphoblastic leukemias predominate 4:1 over myeloid leukemias. In children with NF1, the ratio changes to 9:20 (Bader et al. 1978). This information strongly links NF1 and JMML. Another study compared leukemia patients with and without NF1 for activating *N-RAS* and *K-RAS* mutations in the tumor cells (Kalra et al. 1994). The results showed that leukemia patients with NF1 had no activating *RAS* mutations. However, 20% leukemias without NF1 had activating *RAS* mutations. Since loss of *NF1* increases RAS activity, this suggests another link between leukemia and NF1, via the RAS pathway. But mutations in the two genes are mutually exclusive.

The *NF1* gene, maps to chromosome 17q11.2 in humans and chromosome 11 46.06 in the mouse (NCBI). The gene is over 98 percent conserved between the two species. In humans, the genomic sequence spans over 280kb and its mRNA is >9 kb. There are three embedded genes within the *NF1* genomic region called *EVI2B*, *EVI2A*, and *OMGP*. All three genes are located within an intron of the *NF1* gene and are transcribed in the opposite orientation to the *NF1* gene. Their roles in NF1 and their specific protein functions are still under investigation. The *NF1* gene also undergoes alternative splicing. Specifically, there are three exons that are alternatively spliced, exon 9a, exon 23a, and exon 48a(Geist et al. 1996; Gutmann et al. 1999; Andersen et al. 1993; Gutmann et al. 1995). The isoforms are differentially expressed in a wide range of tissues ranging from the cerebellum to the spleen with 9a predominantly in the brain,

48a in the muscle, and 23a ubiquitous. It has yet to be determined what roles these isoforms play in the function of the *NF1* gene and the disease, although it has been determined that inclusion of exon 23a reduces ras-inactivating activity of the protein.

The NF1 protein is called neurofibromin. Structurally, it is 2818 amino acids long and has at least two conserved domains, a RAS-GAP domain and a Sec14p-like lipid domain (NCBI). The RAS-GAP domain negatively regulates the RAS signaling pathway (NCBI). The NF1 protein acts as a tumor suppressor protein in the sense that it functions by accelerating the hydrolysis of RAS-GTP into RAS-GDP to prevent over-proliferation of cells. The other conserved domain, Sec14p-like lipid binding domain, is found in secretory proteins and in lipid regulated proteins (NCBI). The role of this and some other protein domains remains unclear in the protein function. There is evidence that neurofibromin can be both in the cytoplasm and nucleus (Vanderbroucke et al. 2004). The rest of this large protein is highly conserved but additional functions have not been found.

NF1 has proven to be somewhat complicated genetically. The mutational analysis of the *NF1* gene is difficult due to the large size of the gene and because there are many different mutations. The NF1 consortium has categorized mutations in 246 patients (www.ctf.org). In the consortium study, it was found chromosomal abnormalities were found in 1.6 percent of the patients. Deletions of the entire *NF1* gene were found in 7.2 percent, whereas small intragenic deletions were found in 15.5 percent. Also, large intragenic deletions were found in 1.2 percent of the patients, whereas small insertions accounted for 11 percent of the mutations. Missense and nonsense mutations accounted for 11.8 percent and 17.6 percent, respectively. Finally, putative 3'UTR mutations were found in 1.6 percent of patients, and intronic mutations affecting RNA splicing accounted for 10.2 percent. Furthermore, it has been shown that somatic mutation

of the other allele is associated with neurofibroma, café au lait spots, JMML, and bone dysplasia (Side et al. 1997; Coleman et al. 1995; Stevenson et al. 2006). Virtually all mutations can be predicted to be disruptive or inactivating, and thus, reduction/loss of neurofibromin activity is an initiating event in many NF1-related phenotypes.

## Mouse Models of Nf1

There are no known naturally existing animal models for NF1, a hindrance to research. Two attempts were initially made to model NF1 in mice through knockout technology. These two labs made mouse knockouts for the *Nf1* gene in different locations. One lab constructed a mouse knockout deleting exons 30 to 32 (located after the GAP related domain) (Jacks et al 1994). 250 heterozygous mice, $Nf1^{+}/Nf1^{n31}$, were followed from 7 months to 2 years of age. The other mutation was a neo gene insertion into exon 31 (Brannan et al. 1994). The results were the same in both labs: homozygous knockout mice were embryonic lethal and heterozygous mice didn't develop the cardinal features of NF1 (neurofibromas, café au lait, or Lisch nodules). However, the mice did have an increased rate of tumorigenesis. It was found that 75 percent of the heterozygous animals died as a result of the tumors over a period of 27 months compared to 15 percent of wild type animals. Jacks et al. (1994) looked into a larger series of heterozygous animals (n=64) and found a variety of tumor types. Lymphoma presented in 14 animals, lymphoid leukemia in 2 animals, lung carcinoma in 9 animals, hepatoma in 4 animals, and fibrosarcoma in 3 animals. The heterozygotes also developed a few tumors characteristic of human NF1. One animal had an MPNST at 21 months of age, and 12 heterozygotes had adrenal tumors (pheochromocytomas) at 15 to 28 months of age. Seven of their heterozygotes had chronic myeloid leukemia at 17.7 to 27 months of age. In addition, homozygous lethality occurred between days 12.5 to 14 dpc. (Jacks et al. 1994). Cami Brannan's exon 31 mouse model (Nf1, Fcr) was slightly different than the previous model. Dr. Brannan observed some

similarities with the Jacks mouse model, but found additional developmental defects that were not present in the Jacks mouse model (Brannan et al. 1994). The homozygous mice, $NF1^{Fcr/Fcr}$, were also embryonic lethal, between 11.5 and 14.5 dpc. The $Nf1^{Fcr/Fcr}$ embryos were studied for developmental problems between 11.5dpc and 13.5dpc. These mice had obvious cardiac, renal, hepatic, and skeletal muscle defects, and hyperplasia of the vertebral sympathetic ganglia (Brannan et al. 1994).

**Molecular and Biochemical Mechanisms Underlying Myeloid Leukemogenesis.**

Myeloid leukemia is the overexpansion of a myeloid hematopoietic precursor (blast), which reduces number and function of the other blood cell types. These cells can invade tissues as well in the acute form (>30% blasts in the blood). The chronic form is <30% blasts and can be fatal in itself, or can progress to AML. Somatic genetic mutations lead to chronic leukemia and other genetic events cause its progression to acute stage. These are very difficult to treat for patients. Functional analysis of genes isolated from recurring chromosomal translocation breakpoints in leukemia cells such as *AML1*, *MLL*, and *HOXA9* strongly implicate aberrant transcription in leukemogenesis (Look 1997). A second group of specific genetic lesions (e.g., *RAS* and *FLT3* mutations, the *BCR-ABL* translocation, and *NF1* inactivation) undermine hematopoietic growth control by providing hyperproliferative and survival signals (Daley GQ et al. 1990; Largaespada et al. 1996, Kelly LM et al. 2002). Mutations in both classes of genes are common in acute myeloid leukemia (AML). Based on these data, Gilliland and coworkers proposed that transcription factor fusion proteins cooperate with genetic lesions that deregulate growth-promoting signaling pathways in the progression to AML (Kelly et al. 2002). Whereas data from mice generally support the idea that neither type of genetic lesion is sufficient to cause AML by itself, these studies have also shown that *Nf1* inactivation and other genetic lesions that result in hyperactive Ras are sufficient to induce myeloproliferative disorders (MPDs) (Le et al.

2004). However, the requirement for cooperating mutations in the pathogenesis of JMML and other human MPDs, and the mechanisms that contribute to progression to overt AML, are poorly characterized.

## Hyperactive Ras in JMML

Somatic *KRAS*, *NRAS*, and *HRAS* mutations, which introduce amino acid substitutions at codons 12, 13, and 61, are the most common dominant oncogenic mutations found in human cancer (Bos JL 1989; Malumbres M et al. 2003). Mutant Ras proteins accumulate in the GTP-bound conformation due to defective intrinsic GTPase activity and resistance to GAPs (Bos JL 1989; Vetter IR 2001; Donovan et al. 2002). *NRAS* and *KRAS2* mutations are highly prevalent in MDS, MPD, and AML (Malumbres M et al. 2003; Boguski M et al. 1993), are particularly common in CMML (~40% of cases) (Onida F et al. 2002), and are found in ~25% of JMMLs. (Miyauchi et al. 1994; Kalra et al. 1994) The elevated risk of JMML in children with NF1 and Noonan syndrome (NS) provide additional evidence that hyperactive Ras can initiate myeloid leukemogenesis. Loss of the normal parental *NF1* allele occurs in JMML cells from children with NF1, which results in elevated levels of Ras•GTP and activation of the downstream effector extracellular signal-regulated kinase (ERK) (Shannon KM et al. 1994; Bollag et al. 1996; Side L et al. 1997). Approximately 50% of children with NS demonstrate germline missense mutations in the *PTPN11* gene, which encodes the SHP-2 protein tyrosine phosphatase. *PTPN11* mutations are found in nearly all NS patients with JMML, and somatic *PTPN11* mutations are detected in about 35% of sporadic JMML (Tartaglia M et al. 2003; Loh M et al 2004). Most of these mutations decrease SHP-2 phosphatase activity by destabilizing an auto-inhibitory interaction and thereby increase signaling to Ras and other downstream effectors. Overall ~90% of JMML bone marrows have mutations in either, *KRAS2*, *NRAS*, *NF1*, or *PTPN11*, which are largely mutually exclusive.

## Nf1 Reconstitution Mouse Model

Further research of the Nf1 knockout mouse showed that when $Nf1^{Fcr/Fcr}$ fetal liver cells were transplanted into lethally irradiated recipient mice, to reconstitute their bone marrow, all of these mice developed a chronic myeloproliferative-like syndrome similar to human JMML (Bollag et al 1996, Largaespada et al 2004, Birnbaum et al 2000). Approximately twenty seven percent of these mice died of complications or developed or AML. Largaespada et al. 1996, also observed an increase in colony formation of hematopoetic cells response to granulocyte/macrophage-colony stimulating factor (GM-CSF) (Bollag et al 1996, Largaespada et al 2004). GM-CSF binds to receptors expressed on some myeloid lineage cells to promote their differentiation, proliferation and cell survival (Birnbaum et al. 2000). Flow cytometry experiments showed that these tissues had more myeloid progenitor cells as well (Largaespada et al, 1996; Bollag et al, 1996, Birnbaum et al. 2000).

## Identification of Epi Loci in Nf1-Related Myeloid Leukemia

The discovery of the *Epi2* locus employed the BXH-2 mouse that is a cross between the C57/BL6J and C3H/HeJ strains (Bedigian et al. 1984). In the parental strains, the incidence of leukemia is low. The high incidence of AML in BXH-2 is associated with high levels of natural expression of B-ecotropic murine leukemia virus (MuLV) that is passed from mother to offspring in utero (Bedigian et al 1984, Blaydes et al. 2001). Ninety five percent of BXH-2 mice die of AML by one year of age. This 8kb murine leukemia virus has a 5'and a 3' long terminal repeat with gag, pol and env genes (NCBI). These genes are necessary for the retrovirus's life cycle so that it can synthesize more virus particles, package itself, and infect other cells (Bedigian et al 1984, Blaydes et al. 2001). Also, it's important to note that these viruses are of non-T cell origin and replication competent. The BXH-2 mouse was used here as a tool to find genes that cooperate with *Nf1* loss to cause Nf1-associated leukemia. To accomplish this task,

the BXH-2 mouse was backcrossed to the *Nf1*$^{+/Fcr}$ mouse that was created by Dr. Cami Brannan (Brannan et al. 1994, Blaydes et al. 2001). It was backcrossed for 3 generations and aged until the BXH2 *Nf1*$^{+/Fcr}$ mice developed leukemia. Interestingly, fifty percent of the mice developed AML at an average earlier time than the controls, t=5.5 months versus t=8.5 months. Tumors were collected from all the mice and analyzed by Southern Blot analysis to test for a second genetic hit in the *Nf1* locus. It was determined by Blaydes et al (2001), that 89% of the tumors had a second hit at the *Nf1* locus by LOH or by viral integration into Evi2 (internal to *Nf1*) integration. It was then determined that each tumor had at least 3-4 somatically acquired viral integrations (Brannan et al. 1994, Blaydes et al. 2001). This suggested that loss of *Nf1* on the BXH-2 background was not sufficient to cause acute disease. In fact, it is the additional acquired somatic mutations that are required for progression to acute disease. The actual identification of the common sites of viral integration (presumably at the sites of cooperating genes) was done through the use of Southern Blot analysis, a mouse mapping panel, and an ecotropic viral probe, pAKV5 (Brannan et al. 1994, Blaydes et al. 2001). After the first isolation with probe pAKV5, the genomic fragment was isolated and a new non-repetitive probe was made based on the fragment isolated from the tumor. This new probe was used to test the whole collection of tumor samples and see if the same rearrangement was also present in another tumor. Indeed, this was the case (Brannan et al. 1994, Blaydes et al. 2001). Dr. Brannan identified three new common sites of viral integration, termed *Epi1*, *Epi2*, and *Epi3*. These names were abbreviated based on the original name, ecotropic proviral integration site X where X denotes the number of the site. In order to map the location of the viral integration on the mouse genome, a mapping mouse panel was used in collaboration with Jenkins and Copeland's lab at the NCI (Blaydes et al. 2001). Once the three common sites of viral integration were localized, subsequent experiments

were focused on elucidating how these sites of common proviral integration cooperate with loss of *Nf1* to cause AML (Brannan et al. 1994, Blaydes et al. 2001). My dissertation work focused on the locus termed *Epi2*. This site was found in 2 independent tumors (33T, 419T) out of 67 in the Brannan series, and was also seen twice in the Copeland and Jenkins' Lab. In all four cases, the virus was inserted into *Mrps18b* in intron 1 in the same orientation (Walrath et al., in preparation).

**Viral Insertional Mutagenesis**

The integration of the virus can theoretically have many effects on that region of the genome. One mechanism is enhancer insertion, where the virus integrates either at the 3' or 5 end of a gene (McCormick et. al. 2005) and the viral enhancer causes improved efficiency of the native promoter. Another mechanism is activation by enhancement where the virus integrates in the 3'UTR. This is thought to increase the stability of the transitory mRNA (McCormick et. al. 2005). A third mechanism is promoter insertion, which occurs when the virus integrates upstream or within the 5' domain of the host target gene with the same transcriptional orientation as the target gene. This causes elevated long terminal repeat constitutive gene activation and transcription (McCormick et al. 2005). This and the former mechanisms would cause overexpression of the endogenous gene along the lines of oncogenes. The next mechanism is protein truncation by transcription termination/promoter insertion where the virus integrates within the coding region of the gene. This may result in the inactivation of the gene. The last mechanism is also protein truncation by transcription termination at a cryptic poly A site (McCormick et al 2005). This is thought to produce aberrant protein products exhibiting anomalous biological function. In the Epi2 locus the virus intergrated into intron 1 of *Mrps18b* and in the same transcriptional orientation of *Mrps18b*. This could cause promoter insertion, where one gets constitutive gene activation and transcription (McCormick et al. 2005). Another

possible theory is protein truncation by transcription termination/promoter insertion since the integration is near the beginning of the coding region of *Mrps18b/Ppp1r10*.

**MRPS18B**

*Mrps18b*, which encodes a mitochondrial ribosomal protein, is located on chromosome 17 B3 in mouse and chromosome 6p21.3 in humans. In mice and humans, the gene has 7 exons and a 5' as well as 3' UTR. The mouse full length mRNA is 1073 bp (NM_025878) and the human mRNA is 1439 bp (NM_014046). The mouse protein is 254 amino acids (NP_080154), and in humans it is 258 amino acids (NP_05765). This is one of a family of mitochondrial ribosomal proteins encoded by nuclear genes, which aid in protein synthesis in the mitochondria. Mitochondrial ribosomes consist of a 5, 18 and 28S subunits. *Mrsp18b* is one of three genes that encode the 28S specific ribosome proteins (NCBI). MRPS18B has only one conserved domain (encoded in exon 2), which is the ribosomal protein domain. However, it is thought that exon 1 may contain sequence that localizes the protein to the mitochondrial ribosome. If *MRPS18B* were disrupted, then the mitochondrial ribosome, might function aberrantly, affecting energy metablosim and apoptosis. Less than one kb upstream of *Mrps18b*, and in the opposite transcriptional orientation is the gene *Ppp1r10*. Because of its proximity, the gene was also a candidate to be involved in NF1 leukemogenesis.

**PPP1R10**

*PPP1R10* consists of 20 exons in humans and 19 exons in mice. The mRNA is 4203bp in mouse (NM_175934) and 4504bp in humans (NM_002714), although it is not clear that the absolute transcription start has been identified. *Ppp1r10* in the mouse encodes a protein that contains 874 amino acids (NM_175934), with the human protein being 940 amino acids long (NP_787948). Also, the Ppp1r10 protein is 89 percent conserved between mice and humans, and Mrps18b is 86 percent conserved (NCBI). It is also important to note that neither gene has yet

been implicated in any human disease. PPP1R10, whose protein product is PNUTS, has 3 conserved domains. One is in the N terminal region, a TFIIS site, which is located in exon 5, 6, and 7. Its function in PPP1R10 activity is unknown. However, TFIIS is thought to function in eukaryotic transcription elongation by suppressing transient pausing of the RNA polymerase. The second conserved domain is a PP1-binding domain encoded in exons 13 and 14. This region of the protein binds to PP1, an important serine-threonine phosphatase (see below). The rat PPP1R10 homolog has been shown to have an inhibitory effect on PP1, and co-localizes with PP1 at distinct phases during mitosis (NCBI, Allen et. al. 1998, Watanabe et. al. 2001, Kim et. al. 2003, Udho et. al. 2002). The third conserved domain is a C3H1 zinc finger encoded by exon 19, which suggests that PPP1R10 may affect transcription of target genes. In addition, recent research has shown that PPP1R10 might be involved in regulating cell death due to hypoxia or cell stress (Lee et al. 2007).

**PP1, a Serine/Threonine Protein Phosphatase**

One third of all eukaryotic proteins are controlled by serine/threonine phosphatases, which affect protein activity and localization (Ceulemans et al. 2004). Protein Phosphatase type 1(PP1), 35-38kDa, is a serine/threonine phosphatase that contributes to many important cellular functions (Ceulemans et al. 2004, Aggen et al. 2000, Klumpp et al. 2002, Ludlow et. al. 1995): cell cycle progression, protein synthesis, muscle contraction, carbohydrate metabolism, transcription, and neuronal signaling. Most protein phosphorylations are reversible and there is a balance between the phosphatases and the kinases. This phosphatase exists in many isoforms: PP1alpha, PP1beta/delta, as well as two from splice variants, $PP1y_1$ and $PP1y_2$. The protein isoforms are conserved in the central three fourths of the protein, however the amino and carboxy termini are the most divergent.

As reviewed by Ceuleman's et al (2004), PP1's catalytic subunit does not exist freely in the cell and requires a regulatory subunit to determine specificity, sub-cellular localization, and regulation of the phosphatase. These regulators are important in bringing PP1 into close proximity to its substrate so that the phosphatase can be anchored in specific cellular compartments via the targeting motifs of the regulators. The regulators, of which there are dozens, are considered either primary or secondary based on whether the protein has or lacks a PP1 binding site, respectively. Some primary regulators include Inhibitor-1, Inhibitor-2, NIPP-1, PPP1R10, and SDS22. Regulatory proteins interact with PP1 via short, degenerate sequence motifs of 4-6 residues, the PP1 binding sites. Most of these proteins have multiple points of interaction with PP1 and some of them can share PP1 interactions sites as well. It has been theorized that PP1 is subject to a combinatorial control that relies on competition of different regulators for a combination of interaction sites. This allows the formation of large variety of holoenzymes with distinct specific activities and substrate activities. There are also secondary PP1 binding sites that can serve as anchor sites to promote the cooperative binding of secondary sites with lower affinity. These secondary PP1 binding sites are called RVXF sites. Most of the regulators contain an RVXF motif, although the binding is not associated with any conformational changes or effects on catalytic activity.

PP1 has many cellular functions important to this project, such as in the cell cycle. First, PP1 interacts with AURORA-B to ensure that cytokinesis works properly (Andrews et al 2000; Sugiyam et al. 2002). Second, PP1 is involved in preventing centrosomes from splitting before G2/M phase (Eto et al. 2002). Third, PP1 contributes to reassembly of the nuclear envelope at the end of mitosis by dephosphorylating Laminin-B (Thompson et al. 2002). Fourth, PP1 dephosphorylates Bcl-2, an anti-apoptotic protein that is an integral membrane protein in the

endoplasmic reticulum and the mitochondria. The dephosphorylation of Bcl-2 by PP1 targets Bcl-2 for proteosome mediated degradation (Brichese et al. 2002). Finally, PP1 has been shown to dephosphorylate the retinoblastoma protein (pRB) in late M phase (Nelson et al. 1997).

My project focused on understanding whether or how PPP1R10 is involved in myeloid leukemia, NF-related or otherwise. I took 3 approaches: (1) mutation analysis of *PPP1R10* in human myeloid dysplasia/leukemia samples+/-NF1 involvement, to look for oncogenic or loss-of-function mutations (Chapter 2); (2) in vitro analysis of mouse fetal liver cells to test whether overexpression of PPP1R10 was tumorigenic (to test oncogene hypothesis)(Chapter 3); and (3) characterize a *Ppp1r10* knockout mouse to test the tumor suppressor hypothesis, including the cross of this mouse to the Nf1 knockout mouse (Chapter 4)

# CHAPTER 2
# MUTATIONAL ANALYSIS OF *PPP1R10* IN LEUKEMIA

## Introduction

JMML is characterized by splenomegaly, leukocytosis, hypersensitivity to granulocyte/macrophage stimulating factor, and absence of the Philadelphia chromosome in tumor cells (reference diagnostic paper). There have been several genes implicated as a primary step in JMML: *NF1*, the *RAS* gene family, and *PTPN11* (a tyrosine kinase phosphatase)(Side et al., 1997; Side et al., 1998; Tartaglia et al., 2003). Mutations in these genes are mutually exclusive initiating genetic events, and together account for ~85% of genetically predisposed JMML. All of these gene mutations lead to an increase in Ras signaling. The Epi2 mouse model implicates *Ppp1r10* as a possible oncogene or tumor suppressor. Since there is so little material from the two mouse Epi2 tumors, we chose to screen human myeloid malignancies for further evidence that *PPP1R10* might be a leukemia gene. Identification of any *PPP1R10* mutations in human myeloid leukemia samples may provide insight about whether (and how) this gene is involved in NF1 associated leukemia and/or JMML, myeloproliferative disorder (MPD), or AML.

To test the hypothesis that *PPP1R10* might be genetically altered, we performed mutational analysis in NF1-JMML, JMML, and AML tumor samples. We examined the entire gene and found loss of heterozygosity in intron 15 in a subset of tumor samples by sequence analysis and RFLP analysis. Additional analysis of the sequenced region revealed a putative stop codon mutation in exon 6 of *PPP1R10* in 2 out 40 leukemia samples. Real-time mRNA quantification PCR was also performed on a subset of leukemia samples, which showed a decrease in expression of *PPP1R10* in some samples compared to a GAPDH control.

## Materials and Methods

### Patient Samples

DNA and RNA were extracted from tumor cells using standard methods (Thomson and Wallace et al 2002). Most leukemia samples (bone marrow or blood cells) were obtained from the UF tissue bank and were > 35% blasts. Tumor and germ-line samples were obtained with IRB approval from the UF Tissue Bank (MDS (n =7), AML (n=54), CML (n=6)) and UCSF (courtesy of Dr. Kevin Shannon, (NF1-JMML (n=50), JMML (n=25), CMML (n=50)).

### Polymerase Chain Reaction and Sequencing of *PPP1R10* Exons

Tumor DNA was PCR-amplified in a reaction mixture containing 100ng for each forward and reverse primer, 200umol dNTP's (Invitrogen), 0.5U Hotstart Taq Polymerase (Qiagen), and 1X Roche PCR buffer. See Appendix A for a list of primer sets and PCR product size for *PPP1R10*, which were designed using PRIMER3 (http://fokker.wi.mit.edu/primer3/input.htm). The following cycling conditions were used: 1 cycle of 95°C for 15 minutes, 35 cycles of 95°C for 15 seconds, 60°C for 30 seconds, 72°C 1 minute; a final extension of 72°C for 10 minutes. All PCR products were examined on ethidium bromide stained 1.2 percent agarose gels to verify quality and quantity of PCR product. PCR products were purified using Exosapit (Amersham Pharmacia) and 5.8ul were used in the sequencing reaction: 2ul of 5X Sequencing Buffer, 2ul of Big Dye 3 (ABI), and 20ng/ul of forward or reverse primers. The following cycle sequencing conditions were used: 25 cycles of 95°C for 1 minute, 50°C for 30 seconds, and 60°C for 4 minutes. Sequencing reactions were run on a ABI 3130XL Genetics Analyzer at the UF Center for Epigenetics. Sequence data were analyzed using Sequencher software (Gene Codes).

### Restriction Fragment Length Polymorphism for Intron 15 Loss of Heterozygosity

Sequence analysis uncovered a polymorphism in *PPP1R10* intron 15 close to exon 16 and was used for a loss of heterozygosity analysis. Loss of heterozygosity of a polymorphism can be

used to test for deletions. The heterozygosity frequency in this A/G polymorphism (rs126443) was reported to be .478 in Caucasians and confirmation of this was done with normal patient DNA through RFLP. P115RsaF and P115RsaR primers (see Appendix A) were used to amplify the intron 15 polymorphism and create an RsaI site to distinguish the alleles. With RsaI digest, the G allele causes the 138bp to be cleaved into 26bp and 112bp fragments (two bands), where as, the A allele does not cut with Rsa1 digest (one band). The digest was run on an 8% native gel with ethidium bromide for visualization. Visualization of the RFLP on an acrylamide gel allows for comparison of allele signal intensities. A series of germline heterozygous DNAs were used to establish relative allele intensity, and tumor samples were compared to these DNAs. If there is a deletion in the gene of interest in the tumor there will be a reduction in intensity of one allele relative to the other as compared to the germline genotypes. LOH analysis was also performed at an SNP in the shared PPP1R10/MRPS18B promoter (primers Appendix 1), which used an Ear 1 digest.

**Real-Time mRNA Quantification**

Tumor cells from leukemia patients were used in the real-time quantification of PPP1R10 expression. Tumor total RNA was serially diluted from 400ng to 25ng and subsequently used in a RT-PCR reaction. For the reverse transcription: 200uM of dNTPs (Invitrogen), 50ng random hexamer (Invitrogen), and 5ul of water was added to each dilution of tumor RNA. This mixture was heated at 65°C for 10min. and then placed on ice. Next, 4ul of 5X buffer, 2ul of .1M DTT, 40 units of RNase Inhibitor (Invitrogen), and 200units Superscript II (Invitrogen) was added to each of the tubes on ice. These tubes were heated at 25°C for 10 min and 50°C for 40 min to produce cDNA. For the mRNA quantification, 1ul of cDNA at each concentration was placed in PCR tubes (Biorad cat. #TLS0851, TCS-0803), followed by the addition of 10ul of Master mix

(Biorad, contains hotstart version of a modified Tbr DNA polymerase, SYBR Green 1, optimized PCR buffer, 5mM $MgCl_2$, dNTP mix including (dUTP)), 100ng of forward primer, 100ng of reverse primer, and 8ul of water. These reactions were then analyzed on a Opticon Moniter II machine at the Center for Epigenetics: 95C for 15 min, 94°C for 15sec, 55°C for 30sec, Plate Read, 72°C for 1min, Go to Step 2 for 30 cycles, Melting Curve 50°C to 90°C, Read ever 1sec, Hold for 10sec, 72°C for 15min. The Ct number for each *PPP1R10* tube was compared to the Ct of the *GAPDH* gene results thorough the Pfaffl method formula (Appendix B). Primers chosen for real-time quantification lay in different exons to avoid DNA-PCR contamination and *GAPDH* was used as a housekeeping/normalizing gene (Appendix A).

## Results

A set of 50 NF1-JMML and 25 JMML (non-NF1) myeloid leukemia samples were used in the DNA analysis. A polymomorphism in the promoter region (rs16867845) displayed no loss of heterozygosity and had no mutations (Figure 2-1). A putative nonsense mutation was also uncovered in two separate NF1-JMML samples (Figure 2-2). This substitution in exon 6 encodes a serine->stop at codon 125. A putative missense was also uncovered in exon 6, serine->threonine change at codon 125 (Figure 2-3). Another polymorphism in exon 19 (rs11754215) also did not display loss of heterozygosity in any samples (Figure 2-4). The intron 15 SNP (rs1264423) did reveal potential loss of heterozygosity by sequence analysis in 6/44 NF1-JMML samples (Figure 2-5). To confirm this result by another method, a PCR-based forced RsaI digest system was constructed for the polymorphism. The sequence positive NF1-JMML samples were re-amplified with the new primers, digested by RsaI and the products were visualized by native polyacrylamide gel electrophoresis. The RsaI digest creates 2 fragments if the patient is heterozygous (AG) and 1 fragment if the patient is homozygous (GG or AA). Figure 2-6, shows

the RsaI digest normal germline DNA displaying all three genotypes. Figures 2-7 and 2-8 show digests of some tumor samples of NF1-JMML and JMML displaying loss of heterozygosity. More NF1-JMML and JMML samples were tested with this assay and it was found that 6/44 NF1-JMML and 11/20 JMML samples displayed loss of heterozygosity at the intron 15 polymorphism (Table 2-1 and Table 2-2).

Real time mRNA quantification on a set of leukemia samples also revealed a decrease in *PPP1R10* mRNA expression. The Ct values from the tumor RNA and from normal lymphocytes for *PPP1R10* and control *GAPDH* were inputed into the Pfaffl method formula (Pfaffl et al. 2001). This formula can calculate the fold expression change of *PPP1R10* in the tumor cells compared to *GAPDH* using a standard curve method. Table 2-3 shows the fold change of *PPP1R10* to *GAPDH* is reduced in the human leukemia samples. Interestingly, there is a variable reduction between samples, and different leukemia types (including AMLs).

## Discussion

The human genetic data support the notion that *PPP1R10* is a tumor suppressor gene associated with some NF1-JMMLs, JMMLs, and AMLs since the mutations are inactivating (deletion, stop mutation) and the mRNA expression is reduced in tumor cells. The presence of the *PPP1R10* LOH implicates this gene in non-NF1-related leukemia suggests that this LOH is not specific to NF1-related leukemia.

PPP1R10 is an attractive tumor candidate gene because of its regulation of PP1, which regulates at least 70 mammalian genes. Loss of one allele of PPP1R10 would decrease inhibition of PP1 and may affect the ability of PP1 to regulate its target genes. However, it is still unknown which target genes PP1 regulates as a result of *PPP1R10* binding especially in the hematopoietic system. Traditionally, tumor suppressors have 2 hits. Neither of the two tumors with point changes showed LOH, however, we do not yet have evidence for the 2-hit phenomenon. Further

evidence from real-time data on one mouse Epi-2 tumor revealed a reduction in *PPP1R10* mRNA expression in comparison to the other tumors without Epi-2 viral integration (Walrath, 2005). However, the mRNA reduction was not characteristic of a classic 2-hit mechanism. Recently, several papers have reported that cooperating haploinsufficient tumor suppressors in the mouse can be sufficient reduction in protein function to contribute to tumorigenesis (Kamimura et al. 2007; Vives et al. 2006; Moreno-Miralles et al. 2005; Ma et al. 2005). Thus, the data support a functional contribution by decreased PPP1R10 activity but not necessarily in a classic tumor suppressor mechanism.

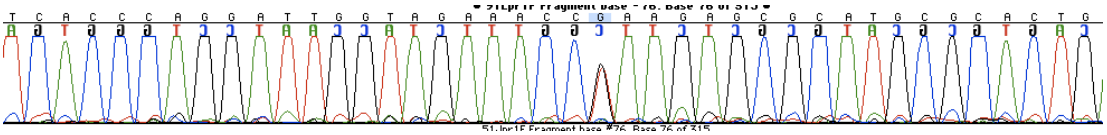

Figure 2-1. Human NF1-JMML analysis PPP1R10, Promoter Polymorphism (rs16867845).

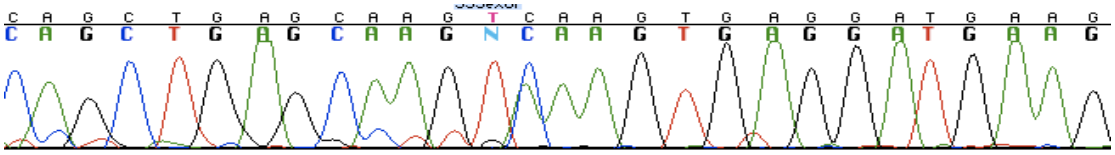

Figure 2-2. Human NF1-JMML analysis, PPP1R10 Exon 6 nonsense, S125X.

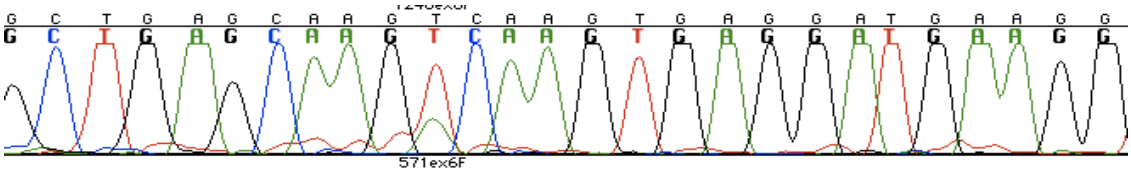


Figure 2-3. Human NF1-JMML analysis, PPP1r10 Exon 6 missense, S125T.

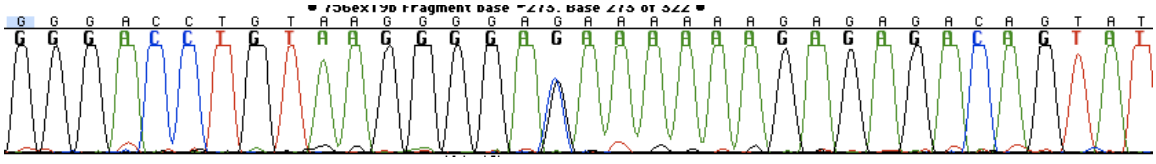

Figure 2-4. Human NF1-JMML analysis, PPP1R10 Exon 19 polymorphism (rs11754215).

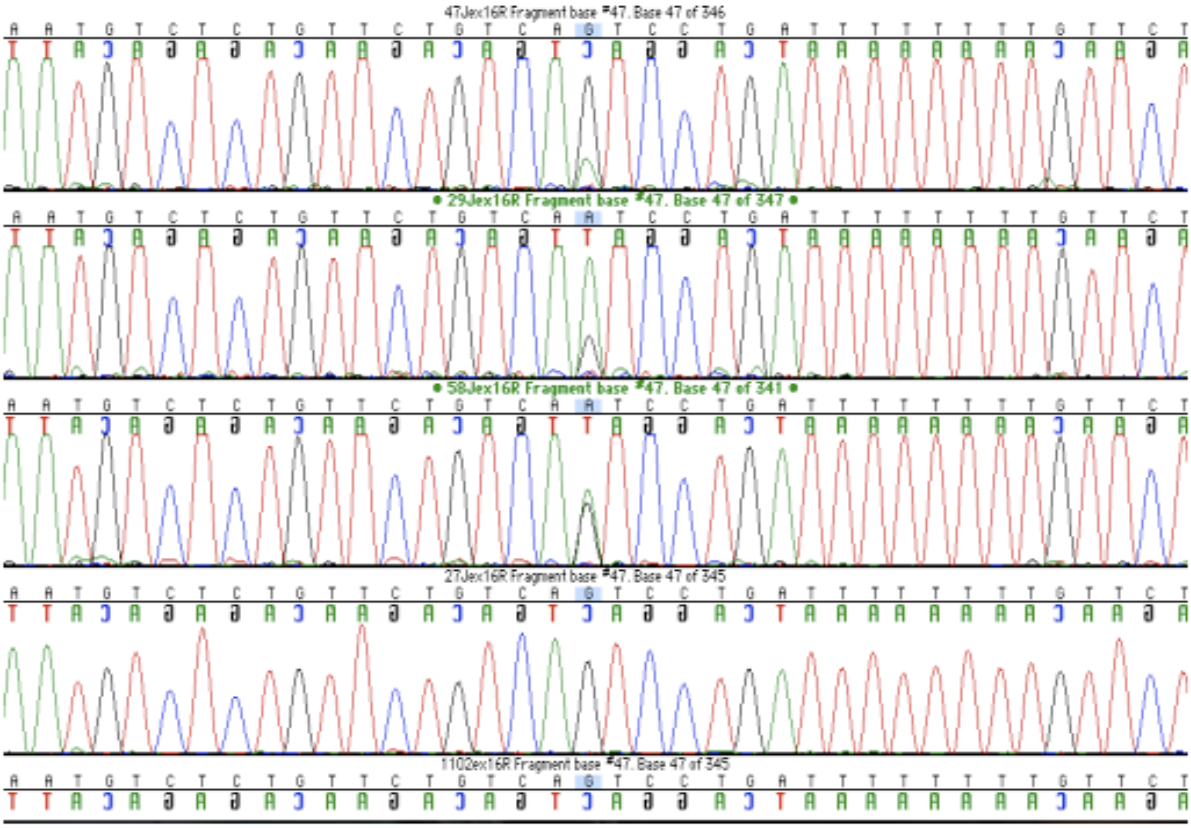


Figure 2-5. Human NF1-JMML PPP1R10 analysis, Intron 15 polymorphism loss of heterozygosity.

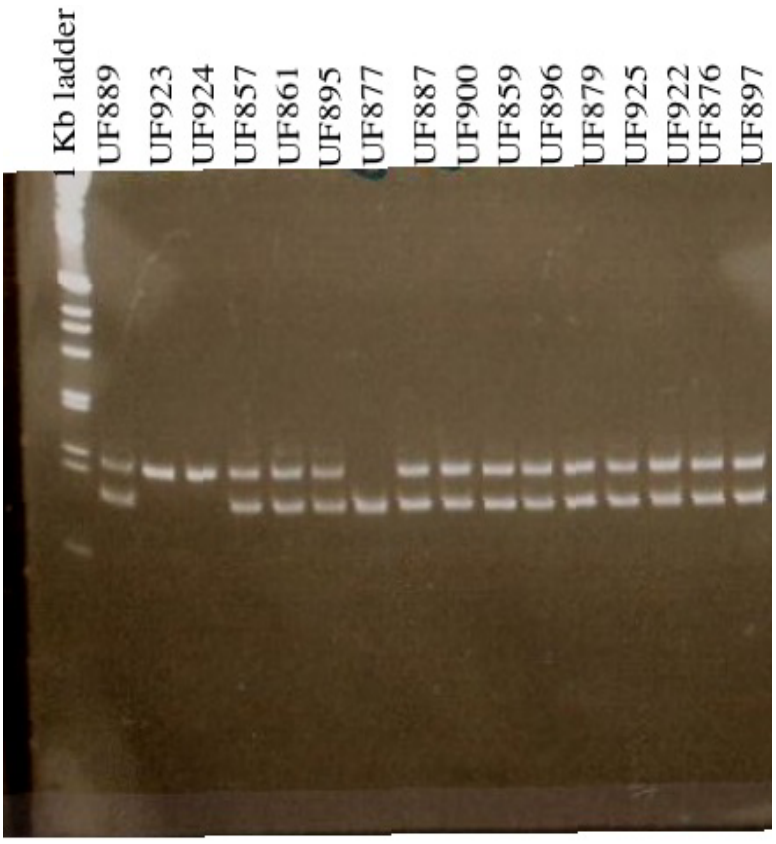


Figure 2-6. RsaI Digest of Intron 15 polymorphism of Control DNA's.

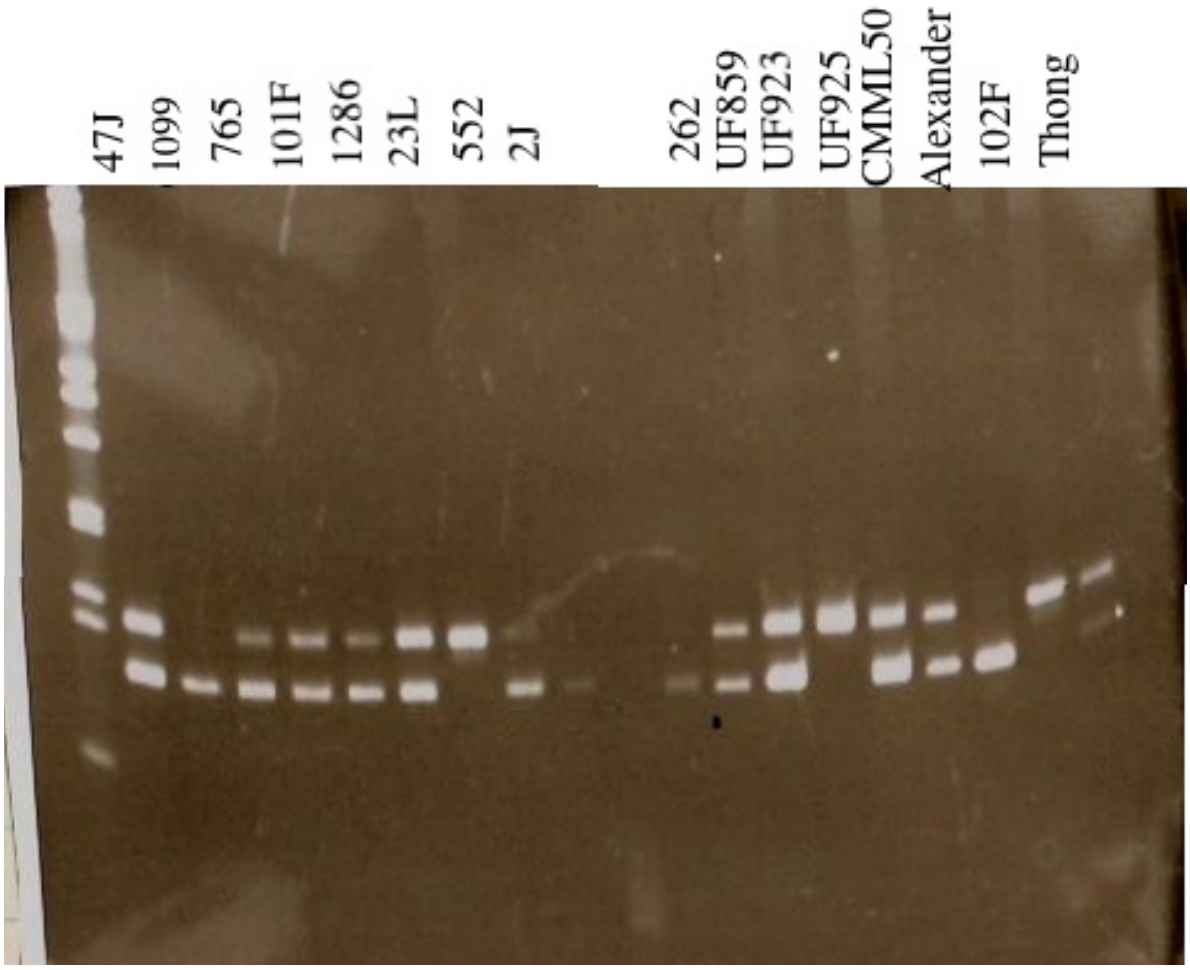


Figure 2-7. RsaI Intron 15 Polymorphism of NF1-JMML and Control DNA.

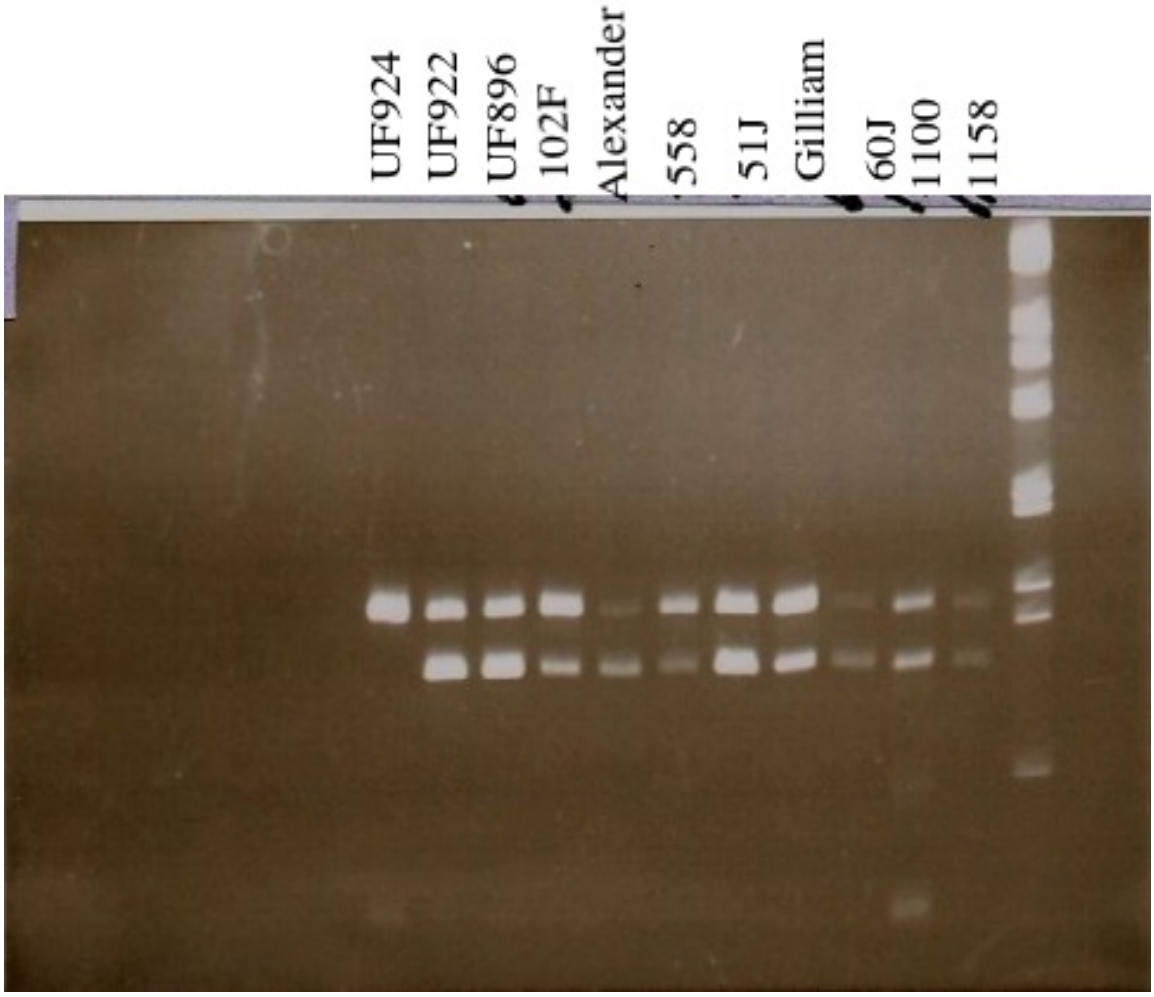


Figure 2-8. RsaI Intron 15 Polymorphim Digest of JMML and an AML sample.

Table 2-1. NF1-JMML human patient samples and Intron 15 polymorphism LOH.

| Sample Name | Diagnosis | Mo. 7 | LOH/NF1 | Mutation | PTPN11done? | Intron15 poly LOH |
|---|---|---|---|---|---|---|
| 1J, 32J | JMML | | yes | yes | no | |
| 2J | JMML | | no | Failed IVTT | no | pLOH AG |
| 18J | JMML | | yes | yes | no | |
| 10L | JMML | | no | Normal IVTT | yes | |
| 29J | JMML | | yes | yes | yes | pLOH AG |
| 29J EBV | | | | | | |
| 26J | JMML | | yes | yes | yes | AG |
| 28J | JMML | | no | Failed IVTT | yes | |
| 27J | JMML | | no | Normal IVTT | yes | GG |
| 61L | JMML | | no | Failed IVTT | yes | |
| 35J | | | | | | |
| 35L | JMML | | no | Normal IVTT | no | AG |
| 33J | JMML | | no | Failed IVTT | yes | |
| 34J | JMML | | prob. | Failed IVTT | no | pLOH AG |
| 33L | JMML | | no | Failed IVTT | yes | pLOH AG |
| 37J | JMML | | yes | Normal IVTT | yes | |
| 45J | JMML | | no | Failed IVTT | yes | |
| 46J | JMML | | no | Failed IVTT | yes | GG |
| 47J | JMML | | yes | Failed IVTT | yes | AG |
| 49J | JMML | | yes | yes | no | |
| 57J | JMML | | no | yes | no | GG |
| 60J | JMML | | no | Normal IVTT | yes | AG |
| 35J | JMML | | prob. | no rna | yes | |
| 51J | JMML | | no | yes | yes | AG |
| 56J | JMML | | yes | yes | no | AG |
| 58J | JMML | | yes | Normal IVTT | yes | |
| 58J EBV | | | | | | |
| 89L | JMML | | yes | yes | no | AA |
| 75J | JMML | | no | not tested | no | |
| 61J | JMML | | no | Normal IVTT | no | |
| 71J | JMML | | no | Normal IVTT | yes | |
| 74J | JMML | | yes | Normal IVTT | yes | |
| 77J | JMML | | | | no | GG |
| 83J | JMML | | | | no | |
| 91L | JMML | | | | no | GG |
| 88J | JMML | | | | no | pLOH AG |
| 63J | JMML | | | | yes | GG |
| HM695 | | | | | | |
| HM725 | | | | | | |
| HM170 | | | | | | |
| HM756 | | | | | | |
| HM853 | | | | | | |
| HM189 | | | | | | |
| HM520 | | | | | | |
| HM549 | | | | | | |
| HM654 | | | | | | |
| HM678 | | | | | | |
| HM609 | | | | | | |
| HM546 | JMML | neg | | | | AA |
| HM552 | JMML | | | | | AA |
| HM553 | | | | | | AA |
| HM605 | JMML | | | | | |
| HM676 | | | | | | pLOH AG |
| HM571 | JMML | pos. | | | | AG |
| HM558 | | | | | | pLOH AG |
| HM660 | JMML | | | | | |
| HM548 | JMML | pos. | | | | |
| HM263 | | pos. | | | | |
| HM264 | | pos. | | | | |
| 19L | | pos. | | | | |
| 20L | | pos. | | | | |
| 17L | | pos. | | | | AG |
| 18L | | pos. | | | | |
| 22L | | pos. | | | | AG |
| 1100 | | | | | | AG |
| 1098 | | | | | | AA |
| 1099 | | | | | | GG |
| 1102 | | | | | | |
| 1101 | | | | | | |
| 1238 | | | | | | GG |
| 1239 | | | | | | |
| 1240 | | | | | | AG |
| 1241 | | | | | | AG |
| 1242 | | | | | | AG |
| 1243 | | | | | | AG |
| 1244 | | | | | | AG |
| 1245 | | | | | | AG |
| 27F | | | | | | AG |
| 28F | | | | | | |

Table 2-2. JMML human samples and Intron 15 polymorphism LOH.

| Patient number | Intron 15 poly. Pcr |
|---|---|
| 99L | pLOH AG |
| 80L | |
| 60L | GG |
| 23L | AG |
| 102F | pLOH AG |
| HM262 | AG |
| 98L | |
| HM1286 | pLOH AG |
| 101F | GG |
| HM896 | |
| HM910 | pLOH AG |
| HM933 | AG |
| HM1224 | GG |
| HM920 | pLOH AG |
| HM1236 | |
| HM773 | pLOH AG |
| HM765 | pLOH AG |
| HM1198 | |
| HM1158 | AG |
| 342 | GG |
| Puente | pLOH AG |
| Schultz | |
| Mackley | |
| Booth | |
| Alexander | pLOH AG |
| Jackson | GG |
| Buck | |
| Gillian | pLOH AG |
| Thong | pLOH AG |
| Gonclaves | |
| | |

Table 2-3. mRNA Quantification of human leukemia RNA.

| Tumor Sample | Evi2B polymorphism LOH? | 3'UTR polymorphism LOH? | Fold Expression PPP1R10/lymphocyte |
|---|---|---|---|
| AML 17 | YES | NI | 1/3.57 |
| AML 47 | YES | NI | 1/7.29 |
| AML 259 | YES | NO | 1/9.43 |
| MDS 4 | YES | NO | 1/22.72 |
| AML101404 | YES | NI | 1/66.66 |
| AML 16 | YES | NI | 1/20 |
| CML 20 | YES | NO | 1/18 |
| JMML 1 | YES | YES | 1/6.25 |
| AML BM | NI | NI | 2.56/1 |

# CHAPTER 3
# *IN VITRO* ANALYSIS OF *PPP1R10* AS A POTENTIAL ONCOGENE

## Introduction

*In vitro* studies have been useful in elucidating the role of cancer genes and their signaling pathways. Similarly, *in vitro* studies of *Ppp1r10* might elucidate its role, if any, in the signaling pathways that contribute to cancer. One proposed mechanism for its role in AML was as an oncogene, based on the viral *Epi-2* integration upstream that could be inducing inappropriate transcription. To test this theory, over-expression of *Ppp1r10* was studied in COS7 cells (from African Green Monkey kidney), which were analyzed for altered expression of proteins involved in classic signaling cascades. In addition, I studied *Ppp1r10* over-expression in wild-type mouse fetal liver cells in a colony formation assay using (CFU-GM, specific for the granulocyte/macrophage lineage of the hematopoietic system). These experiments are detailed below. This work led to the conclusion that *PPP1R10* is likely not an oncogene.

## Materials and Methods

### Cloning of *Ppp1r10* in the MSCV Viral Vectors

A plasmid containing the full-length mouse cDNA, pXY-Ppp1r10 (Operon), was digested with EcoRI and NotI restriction enzymes to remove the cDNA from the pXY plasmid. The digested product was ligated into EcoRI/NotI digested pENT4 plasmid (entry vector, Invitrogen). The modified destination vector, pMIG, was provided by the Dr. Kevin Shannon (UCSF) and was already modified to contain an MSCV promoter, multiple cloning site, att sites, and a GFP transgene. Gateway BP Clonase II enzyme mix (Invitrogen) was used to transfer the *Ppp1r10* cDNA from pENT4 into the pMIG-GFP vector. The final vector was called pMIG-PNUTS and DNA sequencing verified correct reading frame and sequence.

**Hematopoietic Cell Isolation and Retroviral Transduction**

Pregnant wildtype C57BL/6 females were humanely killed by $CO_2$ inhalation at post coitus day 14.5 (E14.5) and fetal liver cells were sterily isolated and prepared as described (Birnbaum et al. 2000). The fetal liver cells were cultured in a stimulation medium containing StemSpan SFEM (StemCell Technologies, Vancouver, BC, Canada), 15% FBS, 100 ng/mL stem cell factor (SCF; Peprotech, Rocky Hill, NJ), 50 ng/mL FLT-3 ligand (Peprotech), and 100 ng/mL IL-11 (R&D Systems, Minneapolis, MN) to promote hematopoietic cell lineage growth. Bone marrow cells were cultured in a stimulation medium containing StemSpan SFEM, 15% FBS, 100 ng/mL SCF, 50 ng/mL IL-6, and 10 ng/mL IL-3 (both from Peprotech). Phoenix cells, used to produce MSCV based viruses were co-transfected with empty vector (pMIG) or WT (pMIG-PNUTS) plasmids along with plasmids encoding retroviral gag-pol and env proteins using Lipofectamine2000 (Invitrogen, Carlsbad, CA), to package and excrete the final viral vectors (PNUTS and empty vector). The supernatants from transfected cells, containing the viruses, were harvested 24 hours post-infection, and used to tranduce the murine fetal liver cells for 1.5 hours.

**Colony Formation Unit Granulocyte/Macrophage Colony Assay**

After transduction, fetal liver cells were sorted based on GFP expression by FACSVantage SE flow cytometer (BD Biosciences, San Jose, CA). GFP-positive fetal liver cells (PNUTS, and vector control) were seeded on methylcellulose medium (M3231; StemCell Technologies) containing escalating doses (0.1ng.ml, 1ng/ml and 10ng/ml) of GM-CSF (Peprotech), to test for ability to form colonies in this media, a sign of an oncogene. Granulocyte-Macrophage colony forming units were scored by indirect microscopy on day 7. Images were acquired using a Nikon Coolpix 5000 camera (Torrance, CA).

**Serum Starvation of COS7 Cells**

To test the effect of PNUTS expression on classic oncogene signaling pathways, 10ug of pDEST-PNUTS were transfected into two million COS7 cells (Schubbert et al 2005). Samples were taken at specific time points after serum starvation media (DMEM, 0.01% Fetal calf serum, 1X glutamine, 1X Pen-Strept) was placed on the cells. The 0 time point was taken before addition of the starvation media. Standard protein lysates were made from all cells at all time points (0, 24, and 48 hours) for Western blot analysis. The negative control was untransfected cells.

**Western Blots**

Ten million cells from each time point were lysed in 1% NP-40 Lysis buffer (1% NP-40, 30mM NaF, 30mM b-glycerophosphate, 20mM sodium pyrophosphate, 1mM sodium orthovanadate, and a cocktail of protease inhibitors (phenylmethylsulfonylfloride, benzamidine, leupeptin)), and total protein was quantified (Lowry assay). Each protein sample (40ug) was loaded onto Nupage Novex precast Midi gels (Bis-tris, SDS, MOPS denaturing polyacrylamide gels) and electrophoresed at 175V for 1 hour in manufacturer's buffer. Proteins were electro-transferred onto nitrocellulose membranes (Novex) for 1hour and 30 minutes at 300 mAmp, as recommended by manufacturer, and blocked overnight with 5% BSA. Primary (rabbit) antibodies [(p-mTor (1:750, Cell Signaling), p-PKCa/b (1:600, Cell Signaling), p-Stat3 (1:1000, Cell Signaling), p-Pten (1:500, Invitrogen), p-Akt, p-Erk1/2(1:1200, Cell Signaling), pMek1/2 (1:750, Cell Signaling), b-actin (1:750, Cell Signaling), and PNUTS (1:1000, Zymed)] were incubated at the recommended concentration with membranes in 5% BSA for 1 hour and 15 minutes at room temperature. The membranes were washed twice for 6 minutes each with TBS-Tween (0.05%) before addition of the secondary antibody. The secondary antibody, HRP-conjugated anti-rabbit (1:2000), was incubated with the membranes for 50 minutes and washed

3X for 6 minutes each with TBS-Tween (0.05%). Treatment of membranes with luminescent ECL reagent (Pierce, 1:1) allowed proteins to be visualized by autoradiography (Kodak X-ray film).

## Results

Three replicates each of the fetal liver cells transduced with MSCV-pMIG and MSCV-pMIG-PNUTS viruses were plated on methylcellulose with increasing amounts of GM-CSF, the the ligand that stimulates the granulocyte/macrophage lineage of the hematopoietic compartment. The resulting colonies, at day 7, were scored for size, morphology, and number in the CFU-GM assay in order to observe alterations in granulocyte/macrophage lineage (the pathway affected in JMML). There were no statistically significant differences between the empty vector and PNUTS vector (Figure 3-1, 3-2, and 3-4).

In the other assay, serum-starved COS7 cells transfected with pDEST-PNUTS at 0, 6, and 12 hour time points were probed for amounts of phosphorylated versions of key signaling molecules: p-mTor, p-PKCa/b, p-Stat3, p-Pten, p-Akt, p-Erk1/2, p-Mek1/2, b-actin (loading control), and PNUTS (Figure 3-4). Levels of p-Stat3, p-Pten, and p-Erk1/2 were visibly increased at the 12 hour time point, suggesting that *Ppp1r10* over-expression increases the signaling in these pathways compared to the untransfected COS7 cells.

## Discussion

If *Ppp1r10* is a classic oncogene involved in leukemia, then the CFU-GM colony assay should detect an increase in the size, change in morphology or increase in the number of colonies. *Ppp1r10* over-expression in *Nf1*+/+ fetal liver cells showed no difference in any these measures between *Ppp1r10* and the empty vector control. This suggests that, by itself, *Ppp1r10* is not an oncogene involved in leukemia. Either other cooperating genes are needed for cytokine independent growth, or *Ppp1r10* is a tumor suppressor gene instead (or, *Ppp1r10* is not involved

in leukemia at all). However, Le et al. 2004, showed that conditionally inactivated *Nf1* fetal liver cells are sensitive to low GM-CSF, have an altered morphology, and an increased number of colonies compared to *Nf1*+/+ fetal liver cells. This, confirmed *Nf1* as a tumor suppressor in myeloid leukemia. A similar assay could be used to test knockdown of *Ppp1r10* (see Chapter 5).

Western analysis of phosphorylated proteins allows correlation with actively proliferating cells. In serum starved COS7 cells, Western analysis showed a possible alteration in the MAPK pathway in PNUTS-positive cells. Specifically, p-MEK decreased at 6 hours and then increased at 12 hours post starvation. In addition, p-Erk1/2 was also increased 12 hours post starvation, suggesting that *Ppp1r10* may contribute to the regulation of the Ras->Mek->Erk pathway in COS7 cells. Specifically, increased the signaling in these pathways is positively association with cell proliferation and cell survival. However, these results are weak compared to classic oncogenes such as mutant H, K, or NRAS. For example, Schubbert et al. (2006) showed that germline KRAS mutants associated with Costello Syndrome and JMML, V14I and T58I, were defective in intrinsic GTP hydrolysis and displayed impaired responsiveness to GTPase activating proteins. This impaired GTP hydrolysis rendered primary hematopoietic progenitors very hypersensitive to growth factors, and deregulated signal transduction in a cell lineage–specific manner. These mutants, along with classic others such as codon 12, induce tumorigenic properties in the assays above.

These results indicate that *Ppp1r10* is not a classic oncogene in itself. It could however, be a tumor suppressor gene or cooperate with other genes (as a moderate oncogene or a tumor suppressor) to cause cancer or leukemogenesis. The serum starvation experiment showed that Ppp1r10 could be involved in the Ras-Mek-Erk pathway, or possibly Stat3 or Pten pathways.

The CFU-GM experiment definitively showed that over-expression of *Ppp1r10* did not alter the size, morphology or colony number as seen in other oncogenes like *NRAS*G12D.

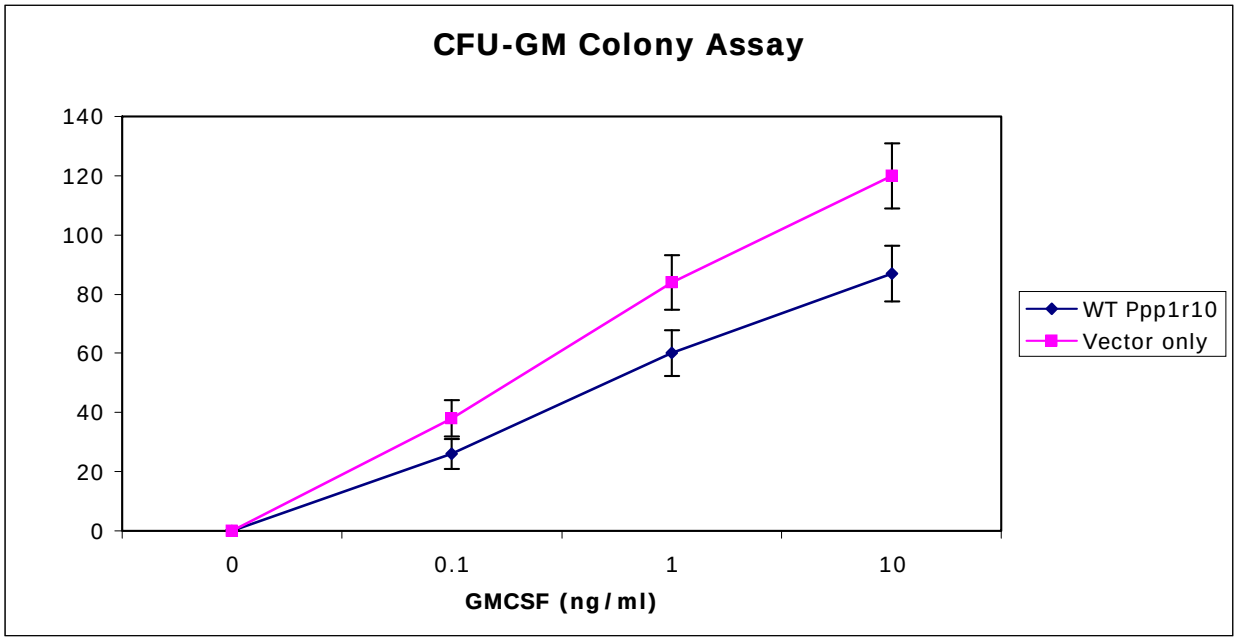


Figure 3-1. CFU-GM Colony assay of pMIG-PNUTS and pMIG in wild-type fetal liver cells.

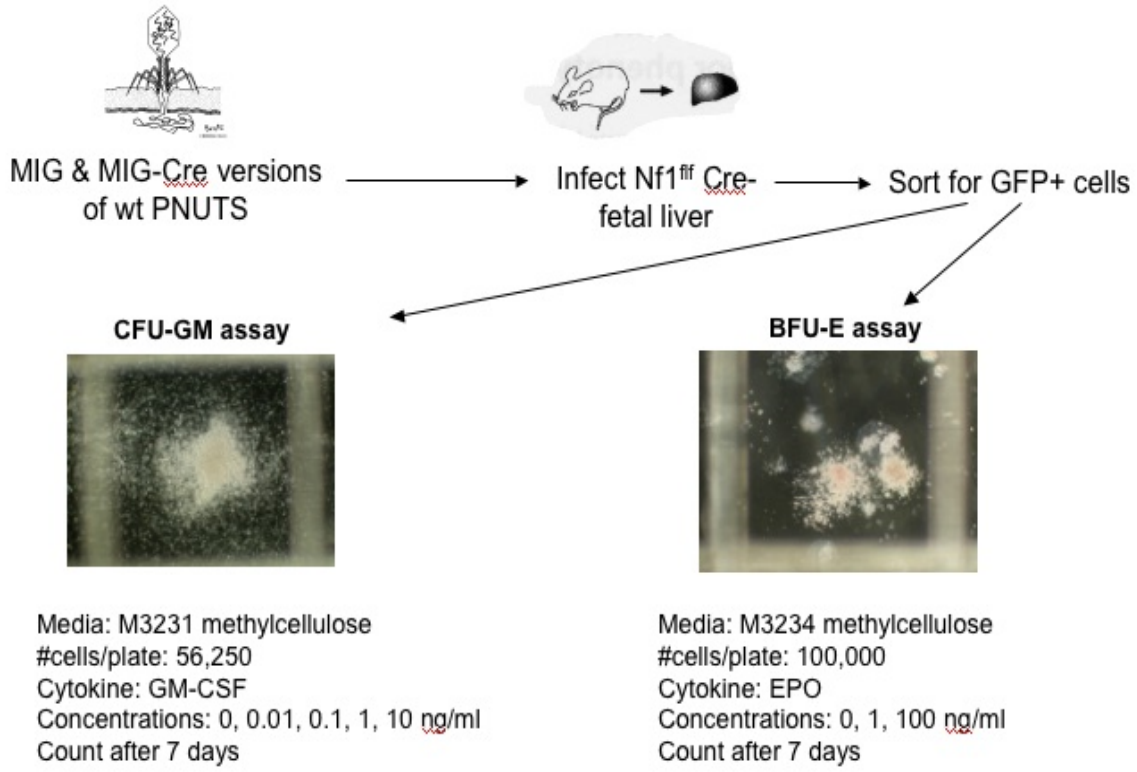


Figure 3-2. Experimental Design of Colony Formation Assay.

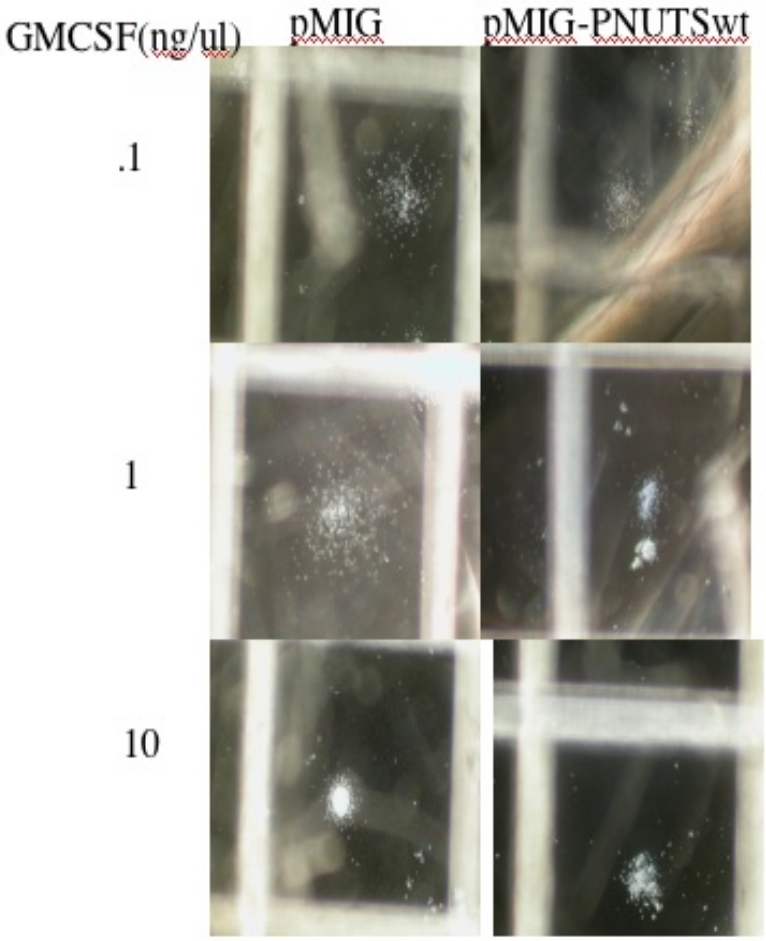


Figure 3-3. CFU-GM of wt PNUTS versus empty vector control.

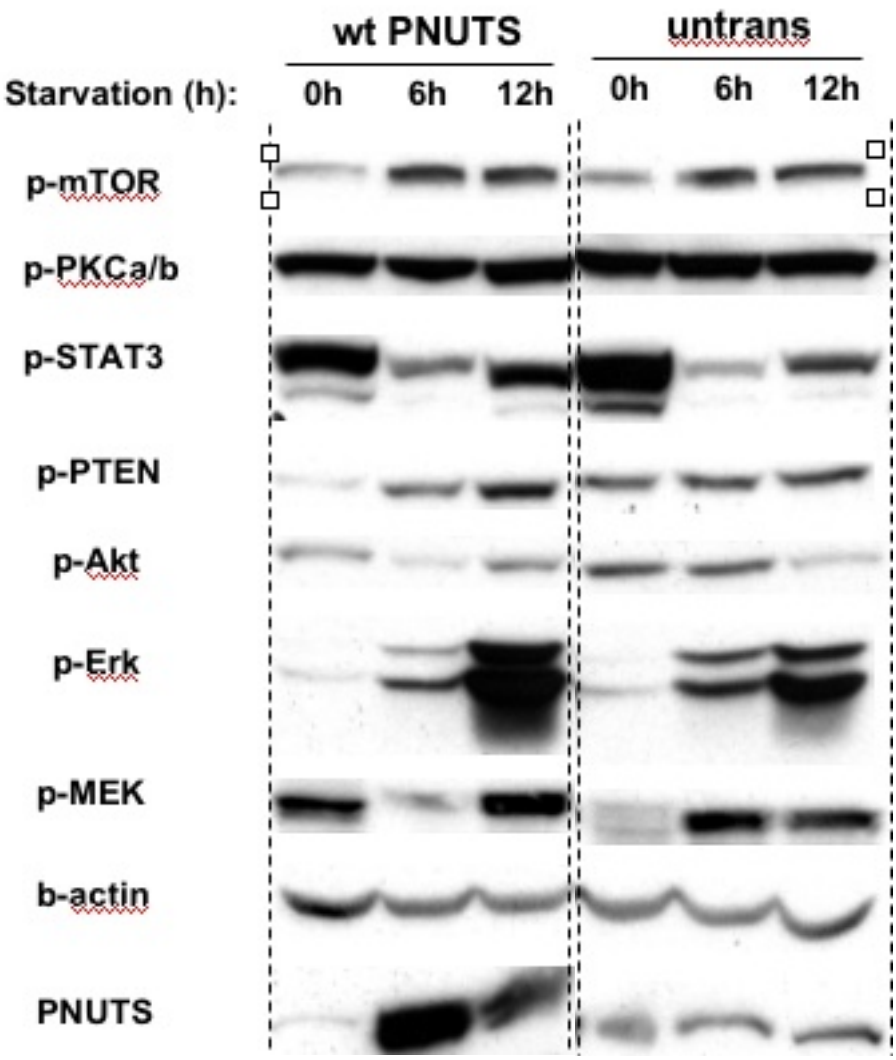


Figure 3-4. Transfection of pDEST-PNUTS in COS7 cells with serum starvation and probing signaling cascades.

# CHAPTER 4
# *PPP1R10* COOPERATES WITH *NF1* INACTIVATION TO CAUSE ACUTE MYELOMONOCYTIC LEUKEMIA IN A MOUSE MODEL

## Introduction

A mouse *Nf1* knockout (*Nf1* KO +/-) created in 1994 displays no characteristic NF1 features, but 11% of mice die of myelodysplasia by 17.7 to 27 months (Jacks et al., 1994). Largaespada et al. (1996) isolated 12.5dpc fetal liver cells from another, similar knockout mouse (Brannan et al., 1994), specifically the *Nf1* $^{fcr/fcr}$ (embryonic lethal 13.5dpc) and transplanted them into lethally irradiated mice. Upon bone marrow reconstitution by these donor cells, the mice developed a JMML-like phenotype, and their bone marrow cells were hypersensitive to granulocyte/macrophage stimulating factor, similar to that seen in JMML patients. It was then hypothesized that additional somatic cooperating mutations were required for progression to more acute disease. Thus, loss of the remaining NF1 allele is required for a child with NF1 to develop JMML (Largaespada et al., 1996; Bollag et al., 1996), but additional somatic mutations in other genes are necessary for progression to AML.

Since *in vitro* studies and previous research suggested that *Ppp1r10* was not an oncogene, I hypothesized that *Ppp1r10* could be a tumor suppressor whose loss cooperates with *Nf1* inactivation in AML. A previous student, Jessica Walrath, made a *Ppp1r10*+/- mouse on the 129S2 background, utilizing the Gene Trap Consortium library of ES cells (Walrath, 2006). The gene trap technology inserts a LacZ gene, which, through splicing, creates a null allele in the host gene. The Consortium mapped the locations of the "trapped" genes and made these available for a nominal fee. Jessica found that homozygosity for *Ppp1r10* knockout was a pre-implantation lethal genotype.

I crossed *Ppp1r10*+/- mice to *Nf1*+/- mice, and aged double heterozygotes for phenotype. I found that these mice become ill and died between 14 and 19 months, compared to 17-27 months

seen in *Nf1*+/- mice. The *Ppp1r10*+/-*Nf1*+/- mice developed acute myelomonocytic leukemia (AML-M4) versus the *Nf1*+/- mice, which developed the more chronic leukemia/JMML-like phenotype. The *Ppp1r10*+/- mice were also aged for phenotype and these mice developed a variety of single occurring solid tumors and became ill by 24 months of age. In addition to solid tumors, the majority developed splenomegaly and acute undifferentiated leukemia (AML-M0). This data support the hypothesis *Ppp1r10* cooperates with *Nf1* inactivation to cause AML, and can cause a slightly different acute leukemia by itself with a high penetrance but extended latency.

## Materials and Methods

### *Ppp1r10*+/- Mouse Construction

The *Ppp1r10*+/- mouse was constructed by a previous student and described elsewhere (Walrath, 2006).

### Breeding *Ppp1r10* Mice

129S2 *Ppp1r10*+/- mice were crossed to 129S1 *Nf1*+/- mice and the F1's were aged for phenotype. There were 21 *Ppp1r10*+/-, *Nf1*+/- (twelve females, nine males) mice aged for phenotype as well as 10 129S2 *Ppp1r10*+/- animals, and 5 129S1 *Nf1*+/- animals. *Ppp1r10*+/- mice were also bred for ten generations to move the knockout allele onto the 129S1 and C57BL/6 backgrounds.

### Pathology/Sectioning/H and E Stain

Mice were aged and observed for abnormal gait, hunching, lack of grooming, and or other signs of illness. Upon observation of illness, the mice were euthanized. Full necropsies were performed on the mice, and fixed paraffin-embedded sections were made from each tissue. These sections were made by the UF Molecular Pathology core and subsequently stained with Hematoxylin and Eosin.

**Blood Smears and Manual Counts**

At the time of observed illness, and euthanasia, five hundred microliters of blood from each mouse were used for standard blood smear analysis. The remaining blood was used to make DNA. Blood smear slides were stained with The Wright Geimsa stain kit (Fisher). Manual cytology counts were performed on blood smears slides from each mouse, counting 200 cells per field of view. In some cases, younger healthy mice had blood samples taken without euthanasia and analyzed by the UF Animal Care Services laboratory for complete blood count. This gave us an indication of whether the white blood cell count was increasing, well prior to death.

**Sudan Black Stain and MPO Stain**

Bone marrow sections were stained with Sudan Black kit for detection of myeloid cells. Paraffin embedded were de-paraffinized, hydrated with water and then stained with the Sudan Black Staining Kit (Sigma). Bone Marrow sections were immuno-stained using a primary mouse monoclonal for Myeloperoxidase (ABCAM mouse monoclonal 16686-50) and a secondary antibody, biotinylated horse anti-mouse IgG made in horse (Vector BA-2001). To de-paraffinize/hydrate paraffin sections, sections were heated in a 60 degree Celsius oven for 15 minutes. Then, the sections were placed in xylene twice for 2 minutes each time, 100% ethanol for 2 minutes, 95% ethanol for 2 minutes, two washes in 70% ethanol for 2 minutes, $H_20$ for 1 minute, and PBS for 5 minutes. Sections were then incubated in 0.3% $H_2O_2$ for 5 minutes. Before adding the primary antibody, the sections were incubated in 10% horse serum for 60 minutes (100ul NHS/1000ul PBS). The excess serum was blotted off and then the sections were incubated overnight with the primary antibody, MPO mouse mAB at 1:100 at 4 degrees Celsius. Before addition of biotinylated horse anti-mouse IgG at 1:100 (10ul of secondary AB, 10ul normal horse serum, 1000ul of PBS), sections were washed for 5 minutes in PBS buffer. The biotinylated anti-mouse IgG was added for 45 minutes at RT and then sections were rinsed in 1%

horse serum for 15 minutes. Finally, the sections were incubated for 30 minutes in vectastain reagent, then PBS for 5 minutes, DAB or Nova Red was added, and the slides were rinsed in water, counterstained with hematoxylin, dehydrated with xylene, and slide coverslips mounted with permanent mounting media.

**Flow Cytometry**

Bone marrow cells were characterized by four-color flow cytometry. Five hundred thousand bone marrow cells were re-suspended in PBS/ .1% BSA, placed into tubes, and incubated with the appropriate antibodies. Three-antibody combinations were used for analysis: (1) PE-Ly6g (Abcam, ab24884), APC-CD11b (BD, 553312), Pacific blue c-kit (Biolegend, 105820); (2) PE-Ly6g, APC-CD11b, Pacific Blue F4/80 (CALTAG, MF48028); (3) Percp-CD45 (BD, 557235), APC-Ter119 (BD, 557909), PE-CD71 (BD, 553267); (4) APC-CD19 (Biolegend, 115511), PE-CD8a (Biolegend, 100707), Pacific Blue-CD3 (Biolegend, 100214); (5) APC-TCRBeta (Biolegend, 109212), PE-CD34 (Biolegend, 119307) (6) PE-CD13 (BD, 558745), AexaFluor647-CD68 (AbD serotec, MCA1957A647); (7) Unstained Control. All antibodies for flow were used according to the manufacturers recommended instructions. Flow cytometry was performed on a BD FACS machine (BD Biosciences) with the help from UF core director Neal Benson. Flow cytometry analysis was performed using FCS Express 3.0 software.

**Nucleic Acid Extraction**

DNA and RNA samples were prepared from blood, bone marrow, tissues and tumors as previously described in Thomson and Wallace (2002). In some cases there were not enough cells for RNA extraction, and only DNA was made.

**Loss of Heterozygosity Analysis**

50ng of DNA from tumors, bone marrow and blood were PCR amplified with the 3-primer system using Pko2Ra, Pko2fb and lac2 to simultaneously genotype the mutant and wild-type

allele in *Ppp1r10* (Appendix A). Similiarly, the *Nf1* mutant and wildtype alleles were also genotyped with NF31a, NF31b, and NeoTkp (Appendix A; Brannan et al. 1994). To PCR amplify *Ppp1r10*: 2.5ul of 10X HotMaster Buffer (Eppendorf), 200umol dNTP, 60ng Pko2ra primer, 60 ng Pko2fb primer, 40ng Lac2 primer, 1.25ul DMSO, 16.325ul $H_20$, 0.125ul Hotmaster Taq (Eppendorf). The following cycling conditions were used for *Ppp1r10*: 1 cycle of 95°C for 15 minutes, 35 cycles of 95°C for 30 seconds, 63°C for 45 seconds, 72°C 45 seconds; and a final extension of 72°C for 10 minutes. To PCR amplify *Nf1*: 2.5ul of 10X Hotstart Buffer (Qiagen), 200umol dNTP (Invitrogen), 65ng of NF31a/NF31b/NeoTkp, 2.5mM $MgCl_2$, 18ul of $H_20$, .125ul of Hotstart Taq polymerase (Qiagen). The following cycling conditions were used for *Nf1*: 1 cycle of 96°C for 15 minutes, 40 cycles of 95°C for 30 seconds, 55°C for 30 seconds, 72°C 1 minute; a final extension of 72°C for 10 minutes. These PCR products were run on an 8% native polyacrylamide gel with controls (germline DNAs), stained with ethidium bromide, to observe whether there was loss of the wildtype allele in *Nf1* and *Ppp1r10*. The *Ppp1r10* PCR product sizes of wildtype/mutant alleles should be 103bp/400bp, and the *Nf1* wildtype/mutant alleles should be 128bp/95bp respectively.

## Results

To test if *Ppp1r10* cooperates with *Nf1* inactivation to cause acute leukemia in mice as a possible tumor suppressor, *Ppp1r10*+/-(129S2) mice were crossed to *Nf1*+/- (129S1) and aged for phenotype. The *Ppp1r10*+/-*Nf1*+/- mice on average died from AMML (AML-M4) at 16.5 months of age (range 14 to 19 months), versus MPD at average 19.5 months of age seen in *Nf1*+/- mice (range 19 to 20 months). Two of the *Ppp1r10*+/-*Nf1*+/- mice died of pulmonary hemmorhage and were not included in the analysis. In addition, the *Ppp1r10*+/- mice on average died of AML (AML-M0) at 23.5 months (range 23-24 months) (Table 4-1). These are illustrated

in the Kaplan Meier survival graph (Figure 4-1). Eighty percent of *Ppp1r10*+/- *Nf1*+/- mice developed AMML, 15% developed MPD, and 5% developed myeloid hypoplasia (Figure 4-14, Table 4-2). At time of death, *Ppp1r10*+/- *Nf1*+/- mice with AMML disease had an average white blood cell count of 15,234 compared to 9187 in *Nf1*+/- mice (Table 4-3, 4-4). The average percentage of blast cells observed in the peripheral blood of these double knockout mice was 42.9% compared to 8.94% seen in the *Nf1*+/- mice, with 30% being the clinical cut-off for "acute" (Table 4-3, 4-4). These mice developed splenomegaly and the leukemic cells had also invaded other organs: kidney, eye-lid, liver, lung, gall bladder and lymph node. By peripheral blood smear analysis, the blast cells appeared to be immature monocytes and immature granulocytes of the granulocyte/macrophage lineage, suggesting that the mutation's effect is at the CFU-GM pathway (Figure 4-14, 4-26). Other than AMML, these mice also developed more (and somewhat different) solid tumors than originally reported in *Nf1*+/- mice (Jacks et al. 1994). These tumors included hemangiosarcomas of the uterus and ovary in 3 out of 19 mice, and a proliferative mesenchymal process of the skin in 2 out of 19 mice. This latter finding appears to consist of leukemic and immature mesenchymal cells (Figure 4-8, 4-5). Other solid tumors in the double heterozygotes that were only observed in one each included: lung adenocarcinoma, hepatocellular carcinoma, granulocytic sarcoma, and squamous cell carcinoma (Figure 4-2, 4-4, 4-15, and 4-16). In comparison, *Nf1*+/- mice also develop lung adenocarcinomas and hepatocellular carcinomas. However, the double heterozygotes did not develop lymphomas or adrenal tumors that are observed in the *Nf1*+/- mice as well. Overall, 55 percent of the mice had solid tumors compared to the reported 25 percent of the 129S inbred background and had a reduced latency (Jacks et al 1994; Bronson et al 1990). However, the cause of death our mice

stemmed from a dysfunctional hematopoietic system typical of acute leukemia (anemia, bleeding).

*Ppp1r10*+/- (129S2) mice lived to about 2 years of age, when they became ill and had to be euthanized. Seven of eight of these mice had acute undifferentiated leukemia (AML-M0) and splenomegaly, with infiltrating immature neutrophils and giant multinucleated cells (Figure 4-12, Table 4-1). The peripheral blood smear analysis showed an increase in white blood cells, and blast cells. On average 16, 265 white blood cells and 44% blasts (Table 4-3, 4-4). The bone marrow histology showed irregularly shaped cells that could not be distinguished as myeloid or lymphoid, in origin, and as well showed a 2-fold decrease in the percentage of granulocytes compared to *Nf1*+/-*Ppp1r10*+/-mice (Figure 4-12, Table 4-3). This result suggests that loss of one allele of *Ppp1r10* affects the hematopoietic system at an earlier precursor than that seen in the *Nf1*+/-*Ppp1r10*+/- (CFU-GM). Besides leukemia, the same seven heterozygous mice developed solid tumors, one each of the following: myoepithilioma of the salivary gland, myoepithelioma of the thymus, hepatic hemangiosarcoma, pulmonary adenocarcinoma, pituitary tumor, and leiomyosarcoma (Figure 4-6, 4-7, 4-8, 4-9, 4-10, 4-11). Our heterozygous *Ppp1r10* mice showed an increased rate of tumorigenesis, with over 75 percent of the mice developing tumors compared to 25 percent of inbred 129S mice (Jacks et al. 1994).

To determine the subtype of acute leukemia, bone marrow sections were stained with Sudan Black or mouse monoclonal myeloperoxidase antibody. Sudan Black stains acute myelogenous leukemia (AML-M1, M2, M3, M6) strongly, weakly stains acute myelomonocytic leukemia M4 (AMML), and positively stains auer rods. However, Sudan Black does not stain AML-M0, AML-M7, AML-M5 and acute lymphocytic leukemia (ALL). Myeloperoxidase, on the other hand, stains acute myelomonocytic leukemia (AML-M4) and auer rods. This antibody

does not recognize AML-M5, AML-M7, and ALL. The *Ppp1r10*+/-*Nf1*+/- mice are thus positive for acute myelomonocytic leukemia (AML-M4) and *Ppp1r10*+/- mice have acute undifferentiated leukemia (AML-M0) (Figure 4-19).

Tumor suppressor genes typically lose the remaining normal allele somatically in tumors, often via large deletions, to fit Knudson's 2-hit hypothesis (Knudson et al. 1971). These somatic deletions can be detected in tumor DNA by loss of heterozygosity (LOH) analysis comparing the presence of alleles in germline versus tumor at informative polymorphisms. To test for possible LOH at both genes, we initially tried genotyping for the only known heterozygous polymorphism, the engineered mutations that define these mice. PCR-genotyping of *Nf1* and *Ppp1r10* was performed in available DNA from tumors, blood and bone marrow. The PCR products were visualized ethidium bromide to observe relative ratio of mutant to wildtype allele, in tumors, as compared to the germline. We were unable to get consistent results, indicating that these 3-primer based systems are unreliable for a quantitative measure such as LOH (Figure 4-17, 4-18).

To further confirm leukemia subtypes (AML-M4 for *Ppp1r10*+/-*Nf1*+/-, MPD for *Nf1*+/- and AML-M0 for *Ppp1r10*+/-), flow cytometry was performed on bone marrow cells extracted at the time of death using hematopoietic antibodies. The Gr1 and Mac1 FACS populations usually display increases in granulocytes and monocytes in AML-M4. The results showed an abnormal $Gr1^{+}/Mac1^{+}$ population as well as a $Gr1^{(low\ to\ med)}/Mac1^{+}$ population in *Ppp1r10*+/-*Nf1*+/- bone marrow compared to control, *Nf1*+/-, and *Ppp1r10*+/- bone marrow (Figure 4-20). These two populations, $Gr1^{+}/Mac1^{+}$ and $Gr1^{(low\ to\ med)}/Mac1^{+}$, are characteristic of granulocyte and monocyte populations, respectively, and thus results confirmed AML-M4. In addition, *Ppp1r10*+/-*Nf1*+/- bone marrow displayed slight increases in c-kit and F-4/80, further confirming

that the CFU-GM point is affected in these mice (Figure 4-21, 4-22). However, although no alteration was observed in the B-cell pathway in *Ppp1r10*+/-*Nf1*+/- bone marrow, *Ppp1r10*+/- bone marrow displayed an increase in the B-cell marker CD19 (Figure 4-23). Alterations were also observed in TCRbeta-positive populations for both *Ppp1r10*+/-*Nf1*+/- and *Ppp1r10*+/-, suggesting that *Ppp1r10* affects the myeloid and lymphoid compartment and (Figure 4-24, 4-25). This suggests that Ppp1r10 may be a possible hematopoietic stem cell gene (Figure 4-26).

## Discussion

Creation of a *Ppp1r10* knockout mouse, and crossing it to the *Nf1* knockout mouse, has led to the discovery of a new cancer gene involved in solid tumor formation and myeloid leukemia. Immunostaining and flow cytometry showed that *Ppp1r10*+/-*Nf1*+/- mice develop acute myelomonocytic leukemia (AML-M4) with high penetrance by 20 months, and about 75 percent of *Ppp1r10*+/- mice develop acute undifferentiated leukemia (AML-M0) by age 24.

AML was classified into 7 subtypes (M0-M7), at a conference by the french, british, and american doctors in the 1970's, called the FAB classification system (http://www.cancer.org). AML-M0, undifferentiated acute myeloblastic leukemia, affects 5% of AML patients and has a worse prognosis. AML-M1, acute myeloblastic leukemia with minimal differentiation, affects 15% of AML patients and has an average prognosis. AML-M2, acute myeloblastic leukemia with maturation, affects 25% of patients and has a better prognosis. These patients often have translocations involving chromosome 8 and 21. AML-M3, acute promyelocytic leukemia, affects 10% of AML patients and has the best prognosis of all AML subtypes. These patients often also have translocations of chromosomes 15 and 17. AML-M4, acute myelomonocytic leukemia, affects 20% of AML patients and has an average prognosis. These patients often have an inv (16) genetic abnormality as well. There is another M4 subtype, M4Eos, acute myelomonocytic leukemia with eosinophilia that affects 5% of AML subtypes and has a better prognosis. AML-

M5, acute monocytic leukemia, affects 10% of patients and has an average prognosis. These patients also often have translocations involving chromosomes 9 and 11. AML-M6, acute erythroid leukemia, affects 5% of AML patients and has a worse prognosis for these patients. The last subtype, AML-M7, acute megakaryoblastic leukemia affects 5% of AML patients and has a better prognosis. In addition, 1 out of 3 AML patients have *FLT3* mutations.

Previous research has shown that a knockin allele for inv (16) predisposes mice to impaired hematopoiesis however administering ENU mutagenesis to these mice is necessary to cause an AMML-like disease. These mice had partial myelomonocytic differentiation in a small percentage of cells in most mice. The majority of these cells are ckit+, Gr1-, Mac1-, B220-, and CD3- (Castilla et al. 1999). However, two cooperation studies with inv (16) with either loss of *ARF* or a tandem duplication in *FLT3* (FLT3-ITD) caused AML without ENU mutagenesis. The inv (16); *Arf*-/- mice develop AML and the mutations' effect is on immature myeloid cells, staining positive for c-kit and negative for Sca1. Peripheral blood analysis of these mice shows basophile and eosinophil granules in addition to a slight monocytic component (Moreno-Miralles et al. 2005). In addition, inv (16) with *FLT3*-ITD mice develop AML with an effect on immature myeloid cells (myeloblasts and promyelocytes), which are c-kit+ and Sca1- (Kim et al. 2008). In contrast, our model, *Ppp1r10*+/- *Nf1*+/- mice have an abnormal granulocyte/macrophage population and an abnormal monocytic population of cells. This phenotype is a more mature myeloid phenotype than the immature myeloid phenotype observed in the previous mouse models.

There are no existing mouse models for AML-M0 as observed in the *Ppp1r10*+/- mice. It is hypothesized that the *Ppp1r10*+/- mice have other genetic alterations in genes that cooperate

with *Ppp1r10* to cause AML-M0. These could be targets of PP1, like p53 or RB1 or genes unrelated to the PP1 pathway.

All of the data suggests that *Nf1* has an antagonizing effect on *Ppp1r10*. *Nf1* heterozygous bone marrow effects mature granulocytes and macrophages and *Ppp1r10* heterozygous bone marrow has neither lymphoid or myeloid morphology, suggesting an early hit in the hematopoietic pathway. Therefore, *Nf1/Ppp1r10* cooperate to cause an intermediate hit in hematopoeisis, CFU-GM. However, the effect on *Nf1* is synergistic since, the *Ppp1r10* mutation allows leukemic transformation from MPD seen in *Nf1*+/- mice to AML-M4 in *Ppp1r10*+/-*Nf1*+/-.

In addition to AML-M4, fifteen percent of *Ppp1r10*+/-*Nf1*+/- mice developed hemangiosarcomas and ten percent developed a proliferative mesenchymal process of the skin. Other solid tumors included squamous cell carcinoma, granulocytic sarcomas, lung adenocarcinoma and hepatocellular carcinomas. However, the *Ppp1r10*+/-*Nf1*+/- mice did not develop adrenal tumors, MPNSTs or lymphomas as previously observed in *Nf1*+/- mice (Jacks et al. 1994). The *Ppp1r10*+/- mice, on the other hand, showed some different solid tumors: myoepithelioma of the thymus and salivary gland, hepatic hemangiosarcoma, pulmonary adenocarcinoma, pituitary tumor, and leiomyosarcoma. These data suggest that loss of at least one *Ppp1r10* and *Nf1* allele cooperate to affect myeloid compartment development at slightly different stages than either gene alone.

Other known tumor suppressors that are proposed to be at least indirectly related to PP1 include *p53* and *RB1* (Lee et al 1992; Jacks et al. 1992; Clarke et al 1992). Mice deficient for p53 (homozygous for knockout allele) are developmentally viable, however approximately a fourth of mice develop hemangiosarcomas, and 80% develop lymphomas (Donehower et al.

1992). In contrast, mice deficient for *RB1* die embryonically at day 16, and their hematopoietic system (myeloid compartment) is abnormal, showing increases in immature erythrocytes. Heterozygous *RB1* mice have an increase in pituitary tumors (Lee et al 1992; Jacks et al. 1992; Clarke et al 1992). In addition, other hemangiosarcoma mouse models have suggested a p53-related mechanism of tumorigenesis. For example, one mouse model lacking *p53*, + one *Ink4c* or *Ink4d* allele, develops hemangiosarcomas in over 50 percent of mice (Zindy et al. 2003). Another model, *p18*-/-, *p53*-/- displays a range of tumor types similar to that also observed in our mice: hepatocellular carcinoma, testicular carcinoma, hemagiosarcoma, leiomyosarcoma, fibrosarcoma, and osteosarcomas (Damo et al. 2005). In comparison, *Ppp1r10*+/- *Nf1*+/- phenotype includes affected hematopoeitic system, increases in hemagiosarcomas, proliferation of leukemic cells in the skin, and a range of non-recurring tumor types. This suggests that the tumor mechanism in the double heterozygotes involves *p53* and or *Rb* pathways and further investigation is necessary.

Since the 3-primer systems are unreliable for LOH analysis of tumors in our mice, Southern blots will be performed on DNA from any available tumors or bone marrows. It is expected that the remaining *Nf1* allele is lost in these mice for tumorigenesis since the previous *Nf1* mouse model has shown tumors to be *Nf1*-/- (Jacks et al. 1994). It is unknown whether *Ppp1r10* will be heterozygous or homozygous in the tumors or bone marrow. However, it is believed that *Ppp1r10* will be homozygous in the bone marrow due to tumor heterogeneity and lack of a detectable mRNA transcript in bone marrow. Recently, several papers have reported that cooperating haploinsufficient tumor suppressors in the mouse can be sufficient reduction in protein function to contribute to tumorigenesis (Kamimura et al. 2007; Vives et al. 2006; Moreno-Miralles et al. 2005; Ma et al. 2005).

This work provides evidence that *Ppp1r10* is a new cancer gene, most likely a tumor suppressor gene, and cooperates with *Nf1* inactivation to cause AML-M4 and other cancers. Future work will focus on defining the pathways that are deregulated in these cells in order to develop targeted drug therapy for patients. This is particularly important since AML is a very refractory cancer and few long-term effective treatments exist.

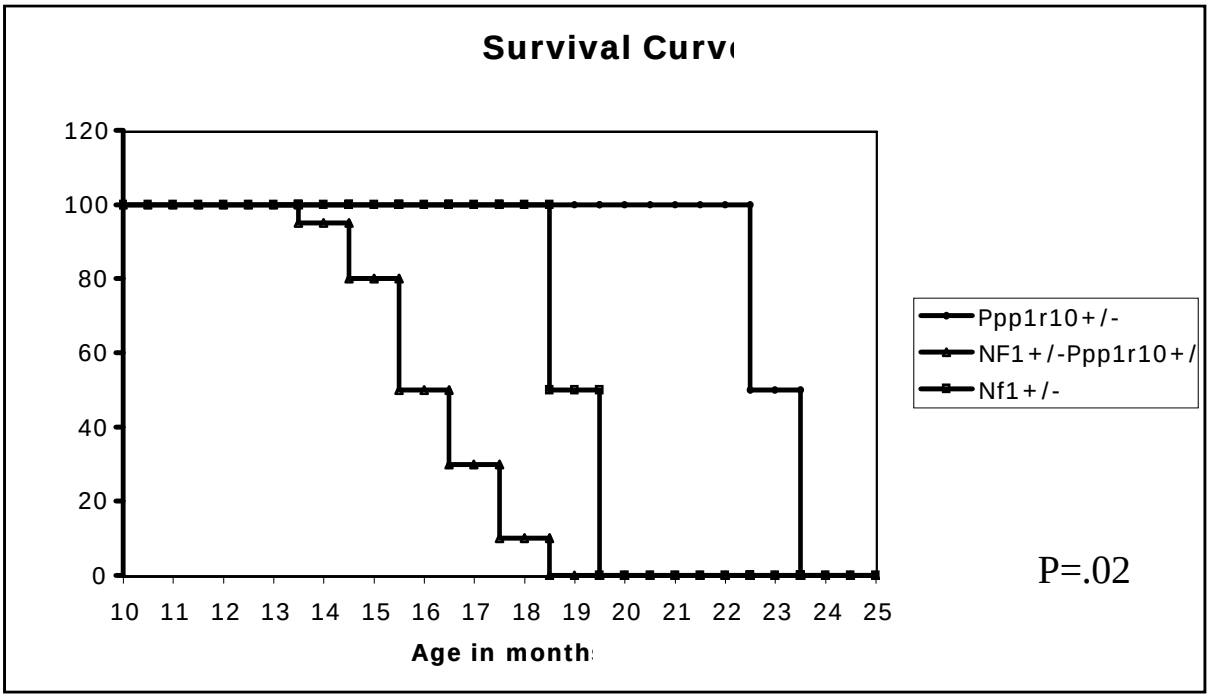


Figure 4-1. Kaplan-Meier survival curve for *Nf1*+/-*Ppp1r10*+/-, *Ppp1r10*+/-, and *Nf1*+/- mice.

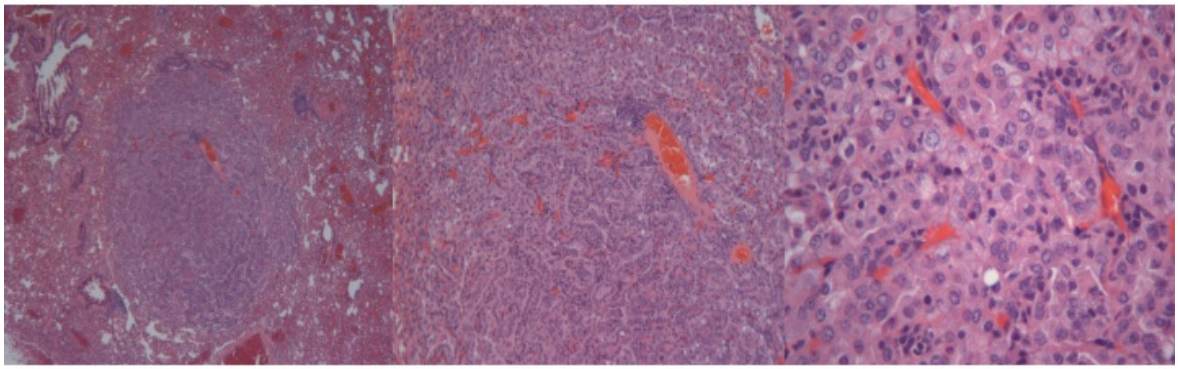

Lung Adenocarcinoma 40X, 100X, and 400X

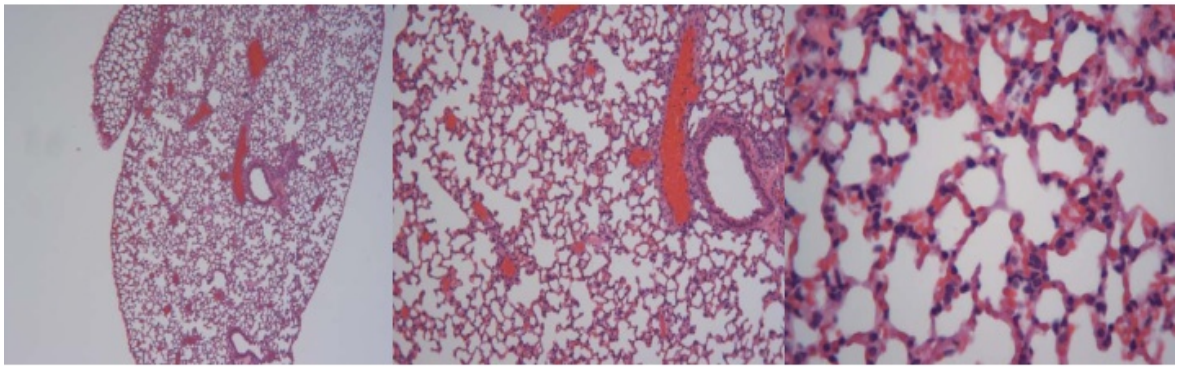

Normal Lung 4X, 10X, and 40X

Figure 4-2. H and E stain sections from *Nf1*+/- *Ppp1r10*+/- pulmonary adenocarcinoma and mouse normal lung.

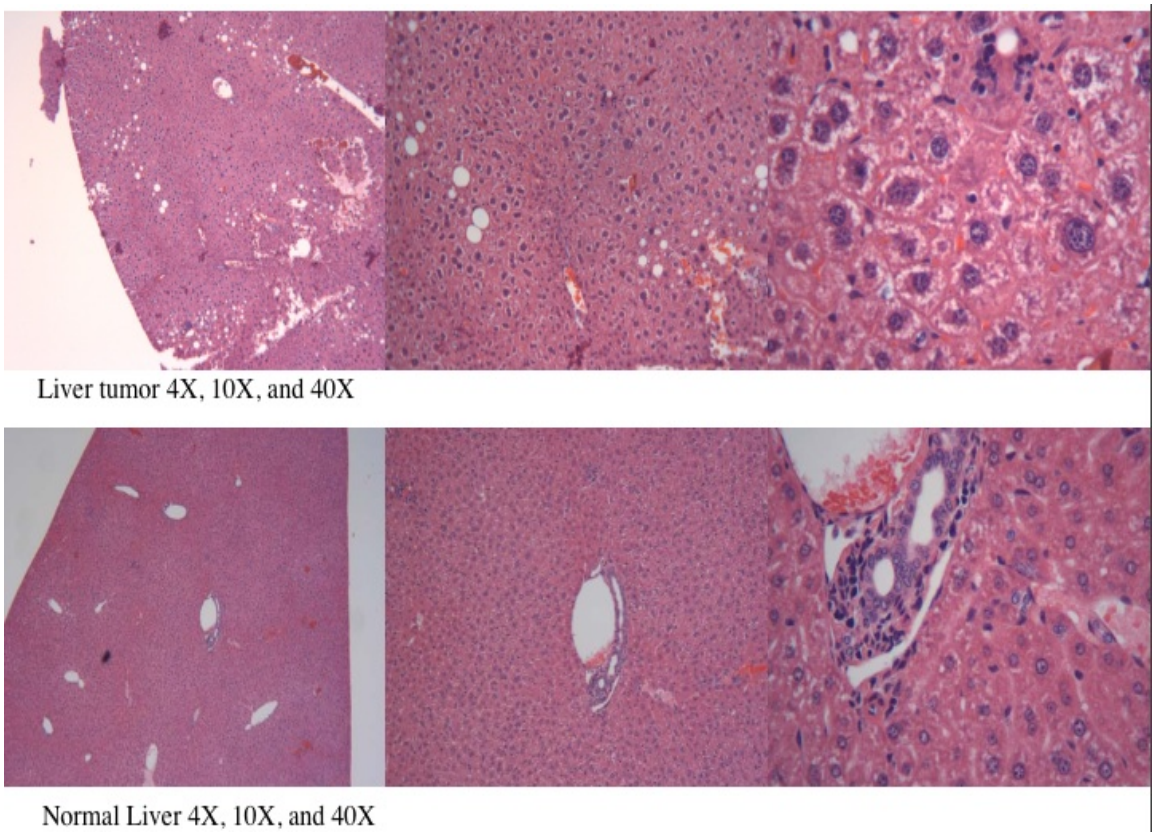


Figure 4-3. H and E stain of sections from *Nf1*+/-*Ppp1r10*+/- liver tumor and mouse normal liver.

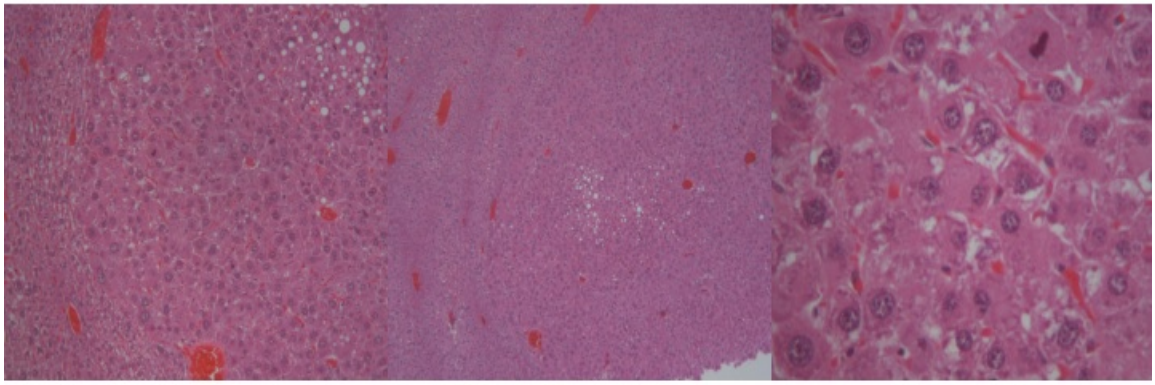

Hepatocellular carcinoma, 40X, 100X, 400X

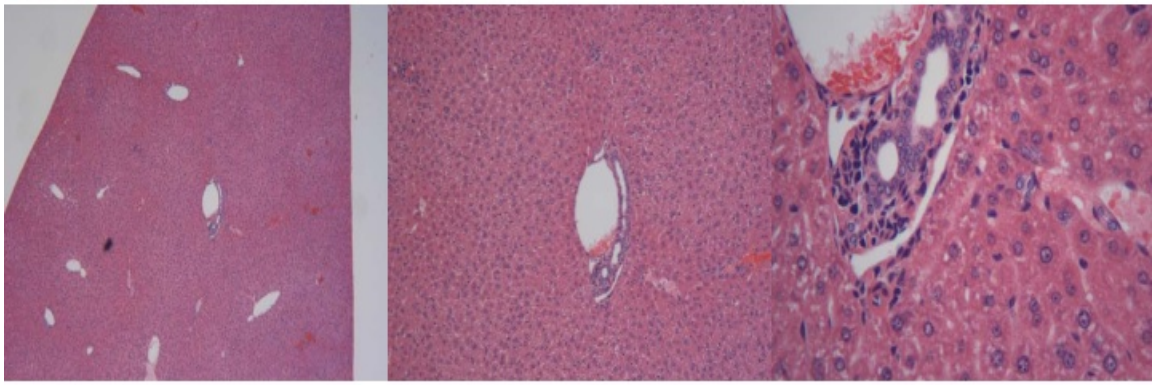

Normal Liver 4X, 10X, and 40X

Figure 4-4. H and E stain of sections from *Nf1*+/-*Ppp1r10*+/- hepatocellular carcinoma and normal liver.

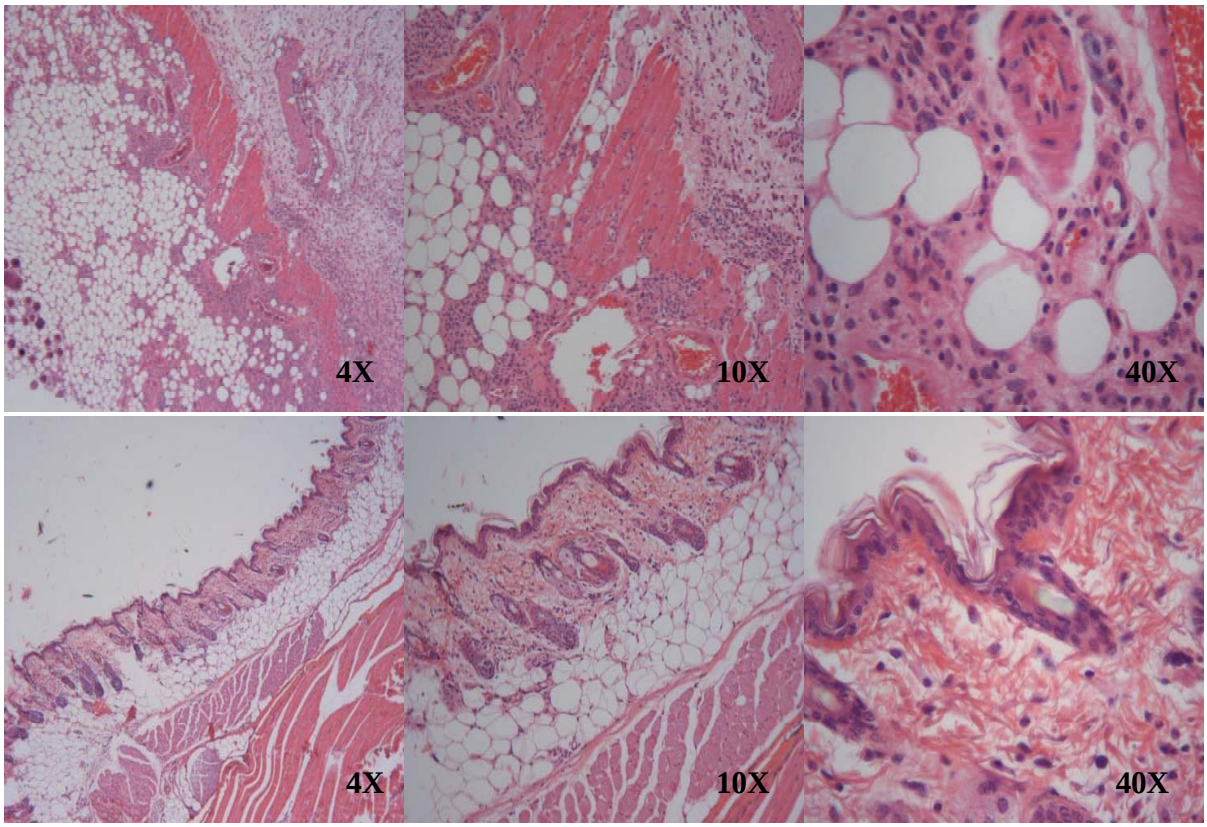


Figure 4-5. H and E stain of sections from *Nf1*+/- *Ppp1r10*+/- proliferative mesenchymal process of the skin (top) and normal skin (bottom).

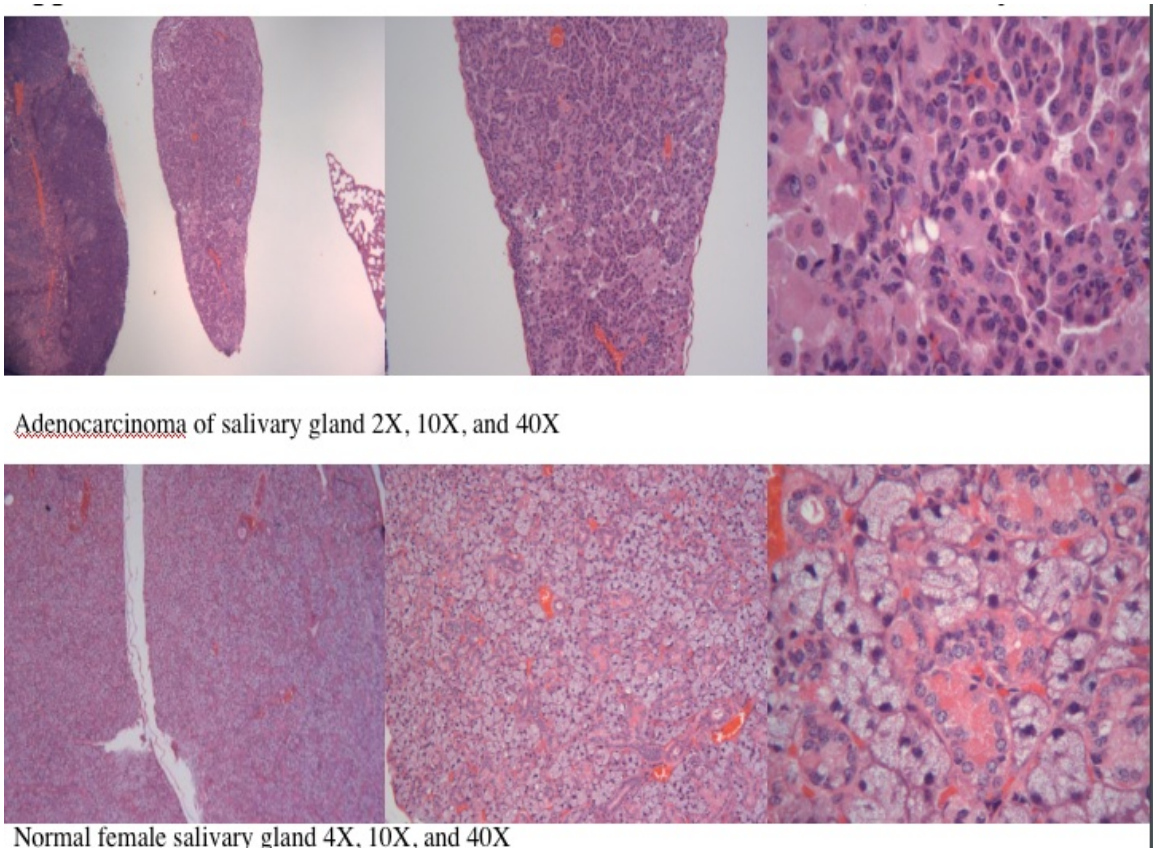


Figure 4-6. H and E stain of sections of *Ppp1r10*+/- adenocarcinoma of the salivary gland and normal salivary gland.

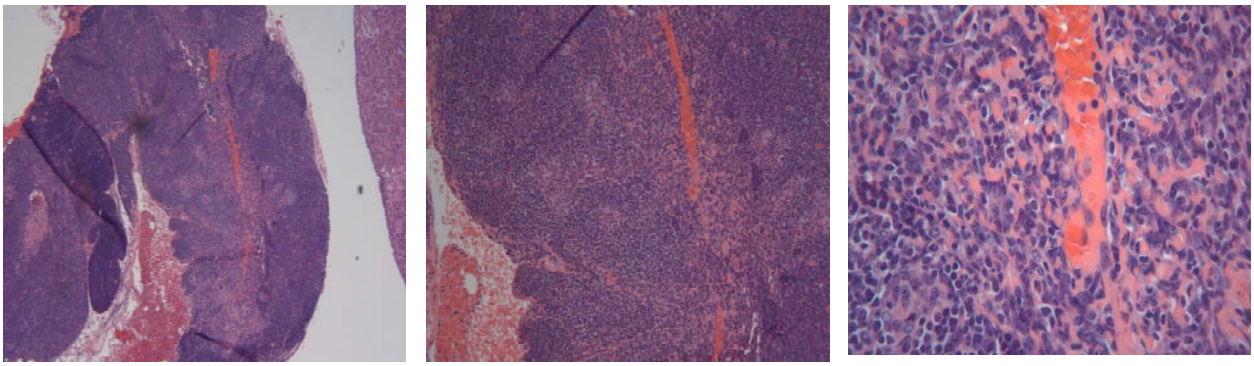

Myoepithelioma 4X, 10X, and 40X

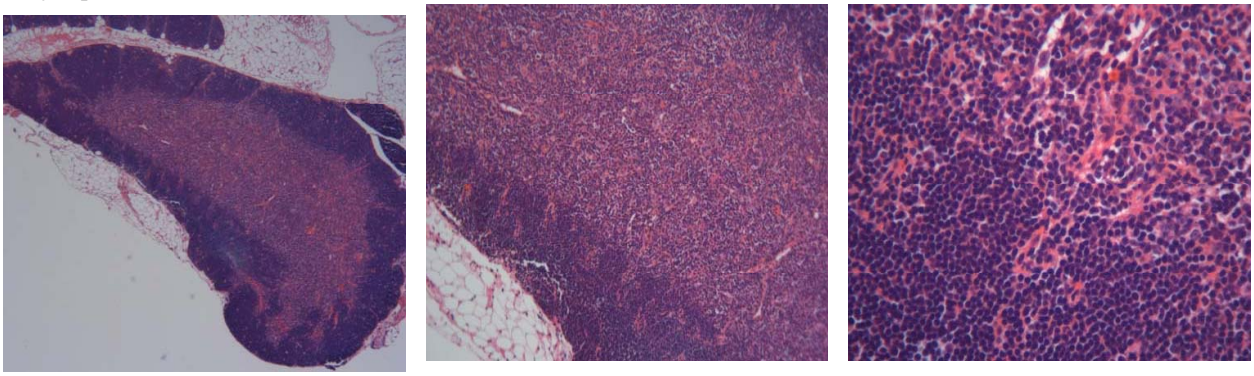

Normal Thymus 4X, 10X, and 40X

Figure 4-7. H and E stain of sections of *Ppp1r10*+/- myoepithelioma, thymus and normal thymus.

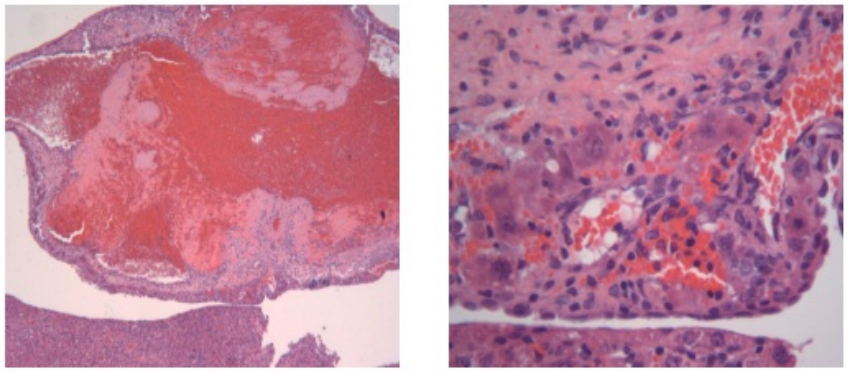

Hepatic hemagiosarcoma 4X, 40X

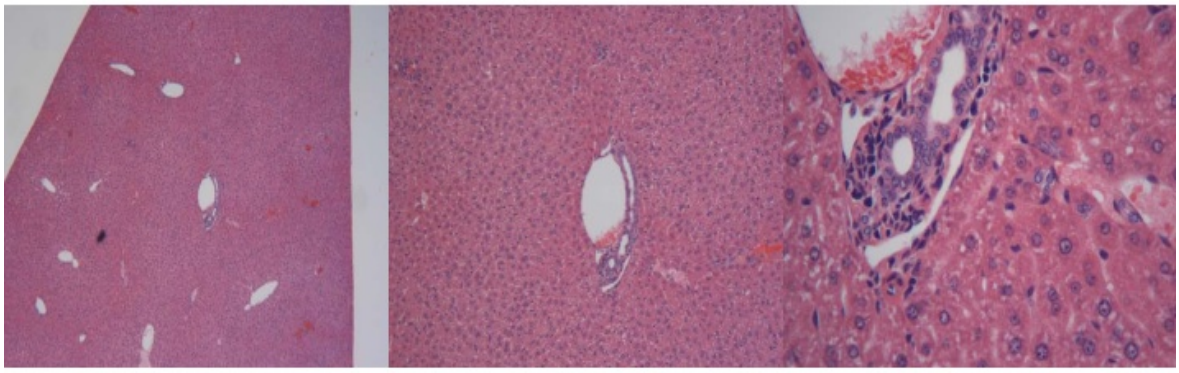

Normal Liver 4X, 10X, 40X

Figure 4-8. H and E stain of sections from *Ppp1r10*+/- hemangiosarcoma and normal liver.

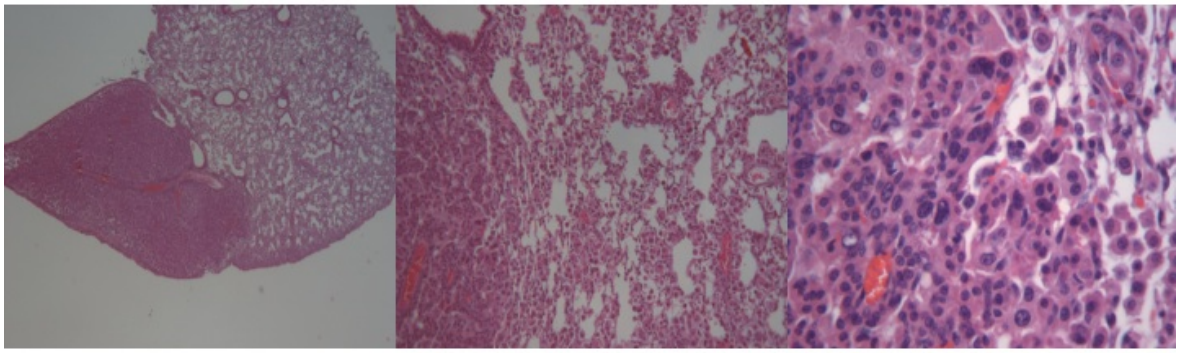

Pulmanary Adenocarcinaoma 4X, 10X, and 40X

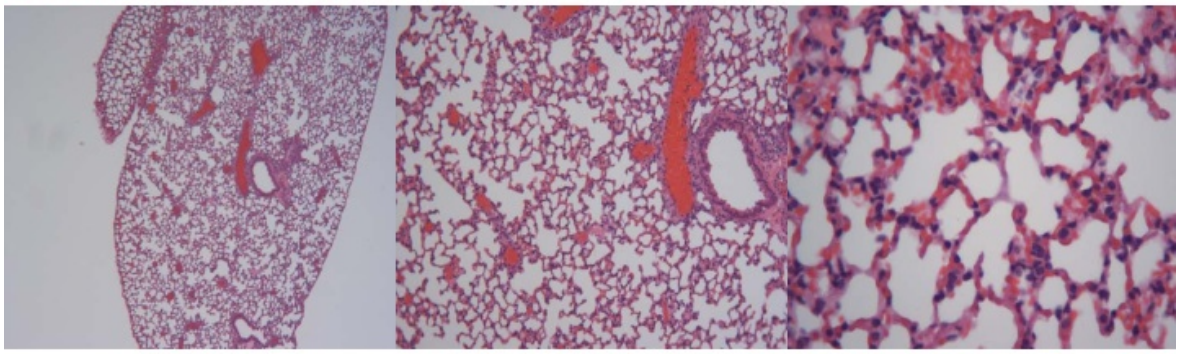

Normal Lung 4X, 10X and 40X

Figure 4-9. H and E stain of sections from *Ppp1r10*+/- pulmonary adenocarcinoma and normal lung.

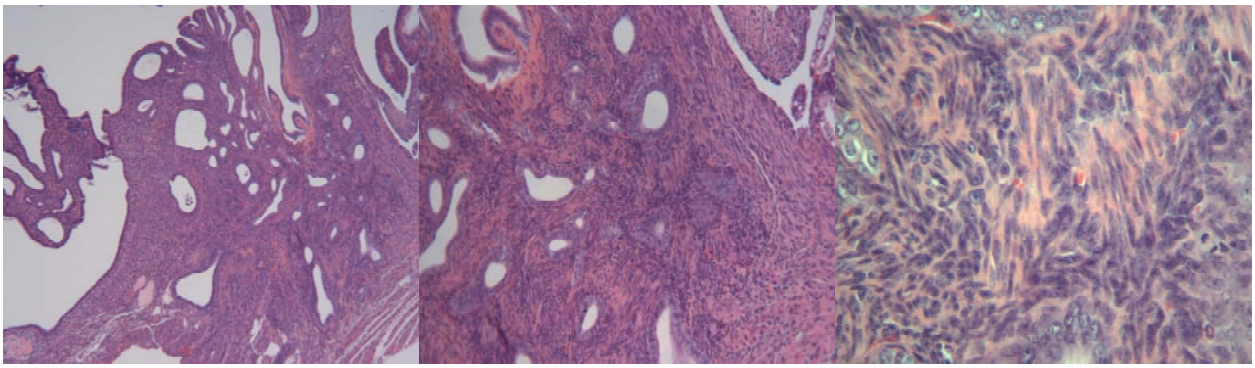

Leiomyosarcoma 4X, 10X, and 40X

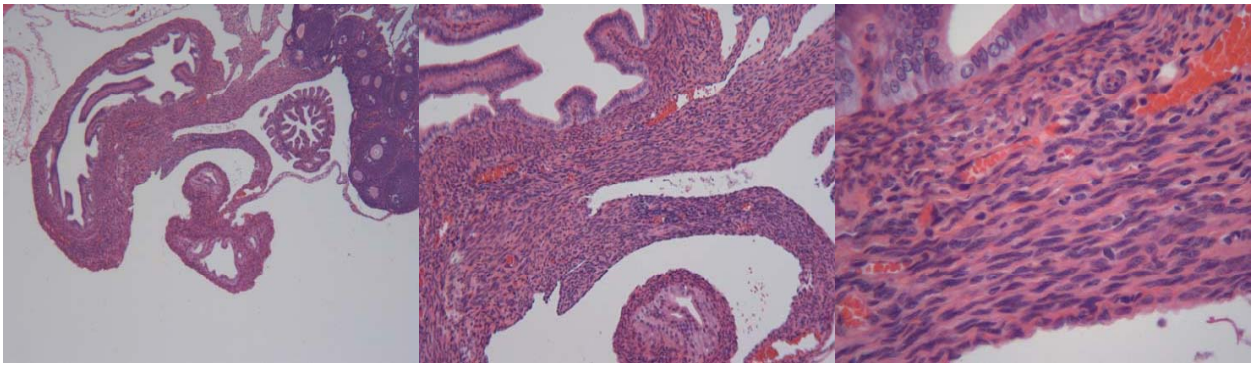

Normal Uterus 4X, 10X, and 40X

Figure 4-10. H and E stain of sections from *Ppp1r10*+/- leiomyosarcoma and normal uterus.

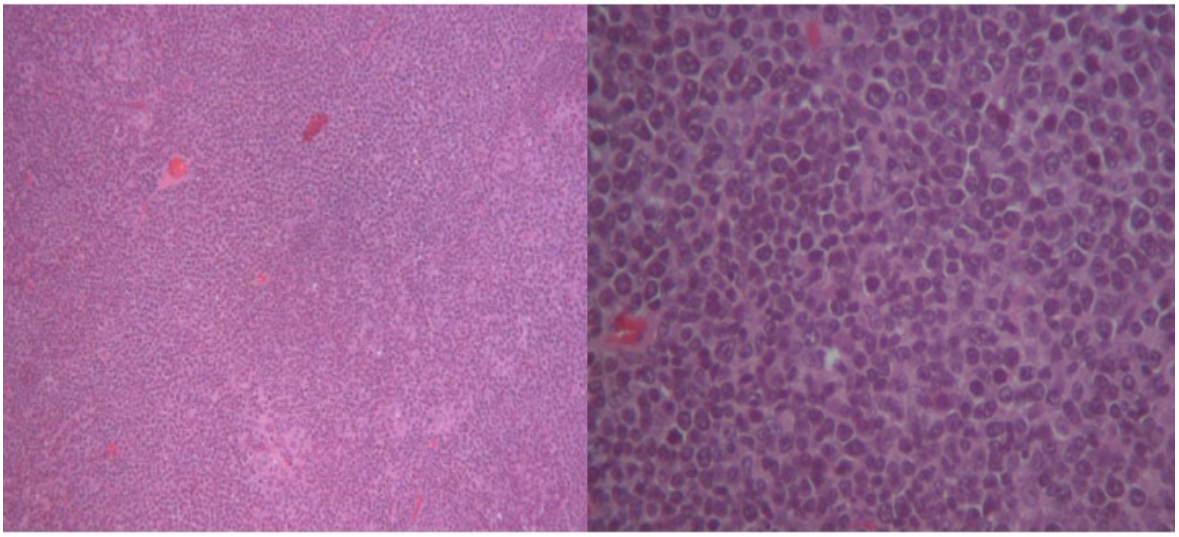

Figure 4-11. H and E stain of sections from *Ppp1r10*+/- chloromas, showing myeloid expansion, 10X (left) and 40X (right).

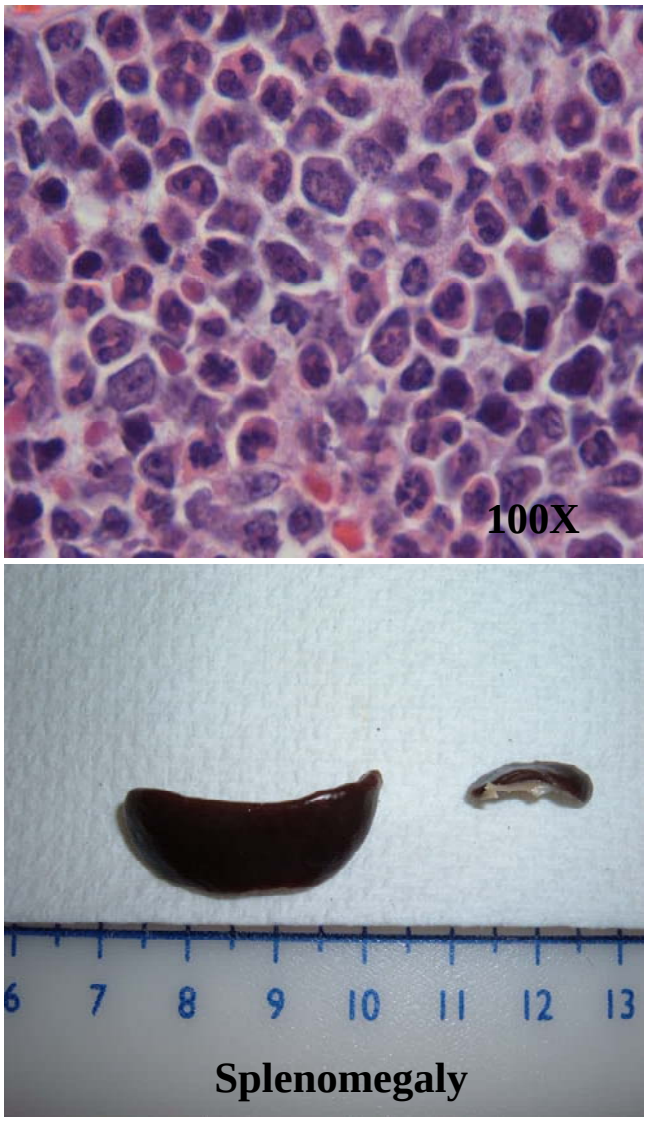


Figure 4-12. H and E stain of sections from *Ppp1r10*+/- acute undifferentiated leukemia (AML-M0) bone marrow (top, 100X) and splenomegaly. Bottom picture shows spleens from a *Ppp1r10*+/- mouse with AML M0 (left) and a normal mouse (right). Scale is in cm.

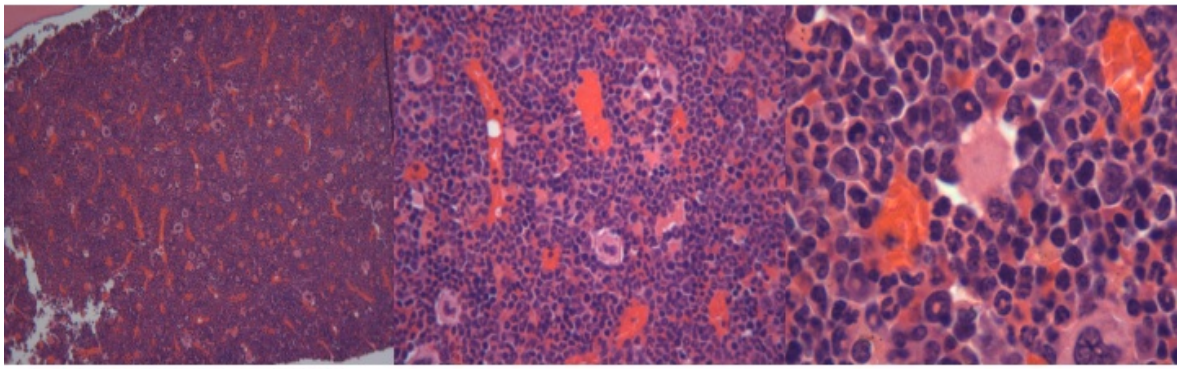


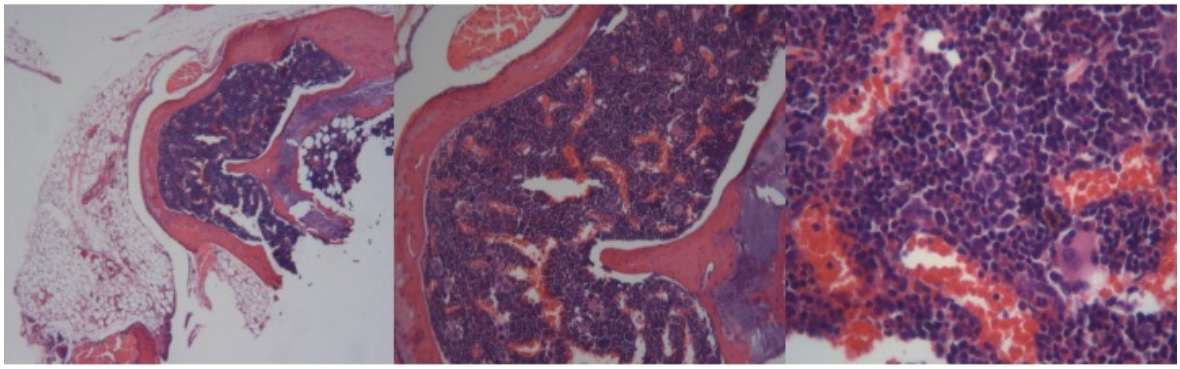

Figure 4-13. H and E stain of sections from *Nf1*+/-*Ppp1r10*+/- acute myeloid leukemic marrow (AML-M4) (top) and normal bone marrow (bottom).

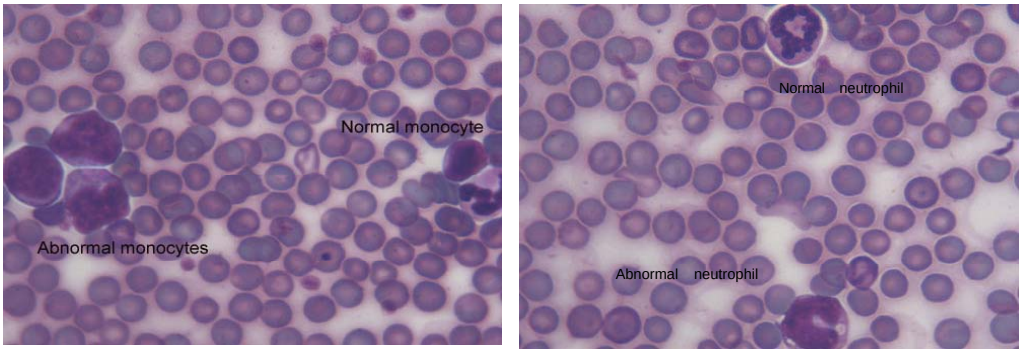


Figure 4-14. Peripheral Blood Smear from *Ppp1r10*+/-*Nf1*+/- mouse, displaying abnormal monocytes and neutrophils.

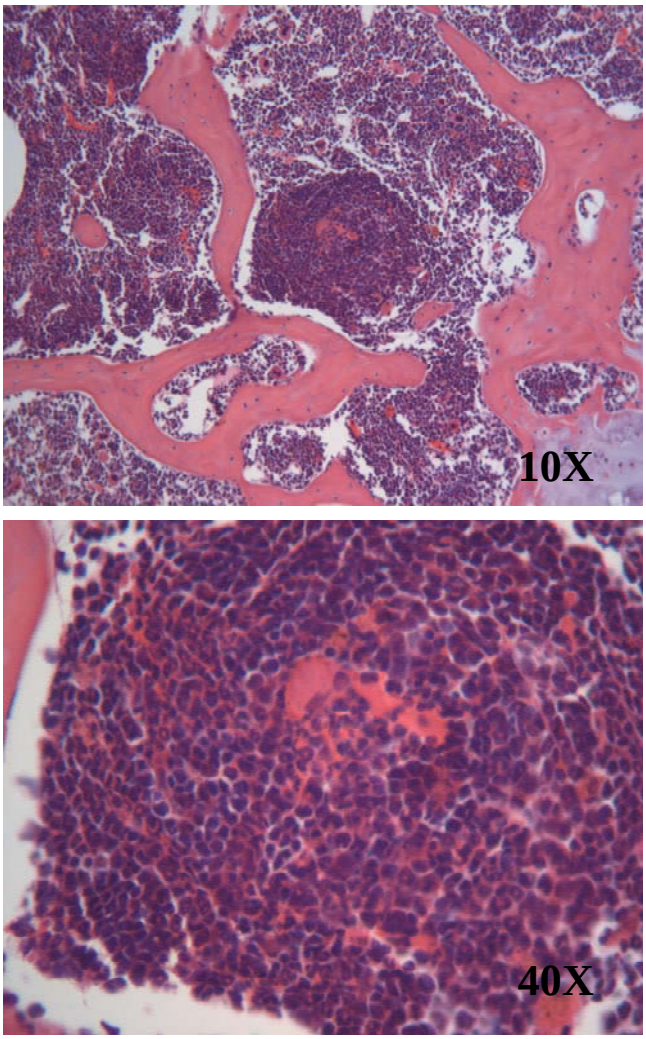


Figure 4-15. An H and E stain of section of a granulocytic sarcoma in a *Ppp1r10*+/-*Nf1*+/- mouse (10X on top, 40X on bottom).

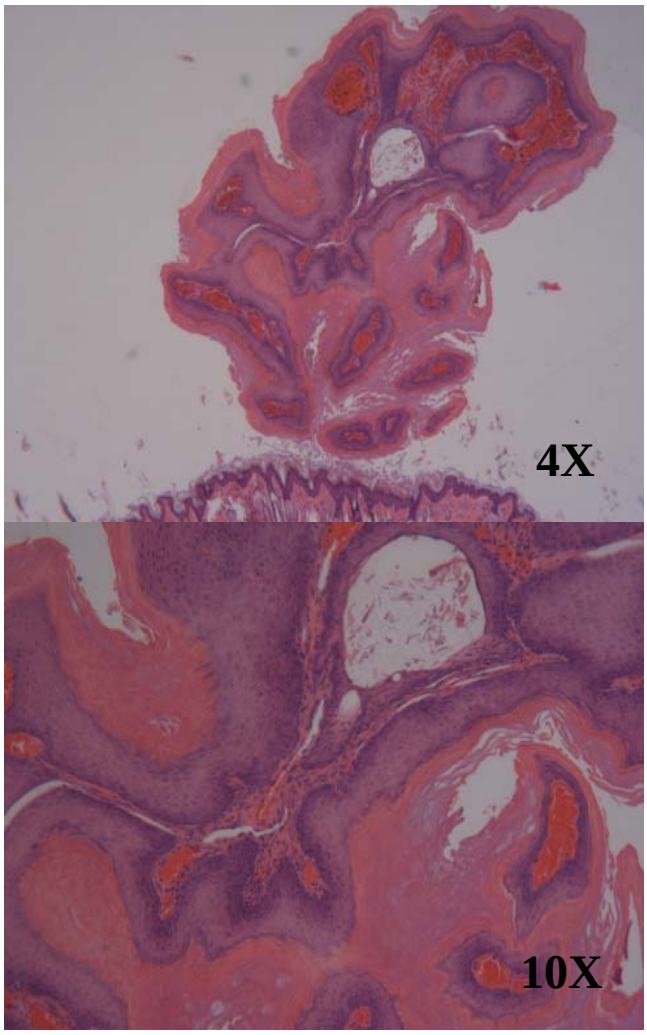


Figure 4-16. H and E stain of a section of a squamous cell carcinoma from a *Ppp1r10*+/-*Nf1*+/, 4X top, 10X bottom.

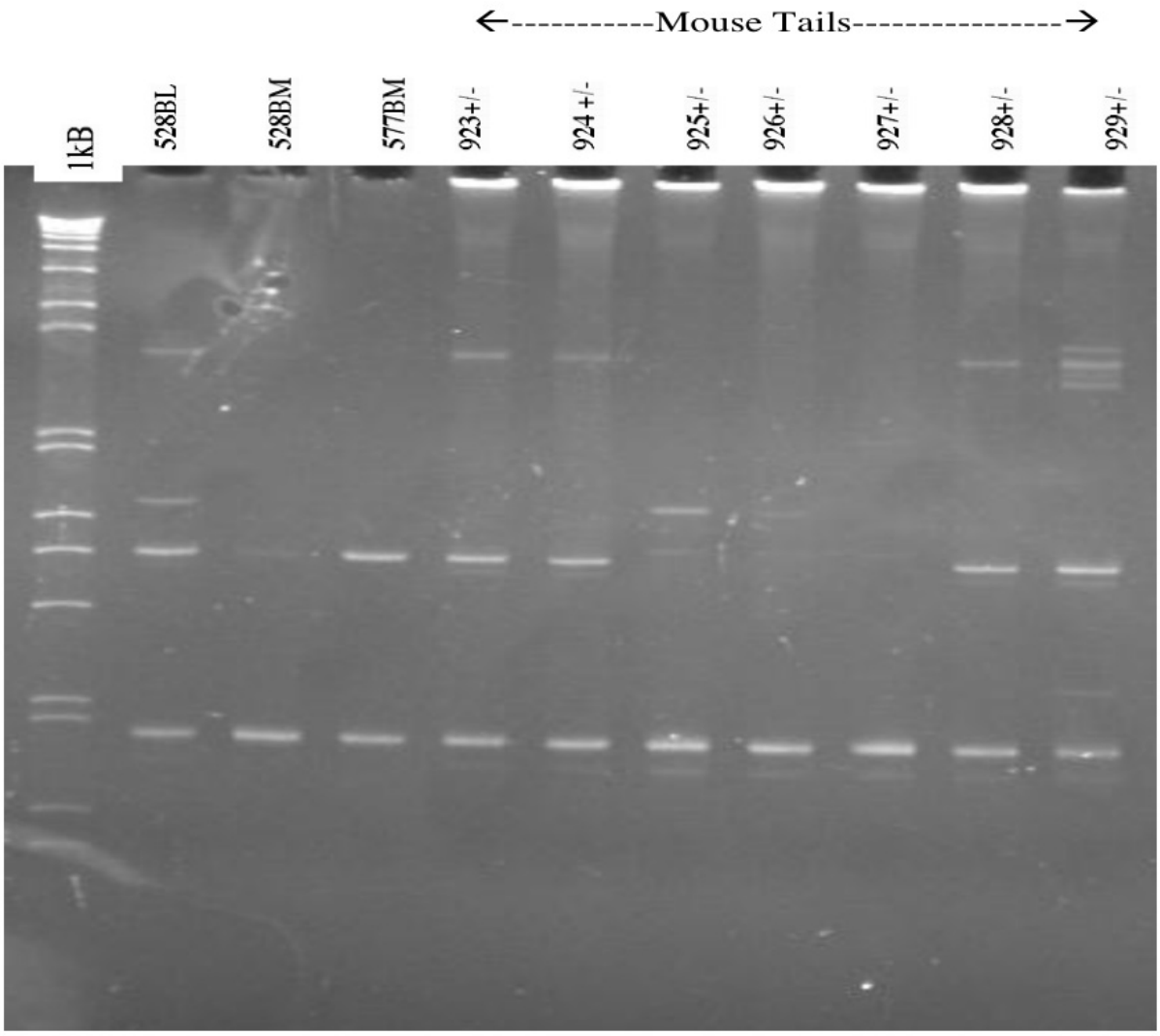


Figure 4-17. Ethidium-bromide stained polyacrylamide gel showing *Nf1* PCR products from blood and bone marrow for *Nf1*+/-*Ppp1r10*+/- mice to test for loss of heterozygosity in the leukemic bone marrow.

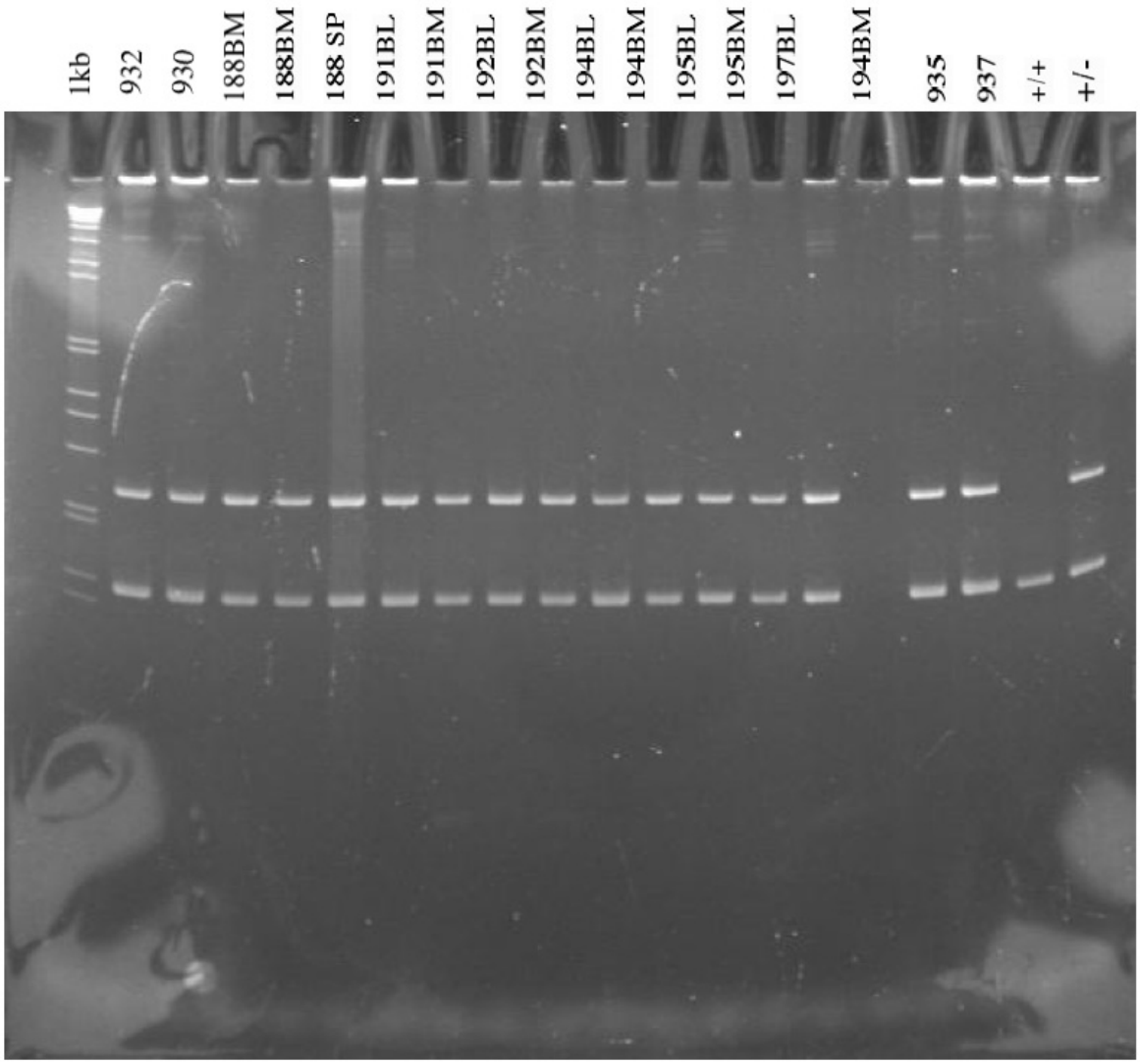


Figure 4-18. Ethidium-Stained polyacrylamide gel showing PCR products from *Ppp1r10* genotyping in *Ppp1r10*+/- mouse tissues to screen for loss of heterozygosity.

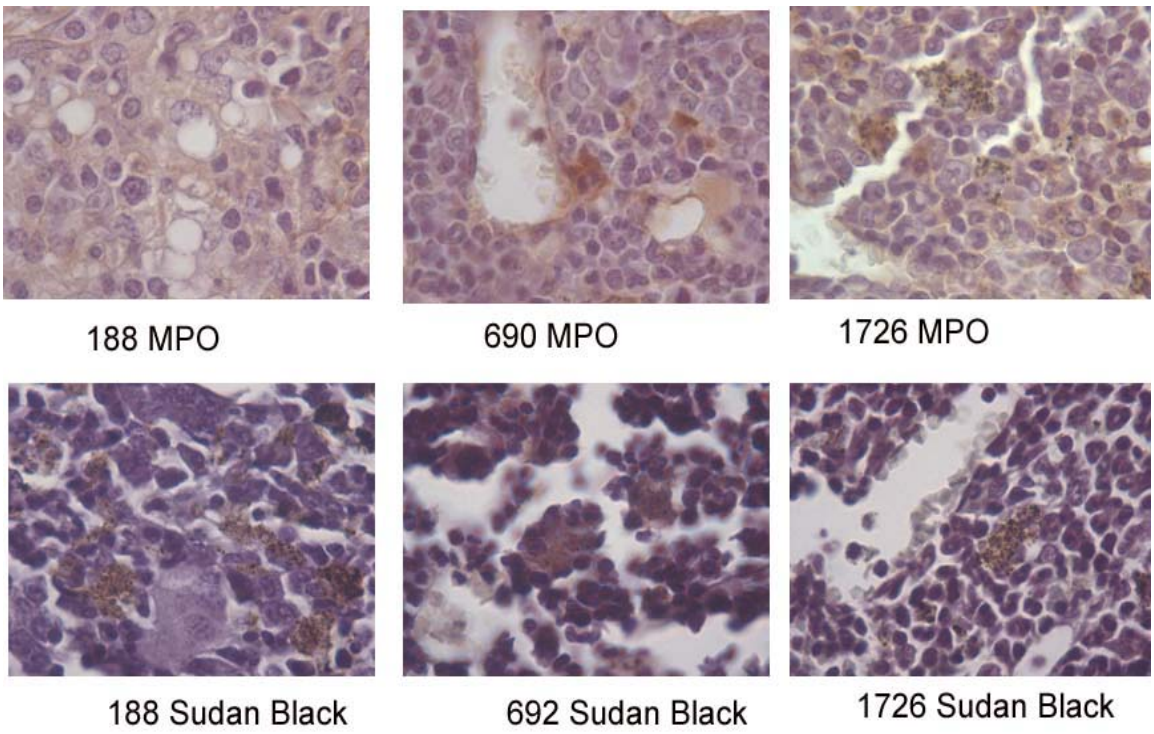


Figure 4-19. Myeloperoxidase and Sudan Black stain of bone marrow sections mouse 188 (*Ppp1r10*+/-), 690 (*Ppp1r10*+/-Nf1+/-), and 1726 (*Nf1*+/-).

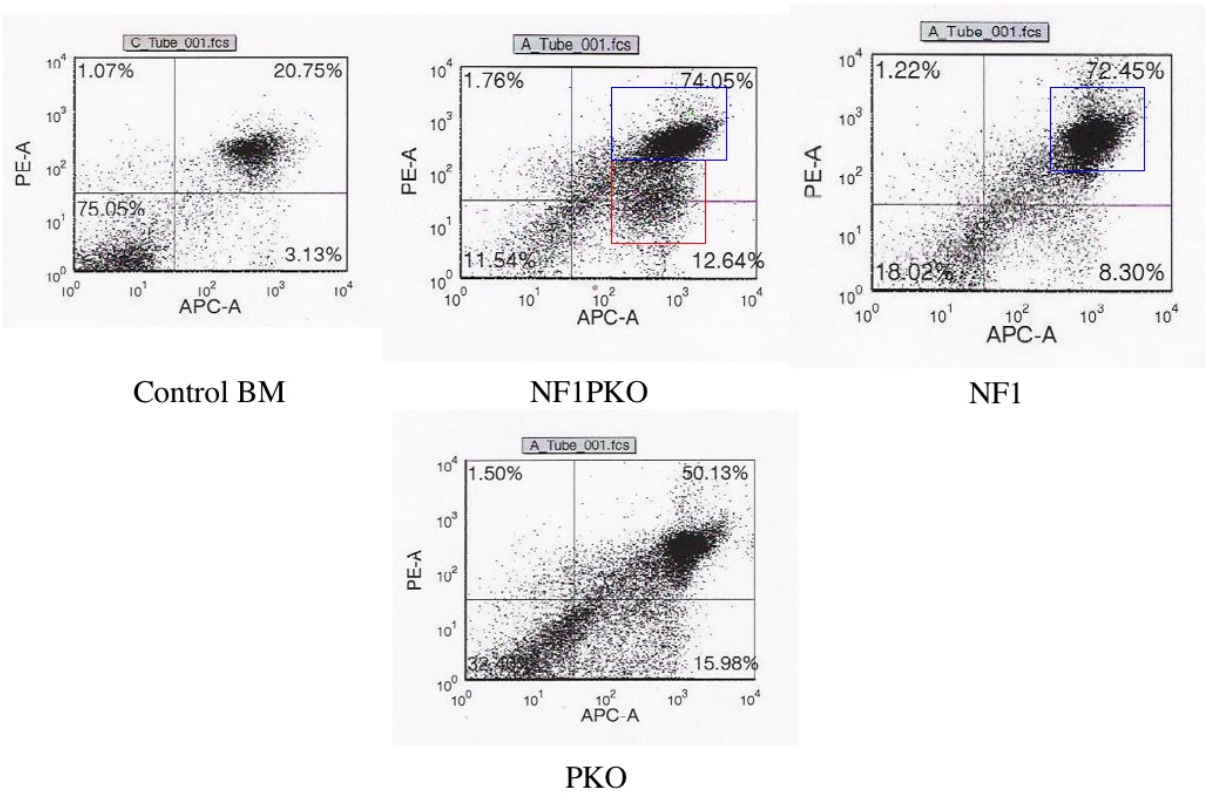


Figure 4-20. Flow cytometry on mouse bone marrow for *Ppp1r10*+/-*Nf1*+/- (NF1PKO), *Nf1*+/, and *Ppp1r10*+/- (PKO) with Gr1 (PE) and Mac1 (APC). Blue box indicates granulocyte population and red box indicates monocyte population.

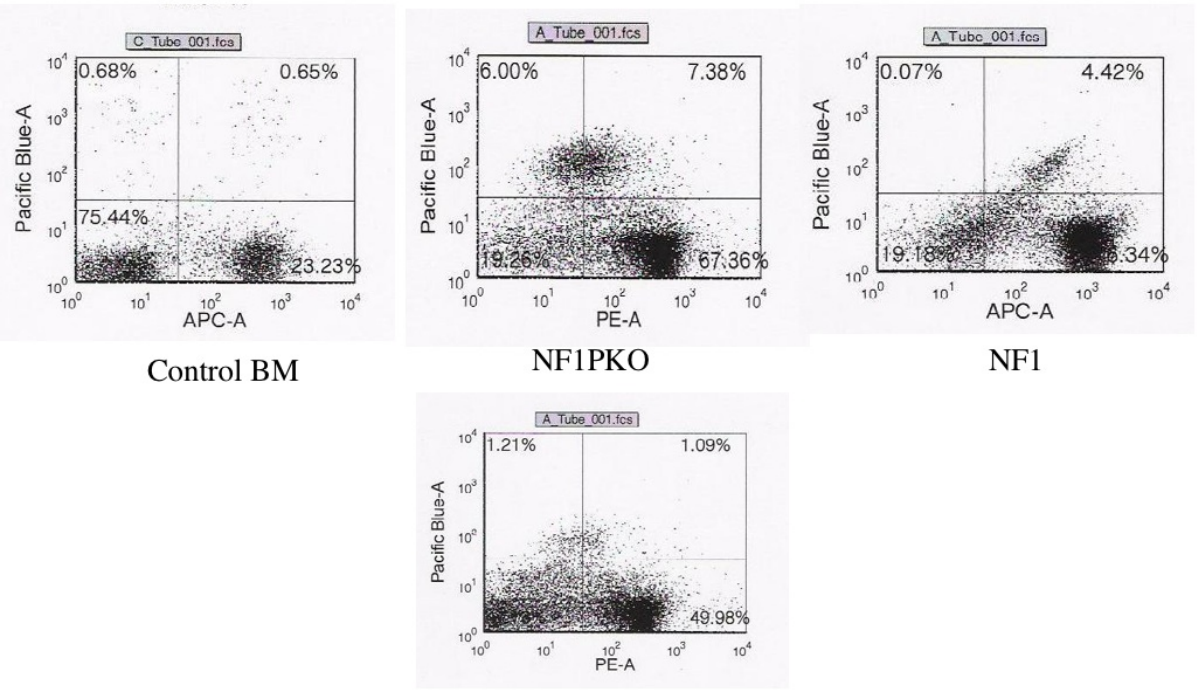


Figure 4-21. Flow cytometry on mouse bone marrow for control bone marrow, *Ppp1r10*+/-*Nf1*+/ (NF1PKO), Nf1+/-, and *Ppp1r10*+/- (PKO) with ckit (Pacific Blue, stem cell marker).

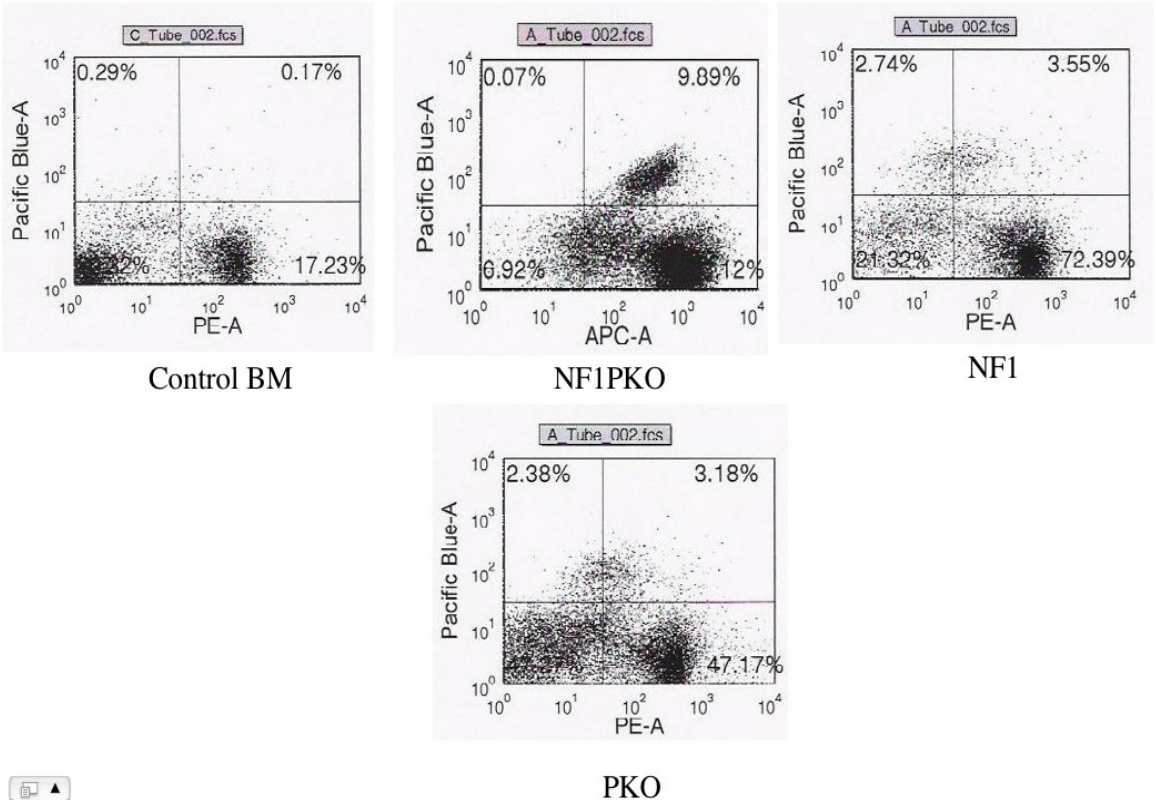


Figure 4-22. Flow cytometry on mouse bone marrow from control bone marrow, *Ppp1r10*+/- *Nf1*+/ (NF1PKO), *Nf1*+/-, and *Ppp1r10*+/- (PKO) with F4/80 (granulocyte/macrophage marker).

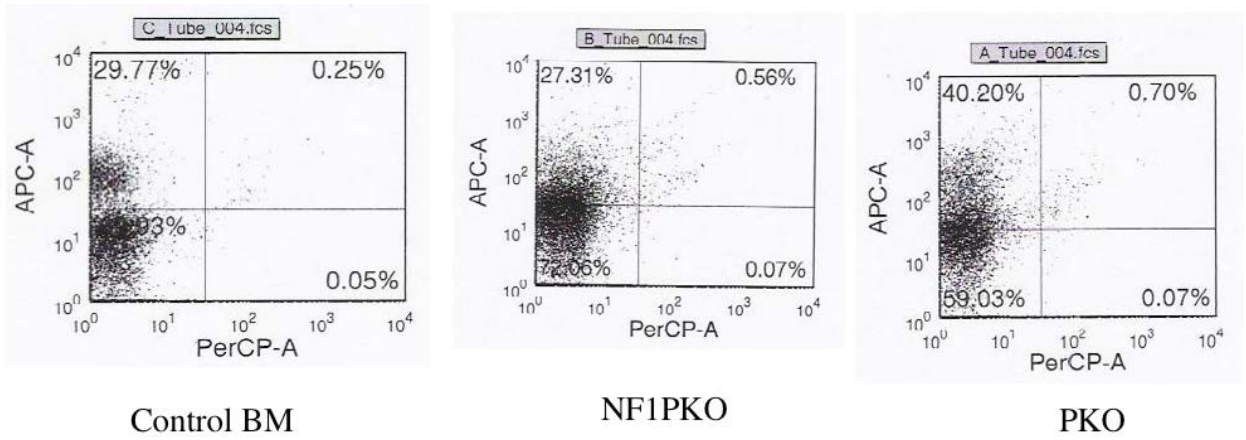


Figure 4-23. Flow cytometry on mouse bone marrow from control bone marrow, *Ppp1r10*+/- *Nf1*+/- (NF1PKO) and *Ppp1r10*+/- (PKO) with CD19 (APC, B-cells).

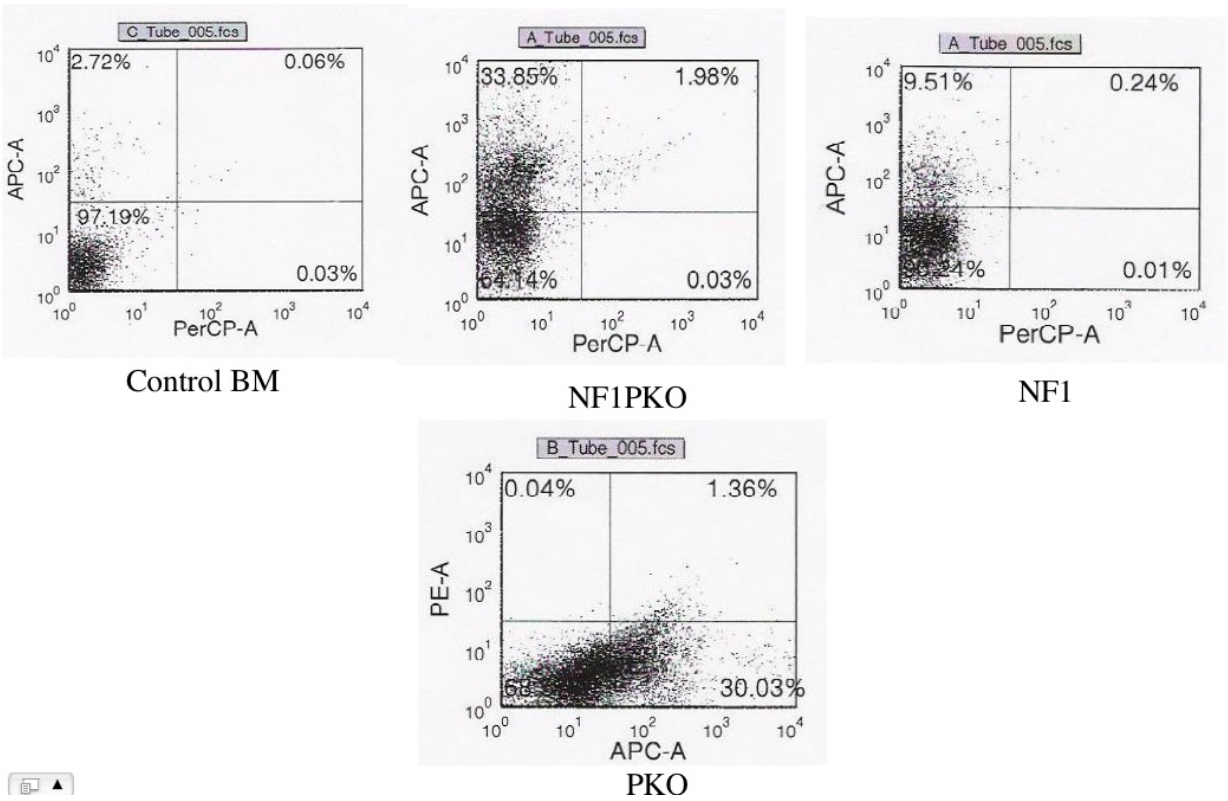


Figure 4-24. Flow cytometry on mouse bone marrow from control bone marrow, *Ppp1r10*+/- *Nf1*+/- (NF1PKO) and *Ppp1r10*+/- (PKO) with TCRBeta (APC, T cell receptor).

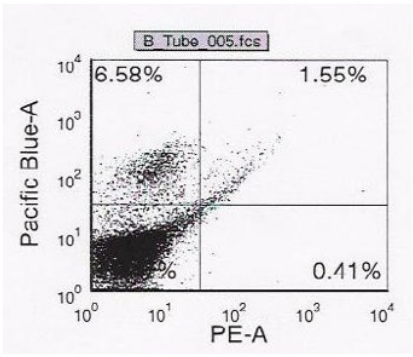


NF1PKO

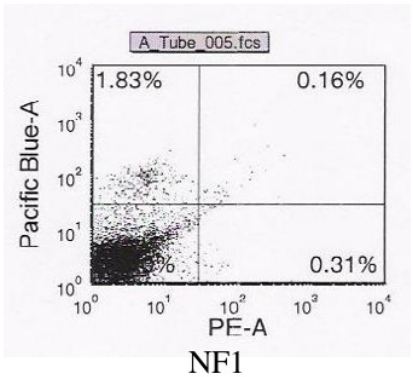


NF1

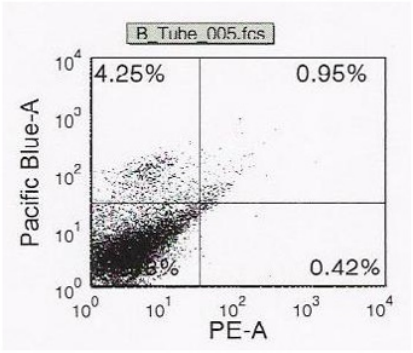


PKO

Figure 4-25. Flow cytometry on mouse bone marrow from *Ppp1r10*+/-*Nf1*+/- (NF1PKO), *Nf1*+/- and *Ppp1r10*+/- (PKO) with CD3 (Pacific Blue, T cell).

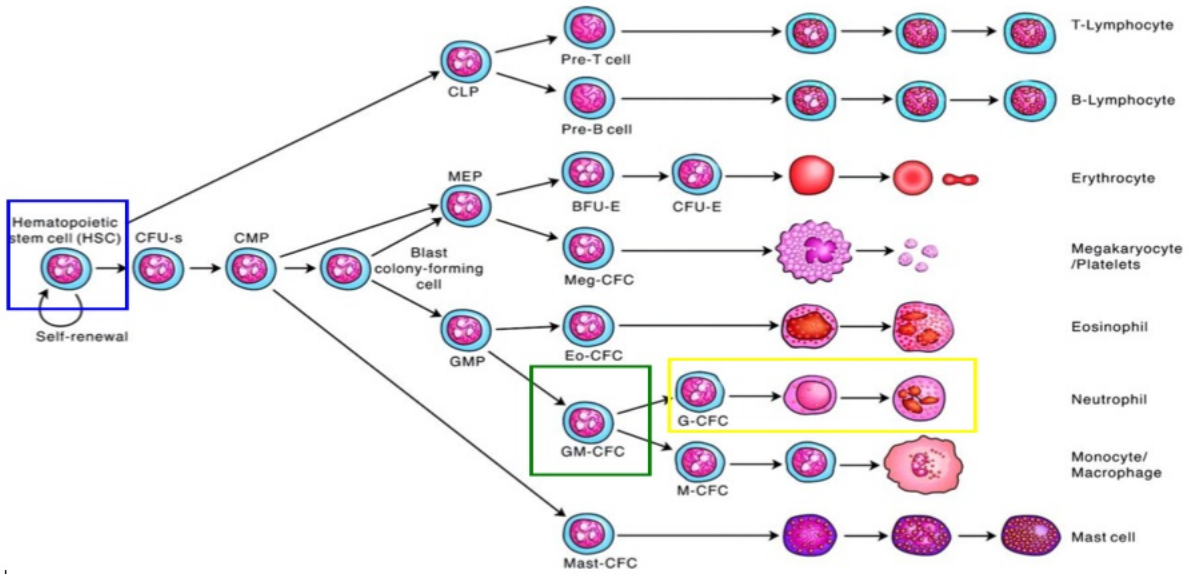


Figure 4-26. An illustration of *Nf1PKO* (green), *PKO* (blue) and *Nf1* (yellow) effect the hematopoeitic lineage.

Table 4-1. *Ppp1r10*+/- aged mice necropsy data, M: E (2 to 8.25) ratios, and blast numbers.

| PKO Hets | DOS | Sex | Age | Necropsy findings | Total no. of solid tumors | Bone marrow diagnosis | Peripheral blood cytology | Final diagnosis |
|---|---|---|---|---|---|---|---|---|
| 195 | 10/05/11 | F | 2 yr | **Myoepithelioma (Ddx ACA), salivary gland, presumptive**<br>**Myoepithelioma, metastatic, thymus**<br>Leukemia (presumptive), spleen<br>Leukemia (presumptive), perirenal LN | **2** | AUL | **AML** | **AUL** |
| 194 | 10/05/11 | F | 2 yr | **Hepatic hemangiosarcoma (gross and micro)**<br>**Pulmonary adenocarcinoma (micro)**<br>**Leimyosarcoma, uterus**<br>Leukemia (presumptive) spleen (gross and micro) | **3** | AUL | **AML** | **AUL** |
| 191 | 10/05/11 | F | 2 yr | **pituitary tumor (gross only)**<br>focal angiectasis (peliosis hepatis), liver<br>Leukemia (presumptive), lung<br>Leukemia (presumptive), small intestine | **1** | AUL | **AUL** | **AUL** |
| 192 | 10/05/11 | F | 2 yr | No significant lesions | 0 | M:E 2:1 (WNL) | **MDS?** | **Normal** |
| 188 | 10/16/11 | F | 2 yr | **Round cell tumors** | **TNTC, visceral and thoracic cavity** | M:E 4.2:1 | | **AUL** |
| 204 | 10/20/11 | M | 2 yr | Thrombosis with fibrinoid necrosis, heart.<br>**Myeloid leukemia poorly differentiated, spleen**<br>**M**yeloid leukemia poorly differentiated, kidney | **1** | M:E 3.68:1 (AUL) | **AUL** | **AUL** |
| 199 | 10/20/11 | M | 2 yr | Myeloid leukemia (presumptive), lung<br>Myeloid leukemia (presumptive), spleen | 0 | M:E 5.1: 1 | **AUL** | **AUL** |
| 197 | 10/20/11 | M | 2 yr | Myeloid leukemia, Heart, lung, liver, LN, **SI**<br>**photo of SI**<br>**Myeloid leukemia poorly differentiated, spleen**<br>similar to 204, have photos | **2** | M:E 8.25:1 (AUL) | **AUL** | **AUL** |

Table 4-2. *Nf1*+/-*Ppp1r10*+/-aged mice necropsy data, M:E (2.33 to 13.25) ratios, and blast numbers.

| PKO NF1 double hets | DOS | Sex | Age | Necropsy findings | No. of Solid Tumors | Bone Marrow results | Final diagnosis |
|---|---|---|---|---|---|---|---|
| 557 | 10/16/11<br>DIC | F | 16 | Infarction with fibrinoid necrosis | unk | N/A | Anemia, platelet dysfunction, infarction |
| (1) 528 | 10/16/11 | M | 17 | **pedunculated liver tumor** | **1** | M:E 2.33 WNL | Normal bone marrow, with liver tumor |
| (2) 552 | 10/20/11 | M | 16 | **Adenocarcinoma, lung**<br>aggressive tumor, photos<br>**Hepatocellular carcinoma, liver** | **2** | M:E 11.5<br>90% bands | **CML** |
| (3) 564 | 10/20/11 | M | 16 | NSL | 0 | M:E 4.88 | **AML** |
| (4) 690 | 11/10/11 | F | 15 | Leukemia (presumptive), spleen. | 0 | M:E 3.7 | **AML** |
| (5) 554 | 12/5/11 | F | 18 | Leukemia, lung with hemorrhage<br>Myeloid leukemia, liver, spleen | 0 | M:E 6.4 | **AML**<br>photos of bone marrow |
| (6) 692 | 12/5/11 | F | 16 | **proliferative mesenchymal process**<br>Splenomegaly, splenic nodule<br>liver nodule (infarction)<br>Leukemia, thymus, liver, spleen | **1** | M:E 8.8 | **AML** |
| (7) 577 | 9/22/11 | M | 15 | Leukemia, salivary gland, lung, spleen | 0 | M:E 8.0 | **AML** |
| (8) 481 | 9/22/11 | F | 17 | leukemia, lung, kidney, spleen, nictitans<br>cystic endometrial hyperplasia | 0 | M:E 7.3 | **AML** |
| 574 | 9/22/11 | F | | Pulmonary hemorrhage, DIC | unk | | did not keep bone marrow, autolyzed |
| (9) 494 | 8/29/11 | F | 16 | Pulmonary hemorrhage | 0 | M:E 4.45 | **AML** |
| (10) 482 | 8/21/11 | M | 16 | Subcutaneous hemorrhage | 0 | M:E 7.92 | **AML** |
| (11) 442 | 8/2/11 | M | 14 | Myeloid leukemia, liver, spleen and bone marrow | 0 | M:E 9.0 | **AML** |
| (12) 630 | 1/5/12 | F | 18 | Leukemia, lung, spleen<br>**Hemangiosarcoma, ovary** | **1** | M:E 5.5 | **AML** |
| (13) 693 | 3/1/12 | F | 19 | **Hemangiosarcoma, ovary**<br>**Pulmonary adenoma**<br>Leukemia, thymus, lung, liver, spleen<br>Palpebral leukemia | **2**<br>possibly 3 solid tumors | | **CML** |
| (19) 710 | 3/1/12 | M | 18 | **Squamous cell papilloma***<br>cystic dilatation of the seminal vesicles*. | 1<br>** may be incidental findings | | **Myeloid hypoplasia** |
| (14) 641 | 1/24/12 | F | 18 | Myeloid leukemia, lung, liver, gall bladder, spleen, kidney<br>Cystic dilatation of the gall bladder<br>Cystic dilatation of the renal pelvis<br>Palpebral leukemia | 0 | | |
| (15) 530 | 2/9/12 | F | 21 | Myeloid leukemia, lung, LN, spleen<br>Cystic endometrial hyperplasia | 0 | | |
| (16) 646 | 12/18/11 | M | 17 | **proliferative mesenchymal process**<br>Myeloid leukemia, spleen, kidney | **1** | M:E 7.48 | **AUL** |
| (17) 684 | 3/27/12 | F | 19 | Myeloid leukemia, lu, li, sp, ki<br>**granulocytic sarcoma of bone marrow**<br>cystic kidney **gross and micro photographs<br>**Hemangiosarcoma, uterus ** photomicrographs.** | **1** | M:E 13.25 | **CML** |
| (18 ) 688 | 3/27/12 | M | 19 | Myeloid leukemia, lu, ki, sp,<br>**Scoliosis and kyphosis, thoracic vertebrae**<br>cystic dilatation of the seminal vesicle. | **0** | M:E 3.86 | **AML** |

Table 4-3. Peripheral blood smear analysis of *Nf1*+/-*Ppp1r10*+/- (NF1PKO), *Ppp1r10*+/- (PKO), and *Nf1*+/-. The yellow color signifies the average count for all mice for that compartment.

| NF1 PKOs | | | | | | | | | | | | | | | | Cytology | Bone Marrow |
|---|---|---|---|---|---|---|---|---|---|---|---|---|---|---|---|---|---|
| mouse ID | Date of smear | Estimated WBC calculation | Est WBC | % Neutrophils in BL | No. neuts/ul blood | %Bands-metas in BL | No. bands-metas/ul blood | %Lymphocytes in BL | No. lymphs/ul blood | % Monocytes in BL | No. monos/ul blood | % Granulocytes in BM | % Blasts in BM | % Blasts in blood | No. blasts/ul blood | Diagnosis | Diagnosis |
| 646 | 12/18/11 | 12x1500=18000 | 18000 | 71 | 12780 | 11.9 | 2142 | 4.4 | 792 | 4.4 | 792 | | | 7.4 | 1332 | CML | AUL |
| 692 | 12/5/11 | 21.6x1500=32500 | 32500 | 18.4 | 6005 | 9.8 | 3175 | 3.2 | 1059 | 3.2 | 1059 | 14% | 86% | 65.2 | 21195 | AML | AML |
| 554 | 12/5/11 | 9.6x1500=14500 | 14500 | 38.6 | 5606 | 1.3 | 193 | 5.3 | 773 | 4 | 580 | 8% | 92% | 50.6 | 7346 | AML | AML |
| 690 | 11/10/11 | 9.6x1500=14500 | 14500 | 21 | 3782 | 2.1 | 315 | 2.1 | 1891 | 2.1 | 315 | 17% | 83% | 56.5 | 8195 | AML | AML |
| 564 | 10/20/11 | 7.2x1500=10800 | 10800 | 48 | 5200 | 1.8 | 200 | 5.5 | 600 | 27.7 | 3000 | 30% | 70% | 16.6 | 1805 | CML | AML |
| 577 | 9/22/11 | 10x1500=15000 | 15000 | 29.2 | 4384 | 1.5 | 230 | 20 | 3000 | 3 | 461 | 10% | 91% | 46 | 6923 | AML | AML |
| 481 | 9/22/11 | 7.5x1500=11250 | 11250 | 16.1 | 1814 | 1.6 | 181 | 29 | 3266 | 3.2 | 362 | 33% | 66% | 50 | 5625 | AML | AML |
| 530 | 2/9/12 | 9x1500=13500 | 13500 | 8 | 1200 | 8 | 1200 | 6 | 900 | 6 | 900 | 13% | 86% | 68 | 9300 | AML | AML |
| 693 | 3/1/12 | 14x1500=21000 | 21000 | 15 | 3181 | 7.5 | 1590 | 16 | 3500 | 0 | 0 | | 4% | 62 | 12727 | AML | CML |
| 688 | 3/27/12 | 6.6x1500=10,000 | 10,000 | 34 | 3424 | 8.2 | 821 | 23 | 2328 | 4.1 | 410 | 40% | 60% | 30.1 | 3013 | AML | AML |
| 641 | 1/24/12 | 8x1500=12000 | 12000 | 25.8 | 3103 | 5 | 620 | 34 | 4137 | 8 | 1034 | 27% | 73% | 25 | 3103 | AML | AML |
| 630 | 1/5/12 | 7.6x1500=11500 | 11500 | 20.4 | 2346 | 8.1 | 938 | 55 | 6336 | 0 | 0 | 22% | 78% | 16.3 | 1877 | CML | AML |
| AVERAGE without CML | | | 15379.16667 | 28.79166667 | 4402.083333 | 5.566666667 | 967.4166667 | 16.95833333 | 2381.833333 | 5.475 | 742.75 | 21% | 72% | 40.975 | 6869.666667 | | |
| 717 | 3/27/12 | 7.6x1500=11500 | 11500 | 50 | 5750 | 4.3 | 522 | 18 | 2070 | 9 | 1045 | | | 18 | 2090 | CML | CML |
| 710 | 3/1/12 | 7x1500=10500 | 10500 | 39 | 4097 | 0 | 0 | 24 | 2560 | 14 | 1792 | | 1% | 19 | 2048 | MDS | myeloid hypop |
| 528 | 10/16/11 | 2x1500=3000 | 3000 | 19 | 570 | 0 | 0 | 30 | 923 | 23 | 692 | | | 26 | 807 | AML | N/A |
| 552 | 10/20/11 | 9.5x1500=13500 | 13500 | 18.5 | 2500 | 11.1 | 1500 | 1.8 | 250 | 1.8 | 250 | | 10% | 66.6 | 9000 | AML | CML |
| NF1s | | | | | | | | | | | | | | | | | |
| 1726 | 11/10/11 | 6.75x1500=10125 | 10125 | 54.5 | 5522 | 0 | 0 | 7.2 | 736 | 34.5 | 3497 | 70% | | 3.6 | 368 | CML | CML |
| 1718 | 9/22/11 | 5.5x1500=8250 | 8250 | 33.9 | 2799 | 1.7 | 147 | 32.14 | 2651 | 17.8 | 1473 | 42% | | 14.28 | 1178 | CML | Borderline CM |
| AVERAGE | | | 9187.5 | 44.2 | 4160.5 | 0.85 | 73.5 | 19.67 | 1693.5 | 34.5 | 2485 | 56% | | 8.94 | 773 | | |
| PKOs | | | | | | | | | | | | | | | | | |
| 204 | 10/20/11 | 33x1500=49500 | 49500 | 11.7 | 5823 | 1.96 | 970 | 1.96 | 970 | 0 | 0 | 11% | 89% | 84 | 41735 | AUL | AUL |
| 199 | 10/20/12 | 9.3x1500=14000 | 14000 | 17.5 | 2450 | 2.5 | 350 | 1.5 | 2100 | 1.5 | 2100 | 12% | 87% | 50 | 7000 | AUL | AUL |
| 197 | 10/20/11 | 6x1500=9000 | 9000 | 20.4 | 1836 | 8.1 | 734 | 0 | 0 | 8.1 | 734 | 3% | 96% | 63.2 | 5693 | AUL | AUL |
| 188 | 10/16/12 | 7x1500=10500 | 10500 | 23.5 | 2470 | 1.9 | 205 | 13.7 | 1441 | 3.9 | 411 | 3% | 96% | 56.8 | 5970 | AUL | AUL |
| 185 | n/a | 8.75x1500=13125 | 13125 | 36.5 | 4795 | 1.8 | 252 | 13.46 | 1766 | 11.5 | 1514 | 15% | 85% | 34.6 | 4543 | AML | n/a |
| 194 | n/a | 1x1500=1500 | 1500 | 18.75 | 281.25 | 0 | 0 | 43 | 656 | 18.75 | 281.75 | 8% | 92% | 18.75 | 281.75 | AML | n/a |
| 192 | n/a | 8x1500=12000 | 12000 | 28.5 | 3428 | 12.5 | 1500 | 25 | 3000 | 32 | 3857 | | | 1.7 | 214 | MDS? | Normal |
| 191 | n/a | 13.6x1500=20500 | 20500 | 21.7 | 4459 | 2.1 | 445.5 | 13.04 | 2673 | 19.59 | 4010 | 18% | 81% | 43.4 | 8913 | AUL | n/a |
| AVERAGE | | | 16265.625 | 22.31875 | 3182.40625 | 3.87 | 557.075 | 13.9675 | 1575.75 | 11.91375 | 1613.46875 | 10% | 89% | 44.05625 | 9263.71875 | | |

Table 4-4. Bone marrow analysis of *Nf1*+/-*Ppp1r10*+/- (NF1PKO), *Ppp1r10*+/- (PKO), and *Nf1*+/- mice. WNL signifies within normal limits.

| Bone Marrow | | | | | | | | | | | |
|---|---|---|---|---|---|---|---|---|---|---|---|
| **PKO** | **total cells** | **erythroid** | **myeloid** | **M:E** | **immature megakaryocytes** | **maturing grans** | **blasts** | **percent total myeloid** | **percent blasts** | **percent grans** | **final diagnosis** |
| 191 | 158 | 18 | 140 | 7.77 | 3 | 26 | 114 | 88% | 81% | 18% | AUL |
| 194 | 153 | 21 | 132 | 6.28 | 1 | 10 | 122 | 86% | 92% | 8% | AUL |
| 195 | 200 | 56 | 144 | 2.57 | 2 | 21 | 123 | 72% | 85% | 15% | AUL |
| 192 | 180 | 50 | 130 | 2.6 | 3 | 124 | 6 | 72% | 5% | 95% | Normal bone marrow |
| 188 | 190 | 36 | 154 | 4.2 | 8 | 5 | 149 | 81% | 96% | 3% | AUL |
| 204 | 150 | 32 | 118 | 3.68 | 20 | 13 | 105 | 89% | 89% | 11% | AUL |
| 199 | 184 | 30 | 154 | 5.1 | 4 | 19 | 135 | 85% | 87% | 12% | AUL |
| 197 | 185 | 20 | 165 | 8.25 | 21 | 6 | 159 | 89% | 96% | 3% | AUL |
| | | | | | | | | | | | |
| 876 | 143 | 25 | 118 | 4.72 | 13 | 26 | 92 | 82% | 78% | 22% | AML |
| 875 | retrim | | | | | | | | | | |
| 737 | 160 | 28 | 132 | 4.71 | 8 | 32 | 100 | 83.00% | 75% | 25% | AML |
| 738 | 190 | 40 | 150 | 3.75 | 17 | 25 | 125 | 78.00% | 83% | 16% | AML |
| 717 | 160 | 27 | 133 | 4.9 | 10 | 118 | 15 | 88.00% | 11% | 89% | CML |
| | | | | | | | | | | | |
| | | | | | | | | | | | |
| | | | | | | | | | | | |
| **PKO NF1** | **total cells** | **erythroid** | **myeloid** | **M:E** | **immature megakaryocytes** | **maturing grans** | **blasts** | **percent total myeloid** | **percent blasts** | **percent grans** | **final diagnosis** |
| 564 | 200 | 34 | 166 | 4.8 | 7 | 23 | 143 | 83% | 70% | 30% | AML |
| 552 | 150 | 12 | 138 | 11.5 | 10 | 123 | 15 | 92% | 10% | 90% | CML |
| 690 | 226 | 49 | 177 | 3.7 | 5 | 30 | 147 | 78% | 83% | 17% | AML |
| 554 | 237 | 32 | 205 | 6.4 | 4 | 16 | 189 | 86% | 92% | 8% | AML |
| 692 | 256 | 10 | 230 | 8.8 | 3 | 33 | 197 | 89% | 86% | 14% | AML |
| 577 | 235 | 26 | 209 | 8 | 5 | 20 | 189 | 88% | 91% | 10% | AML |
| 481 | 150 | 18 | 132 | 7.33 | 3 | 44 | 88 | 88% | 66% | 33% | AML |
| 494 | 180 | 33 | 147 | 4.45 | 3 | 40 | 107 | 81% | 72% | 27% | AML |
| 482 | 223 | 25 | 198 | 7.92 | 3 | 57 | 141 | 88% | 71% | 29% | AML |
| 442 | 100 | 10 | 90 | 9 | 0 | 18 | 72 | 90% | 80% | 20% | AML |
| 646 | 280 | 33 | 247 | 7.48 | 3 | 17 | 230 | 88% | 93% | 7% | AUL undifferentiated |
| 693 | 310 | 22 | 288 | 13.09 | 3 | 278 | 10 | 93% | 4% | 96% | CML |
| 710 | 220 | 116 | 104 | 0.9 | 7 | 101 | 3 | 47% | 1% | 97% | myeloid hypoplasia |
| 641 | 190 | 45 | 145 | 3.22 | 5 | 39 | 106 | 76% | 73% | 27% | AML |
| 530 | 156 | 46 | 110 | 2.4 | 3 | 15 | 95 | 70% | 86% | 13% | AML |
| 630 | 150 | 23 | 127 | 5.5 | 7 | 28 | 99 | 85% | 78% | 22% | AML |
| 688 | 136 | 28 | 108 | 3.86 | 3 | 43 | 65 | 80.00% | 60% | 40% | AML |
| 684 | 171 | 12 | 159 | 13.25 | 3 | 143 | 16 | 93.00% | 10% | 90% | CML |
| 574, DIC | | | | | | | | | | | |
| | | | | | | | | | | | |
| **NF1** | **total cells** | **erythroid** | **myeloid** | **M:E** | **immature megakaryocytes** | **maturing grans** | **blasts** | **percent total myeloid** | **percent blasts** | **percent grans** | **final diagnosis** |
| 1726 | 338 | 61 | 277 | 4.54 | 3 | 190 | 87 | 82% | 30% | 70% | CML |
| 1718 | 225 | 20 | 212 | 10.6 | 2 | 90 | 122 | 94% | 57% | 42% | borderline CML |
| | | | | | | | | | | | |
| | | | | | | | | | | | |
| **Normal control** | | | | | | | | | | | |
| 952 | 210 | 60 | 150 | 2.5 | 3 | 144 | 6 | 71% | 4% | 96% | WNL |

# CHAPTER 5
# DISCUSSION

Previous work in Dr. Brannan's lab has elucidated three common loci that cooperate with *Nf1* inactivation to cause acute leukemia. The focus of this thesis has been one such locus, *Epi2*. The candidate gene I investigated at this locus was *PPP1R10* located on human chromosome 6q21.3. Experiments were designed to help answer the question that if *PPP1R10* is a cancer gene, is it an oncogene or a tumor suppressor gene.

The mouse retrovirus integrated in intron 1 of *Mrps18b* in the same transcriptional orientation. However, since *Ppp1r10* is less than one kilobase away, in the opposite orientation of the virus, it was hypothesized that this gene may also be affected, particularly by the viral LTR. Based on the location of the virus, the most likely mechanisms were protein truncation of *Mrps18b* or down-regulation of *Ppp1r10* through the viral LTR integrating in a transcription factor-binding site. *PPP1R10* seemed to be a more attractive candidate because of its ability to regulate PP1, a serine threonine phosphatase. *PPP1R10*, whose protein product is PNUTS, is a serine/threonine phosphatase regulator that binds PP1, regulates PP1's enzymatic activity and targets PP1 to the nucleus. PP1, a major phosphatase, regulates over 70 mammalian genes in the cell, however the downstream effectors of PNUTS are still unknown or PNUTS/PP1 complex.

The goal of the first specific aim was to sequence *PPP1R10* and *MRPS18B* and look for any genetic abnormalities in human leukemia samples. In *PPP1R10*, two possible point mutations were found, a serine to stop (nonsense) and a serine to threonine (missense) change at codon 125 in exon 6. However, we have not been able to determine if these are somatic or not. Other polymorphisms previously validated were also found, one in the promoter (rs16867845) and one in exon 19 (rs11754215). Both of these displayed no loss of heterozygosity in human leukemia samples. One polymorphism appeared to display loss of heterozygosity in an intron 15

SNP by sequence analysis. This finding was further confirmed by constructing an induced RsaI restriction fragment length polymorphism at the site. This would indicate *PPP1R10*, may have a role in leukemia through a tumor suppressor mechanism. Results, suggested LOH in other samples, although validation with both methods needs to be done and other SNPs need to be examined as well.

The *in vitro* experiments were aimed at testing *Ppp1r10* as a possible oncogene. The first experiment was to over-express PNUTS in COS7 cells, starve the cells and probe for increases or decreases in different effectors in cancer-related signaling pathways. Western blots showed subtle effects in p-Stat3, p-Pten, p-Erk1/2, and p-Mek1/2 but these were not considered to be representative of oncogenic activation. Further work on downstream effectors of Ppp1r10 could focus on probing these pathways by down-regulating PNUTS through siRNA or a conditional gene targeted *Ppp1r10* mouse, to study its role in different tissues. This is important since PNUTS has not been studied in hematopoietic cells.

To further confirm that *Ppp1r10* is not an oncogene, a CFU-GM assay was performed by over-expressing *Ppp1r10* in murine wild-type fetal liver cells and then plating the cells with increasing amounts of GM-CSF. The expected results for an oncogene were increased sensitivity to GM-CSF at low concentrations, with increasing number of colonies as well as an altered cell morphology. The results displayed no altered morphology of the colonies and no cytokine independent growth via GM-CSF. These experiments provide more evidence that *PPP1R10* is not an oncogene.

To further study the hypothesis of tumor suppressor, a *Ppp1r10* gene targeted Gene Trap mouse knockout was created by Jessica Walrath, a previous graduate student. Dr. Walrath showed that homozygosity for *Ppp1r10* is a pre-implantation lethal mutation (Walrath 2006).

Many tumor suppressor genes when knocked out are embryonic lethal (e.g Nf1, Nf2), consistent with *Ppp1r10* being a tumor suppressor gene (Jacks et al. 1994). Jessica also had evidence of decreased *Ppp1r10* RNA levels in an Epi2 tumor (and somewhat less decreased in a few non Epi2 tumors) but the RNA was not absent (Walrath, 2006). This was similar to my human tumor data and is consistent with tumor suppressor but possibly having an effect through heterozygosity (haploinsufficiency). Further evidence fitting a hypothesis of tumor suppressor was found when 21 *Ppp1r10*+/-*Nf1*+/- mice I generated developed cancer at a very high frequency. Results showed a phenotype different than observed originally in *Nf1*+/- mice, which develop a minor percentage of MPD or pheochromocytomas between 17 and 27 months of age (Jacks et al. 1994). Eighty two percent of *Ppp1r10*+/-*Nf1*+/- mice developed AML-M4 and between 14 and 21 months. In addition, fifteen percent of these mice developed hemangiosarcomas of the ovary and uterus, and ten percent had a proliferation mesenchymal process of the skin. In *Ppp1r10*+/- mice, clinical symptoms were not observed until 24 months of age. These mice then became ill and rapidly declined due to AML-M0. Seventy-five percent of these mice also developed one or more non-recurring solid tumors, suggesting an overall increase in tumorigenesis in other tissues as well. This supports the hypothesis that Ppp1r10 is a tumor suppressor whose loss has high penetrance in certain tissues such as bone marrow. Further these mice are novel models for AML-M0 and AML-M4.

Based on this work and the literature, we hypothesize that loss of *Ppp1r10* causes abnormal regulation of PP1, and increased phospho-p53. Recent literature has shown that PP1 dephosphorylates p53 at serine 15 and serine 37 (Li et al. 2006). The dephosphorylation of these sites changes transcriptional activity and apoptotic activity of p53 to the active form (Li et al. 2006). Phosphorylated p53 (inactive) has been associated with tumorigenesis (Feng et al. 2008).

In our model, loss of *Ppp1r10* decreases *PP1* binding with *p53*, which interferes with dephosphorylation of *p53*, raising the amount of phosphorylated p53. This would cause effects in DNA repair, apoptosis, and the other processes regulates by p53, which go awry when it is inactivated as in many cancers. Alternative explanation is that the pRB pathway is affected, since PP1 is known to dephosphorylate (inactivate) this important tumor suppressor in other tissues (Krucher et al. 2006). However, mouse model phenotypes fit with p53 involvement better (Zindy et al. 2003; Damo et al. 2005).

Future work on this project will be geared towards making a conditional knockout for *Ppp1r10*. The PP1 binding site that encompasses exons 13 and 14 will be floxed in order to ensure that all isoforms of *Ppp1r10* lack of ability to regulate PP1. This mouse will be crossed to an Mx1-Cre mouse, whose Cre expression is inducible and affects the hematopoietic system, spleen, and liver (Kuhn et al. 1995). Expression of Cre will be induced with pIpC injection, or interferon, and then mice will be followed for development of AML. Other tissues could be studied by crossing the conditional Ppp1r10 mouse to other Cre genes driven by tissue-specific promoters. For example, hemangiosarcomas are endothelial in origin. Thus, crossing the conditional *Ppp1r10* knockout to a Cre transgenic mouse driven by an endothelial-promoter such as ICAM2 or Tie2 (the latter of which already exists) (Cowan et al.1998; Kisanuki et al. 2001). This could provide an excellent model for hemagiosarcoma, which could be used to understand pathways involved or test treatments. We could also test effects of background strain on penetrance, latency, and or tumor repertoire (i.e. identify modifier genes).

Another area of research will focus on the pathways that are deregulated in the mouse bone marrow by loss or reduction of *Ppp1r10* with or without *Nf1*. We could use siRNA for Ppp1r10 +/- Nf1 in hematopoeitic precursor cell lines (e.g DC13) or primary cells, or possibly establish

cell lines from the tumors or from non-transformed bone marrow cells, for *in vitro* studies. These experiments may be carried out with Western blots and or phosphoFlow cytometry developed by the Nolan lab at Stanford (Krutzik et al. 2005). Some candidate pathways include: p53, pRB, PKA, and the Ras pathway. Once the deregulated signaling pathway(s) is discovered, therapeutics can be identified to help treat patients with these leukemias. This could be specifically targeted to the PP1 level, or utilize therapies already being developed for the pathways implicated.

# APPENDIX A
# PRIMER LIST

| Primer Name | Primer Sequence | Genomic or cDNA | Region of gene | Mse or Hs |
|---|---|---|---|---|
| PNUTSprom1F | 5'-CAGGACAGGAATTGACGGAAA-3' | genomic | promoter | Hs |
| PNUTSprom1R | 5'-CTAGCACCTCCCTTTCCTCTG-3' | genomic | promoter | Hs |
| PNUTSprom2F | 5'-TACCAATCCTGGGTGAGAAATG-3' | genomic | promoter | Hs |
| PNUTSprom2R | 5'-CCGCAAAATTTTACCCACTAGA-3' | genomic | promoter | Hs |
| P115RsAF | 5'-CCCTAAACTCATCCCCCTAGT-3' | genomic | RFLP intron 15 | Hs |
| P115RsaR | 5'-CTGAAAGAAGAACAAAAAAAATCAGTA-3 | genomic | RFLP intron 15 | Hs |
| lac2 | 5'-CAAGGCGATTAAGTTGGGTAACG-3' | genomic | exon 2 | Mse |
| Pko2fb | 5'-CGAAGGACCGTCACCACATAAC-3' | genomic | exon 2 | Mse |
| Pko2fa | 5'-CGAAGGACCGTCACCACATAAC-3' | genomic | exon 2 | Mse |
| NF31a | 5-'GTATTGAATTGAAGCACCTTTGTTTG-3' | genomic | | Mse |
| NF31b | 5'-CTGCCCAAGGCTCCCCCG-3' | genomic | | Mse |
| NeoTkp | 5'-GCGTGTTCGAATTCGCCAATG-3' | genomic | | Mse |
| PPPex2a | 5'-TTGTGTTCCTTTTATCCCAGGT-3' | genomic | exon 2 | Hs |
| PPPex2b | 5'-CTTCGGCCACAGATTTCAAG-3' | genomic | exon 2 | Hs |
| PPPex2c | 5'-CTGCTTGGGACTTGAAATCTG-3' | genomic | exon 2 | Hs |
| PPPex2d | 5'-TTTGCGACGTCAGCACCT-3' | genomic | exon 2 | Hs |
| PPPex3F | 5'-TCCTCTTACCATAGAAACCACCA-3' | genomic | exon 3 | Hs |
| PPPex3R | 5'-CAAAAAGGGGTAAGACTCACC-3' | genomic | exon 3 | Hs |
| PPPex4F | 5'-GGCTGCTTCATTTCTAACCCTA-3' | genomic | exon 4 | Hs |
| PPPex4R | 5'-GCTTACACCTTCCCATTCCAA-3' | genomic | exon 4 | Hs |
| PPPex5F | 5'-CTGCCTGCCTGCAGATTTAT-3' | genomic | exon 5 | Hs |
| PPPex5R | 5'-AAAGGTACCTGCTTGAGATGG-3' | genomic | exon 5 | Hs |
| PPPex6F | 5'-GCCTCCTGGCATTTACCTTT-3' | genomic | exon 6 | Hs |
| PPPex6R | 5'-AAAGCCCATGAGAGAGCAGA-3' | genomic | exon 6 | Hs |
| PPPex7F | 5'-GCATTTCCCCTTTCTGTCAC-3' | genomic | exon 7 | Hs |
| PPPex7R | 5'-AGGACTAAGGAGCTTACCAGCA-3' | genomic | exon 7 | Hs |
| PPPex8F | 5'-TCCCAGTCTGCTTCACCTCT-3' | genomic | exon 8 | Hs |
| PPPex8R | 5'-GAACGGAACTTGGCATGACT-3' | genomic | exon 8 | Hs |
| PPPex9a | 5'-GTCTGGGGTTTGAGTTCAGC-3' | genomic | exon 9 | Hs |
| PPPex9b | 5'-CATTCAGAGCCTGAGAATATGG-3' | genomic | exon 9 | Hs |
| PPPex10a | 5'-GGGGTGAGTCGGAGATGTT-3' | genomic | exon 10 | Hs |
| PPPex10b | 5'TCAAAGTACATCTTCCCCACTTT-3' | genomic | exon 10 | Hs |
| PPPex11a | 5'-CTGTGTTTGCAGGTGTAGGATT-3' | genomic | exon 11 | Hs |
| PPPex11b | 5'-CTTCTGGGAGCCCATACCTT-3' | genomic | exon 11 | Hs |
| PPPex12F | 5'-CACAATAGCCAAGCCCCTTT-3' | genomic | exon 12 | Hs |
| PPPex12R | 5'-ACCCAAGATCCCTCCTTTCAG-3' | genomic | exon 12 | Hs |
| PPPex13a | 5'-TTCTGCTTCCAGCCTCTTTG-3' | genomic | exon 13 | Hs |
| PPPex13b | 5'-CCTCGTTCAGTTTCATCCAA-3' | genomic | exon 13 | Hs |
| PPPex14F | 5'-CCTGCCGACAGTAAATGTGA-3' | genomic | exon 14 | Hs |
| PPPex14R | 5'-CAGGAGTGTCCAAGCACTCA-3' | genomic | exon 14 | Hs |
| PPPex15F | 5'-TCTCACCTGTGTTGTTCCTGA-3' | genomic | exon 15 | Hs |
| PPPex15R | 5'-CAATGACCATCACAACTTCCA-3' | genomic | exon 15 | Hs |
| PPPex16F | 5'-TGAATTCGGTGCATCTTTCA-3' | genomic | exon 16 | Hs |
| PPPex16R | 5'-ACAGTGAGGAGAGCGAGCTT-3' | genomic | exon 16 | Hs |
| PPPex17F | 5'-CTTTCGCCATGGTTGTTACC-3' | genomic | exon 17 | Hs |
| PPPex17R | 5'-CCCAAGCATCTGCTTGATCTT-3' | genomic | exon 17 | Hs |
| PPPex18F | 5'-GCTCATGCTGTGTTACTCTTGTTT-3' | genomic | exon 18 | Hs |
| PPPex18R | 5'-AAGCAGATAAGCCCATTCCA-3' | genomic | exon 18 | Hs |
| PPPex19a | 5'-GGCAGTTCCTGGTAGCTGAT-3' | genomic | exon 19 | Hs |
| PPPex19b | 5'-GGACGATGTCCACTGCTGTT-3' | genomic | exon 19 | Hs |
| PPPex19c | 5'-ATGAAGGCCCTGGTGGTAG-3' | genomic | exon 19 | Hs |
| PPPex19b | 5'-GAGACGGGTACCTCACGTTC-3' | genomic | exon 19 | Hs |
| PPPex19e | 5'-GACCCCCAAATGGACGAG-3' | genomic | exon 20 | Hs |
| PPPex19f | 5'-CCACCCATGCTACCACCA-3' | genomic | exon 21 | Hs |
| PPPex20F | 5'-GCATTGCCCTCAGCTATTTC-3' | genomic | exon 20 | Hs |
| PPPex20R | 5'-GAAAATGGGCCTCACAGAAG-3' | genomic | exon 20 | Hs |
| PPPintron4F | 5'-CCGCCAACGTCAATAAATCT-3' | genomic | intron 4 SNP | Hs |
| PPPintron4R | 5'-GAGAGGCGCTTTTGCTAAGA-3' | genomic | intron 4 SNP | Hs |
| Ppp1r10cDNA1F | 5'-AACAAACAAGCCTCAGCAACA-3' | cDNA | exon 2 | Mse |
| Ppp1r10cDNA1R | 5'-CCTCTCCCTAAATGGAGTTGGG-3' | cDNA | exon 2 | Mse |
| Ppp1r10cDNA2F | 5'-CTCATCCAGCATTTCCGTT-3' | cDNA | exon 2 | Mse |
| Ppp1r10cDNA2R | 5'-TAGACCCCAAAGAACTGCTA-3' | cDNA | exon 4 | Mse |
| Ppp1r10cDNA3F | 5'-GTGCTGACGTCGCAAAAA-3' | cDNA | exon 2 | Mse |
| Ppp1r10cDNA3R | 5'-ATTGGCATCAGTCCTTGTCAG-3' | cDNA | exon 8 | Mse |
| Ppp1r10cDNA4F | 5'-GCAAGTCAAGTGAGGATGAAG-3' | cDNA | exon 7 | Mse |
| Ppp1r10cDNA4R | 5'-CTGTCCCAGGCATCAAAATT-3' | cDNA | exon 10 | Mse |
| Ppp1r10cDNA5F | 5'-CTGGGTTTTCTGGATGCTCTC-3' | cDNA | exon 10 | Mse |
| Ppp1r10cDNA5R | 5'-CAAGATCAAAGACTTCGGGG-3' | cDNA | exon 15 | Mse |
| Ppp1r10cDNA6F | 5'-GGAGGGCAAGCTGAGAG-3' | cDNA | exon 14 | Mse |
| Ppp1r10cDNA6R | 5'-TTATGGGAAGCATGGGAG-3' | cDNA | exon 17 | Mse |
| Ppp1r10cDNA7F | 5'-CTCCAAGCTGCCTCCAGTT-3' | cDNA | exon 17 | Mse |
| Ppp1r10cDNA7R | 5'-GTCGAGGAGGAAAYGAGCCA-3' | cDNA | exon 20 | Mse |
| Ppp1r10cDNA8F | 5'-CTCCCGGACCATACCACAGA-3' | cDNA | exon 20 | Mse |
| Ppp1r10cDNA8R | 5'-CTACCACCCAGGGGTCAATGG-3' | cDNA | exon 21 | Mse |
| GAPDH-5' | 5'-TCATCATCTCTGCCCCCTCTG-3' | cDNA | | Hs/Mse |
| GAPDH-3' | 5'-GCCTGCTTCACCACCTTCTTG-3' | cDNA | | Hse/Mse |
| PPPex2-3F | 5'-TTGAGTTTTGGGTCCTGGTT-3' | cDNA | exons 2-3 | Hs/Mse |
| PPPex2-3R | 5'-TGGAAATCCCATCCACACTT-3' | cDNA | exons 2-3 | Hse/Mse |

# APPENDIX B
# PFAFFL METHOD

$$\text{Ratio} = \frac{(E_{target})^{DCPtarget(control-sample)}}{(E_{ref})^{DCPref(control-samples)}}$$

REFERENCES


1. Aggen JB, Nairn AC, Chamberlain R (2000). Regulation of protein phosphatase-1. *Chem Biol* **7**(1): R13-23.

2. Allen PB, Kwon YG, Nairn AC, Greengard P (1998). Isolation and characterization of PNUTS, a putative protein phosphatase 1 nuclear targeting subunit. *J Biol Chem* 273(7): 4089-95.

3. Andersen LB, Wallace MR, Marchuk DA, Tavakkol R, Mitchell A, Saulino AM, Collins FS (1991). A highly polymorphic cDNA probe in the NF1 gene. *Nucleic Acids Res* 19(13): 3754.

4. Andersen, LB, Ballester R, Marchuk DA, Chang E, Gutmann DH, Saulino AM, Camonis J, Wigler M, Collins FS (1993). A conserved alternative splice in the von Recklinghausen neurofibromatosis (NF1) gene produces two neurofibromin isoforms, both of which have GTPase-activating protein activity. *Mol. Cell. Biol*. **3**(1): 487-95.

5. Andrews PD, Stark MJ (2000). Protein phosphatase is required for maintenance of cell wall integrity, morphogenesis, and cell cycle progression in Sacchromyces Cerevisiae. *J. Cell Science* 133: 507-520.

6. Bader JL, Miller RN (1978). Neurofibromatosis and childhood leukemia. *J. Pediatrics* (16): 926-929.

7. Bedell MA, Largaespada DA, Jenkins NA, Copeland NG (1997). Mouse models of human disease. Part II: recent progress and future directions. *Genes Dev* 11(1): 11-43.

8. Bedigian HG, Johnson DA, Jenkins NA, Copeland NG, Evans R (1984). Spontaneous and induced leukemias of myeloid origin in recombinant inbred BXH mice. *J Virol* 51(3): 586-94.

9. Birnbaum RA, O'Marcaigh A Wardak Z, Zhang YY, Dranoff G, Jacks T, Clapp DW, Shannon KM (2000). Nf1 and Gmcsf interact in myeloid leukemogenesis. *Mol Cell* **5**(1): 189-95.

10. Blaydes SM, Kogan SC, Truomg BT, Gilbert DJ, Jenkins NA, Copeland NG, Largaespada DA, Shannon KM (2001). Retroviral integration at the Epi1 locus cooperates with Nf1 gene loss in the progression to acute myeloid leukemia. *J Virol* 75(19): 9427-34.

11. Bollag G, Clapp DW, Shih S, Adler F, Zhang YY, Thompson P, Lange BJ, Freedom NH, McCormick F, Shannon K (1996). Loss of NF1 results in activation of the Ras signaling pathway and leads to aberrant growth in haematopoietic cells. *Nat Genet* 12(2): 144-8.

12. Brannan CI, Perkins AS, Vogel KS, Ratner N, Norlund ML, Reid SW, Buchberg AM, Jenkins NA, Prada LF, Copeland NG (1994). Targeted disruption of the neurofibromatosis type-1 gene leads to developmental abnormalities in heart and various neural crest-derived tissues. *Genes Dev* 8(9): 1019-29.

13. Brichese L, Valette A (2002). PP1 phosphatase is involved in Bcl-2 dephosphorylation after prolonged mitotic arrest induced by paclitaxel. *Biochem. Biophys. Commun* 294: 504-508.

14. Boguski M, and McCormick F (1993). Proteins regulating Ras and its relatives. *Nature* 366: 643-653.

15. Bos, J.L. (1989). *ras* oncogenes in human cancer: a review. *Cancer Res* 49: 4682-4689.

16. Buchberg AM, Bedigian HG, Jenkins NA, Copeland NG (1990). Evi-2, a common integration site involved in murine myeloid leukemogenesis. *Mol Cell Biol* 10(9): 4658-66.

17. Castilla LH, Garret L, Adya N, Orlic, D, Petra A, Andersen S, Owens J, Eckhaus M, Bodine D, Liu P (1999). The fusion gene Cbfb-MYH11 blocks myeloid differentiation and predisposes mice to acute myelomonocytic leukemia. *Nature Genetics* 23: 144-146

18. Catenacci DV and Schiller GJ (2005). Myelodysplasic syndromes: A comprehensive review. *Blood Rev*. 19(6): 301-19.

19. Cawthon RM, Andersen LB, Buchberg AM, Xu GF, O'Connell P, Viskochil D, Weiss RB, Wallace MR, Marchuk DA, Culver M et al. (1991). cDNA sequence and genomic structure of EV12B, a gene lying within an intron of the neurofibromatosis type 1 gene. *Genomics* 9(3): 446-60.

20. Ceulemans H, and Bollen M (2004). Functional diversity of protein phosphatase-1, a cellular economizer and reset button. *Physiol Rev* 84(1): 1-39.

21. Christensen JL and Weissman IL (2001). Flk-2 is a marker in hematopoietic stem cell differentiation: a simple method to isolate long-term stem cells. *Proc Natl Acad Sci U S A* 98(25): 14541-6.

22. Cho BC, Shaughnessy JD, Largaespada DA, Bedigian HG, Buchberg AM, Jenkins NA, Copeland NG (1995). Frequent disruption of the Nf1 gene by a novel murine AIDS virus-related provirus in BXH-2 murine myeloid lymphomas. *J Virol* 69: 7138-7146.

23. Clarke AR, Maandag ER van Roon M, van der Lugt NM, van der Valk M, Hooper ML, Berns A, te Reilett (1992). Requirement for a functional Rb-1 gene in murine development. *Nature* 359: 328-330.

24. Coleman SD, Williams CA, Wallace MR (1995). Benign neurofibromas in type 1 neurofibromatosis (NF1) show somatic deletions of the NF1 gene. *Nat Genet* 11(1): 90-2.

25. Cowan PJ, Tsang D, Pedic CM, Abbott LR, Shinkel TA, D'Apice AJ, Pearse MJ (1998). The Human ICAM-2 is Endothelial Cell-specific in Vitro and in Vivo and Contains Critical Sp1 and Gata Binding sites. *J Biol. Chem.* 19: 11737-11744.

26. Daley GQ, Van Etten RA, Baltimore D (1990). Induction of chronic myelogenous leukemia in mice by the P210bcr/abl gene of the Philadelphia chromosome. *Science* 247, 824-830.

27. Damo LA, Snyder PW Franklin DS (2005). Tumorigenesis of p27/p53 and p18/p53 double null mice: functional collaboration between pRb and p53. *Mol. Carcinogenesis* 42(2): 109-20.

28. Donehower L, Harvey M, Slagle BL, McArthur MJ, Montgomery CA Jr, Butel JS, Bradley A (1992). Mice deficient for p53 are developmentally normal but susceptible to spontaneous tumors. *Nature* 356 (6366): 215-21.

29. Donovan, S., Shannon, K.M., Bollag G (2002). GTPase activating poteins: critical regulators of intracellular signaling. *BBA Rev Cancer* 1602, 23-45.

30. Erkeland SJ, Valkhof M, Heijmans-Antonisseb C, van Hooven-Beijen A, Delwel R, Hermans MH, Touw IP (2004). Large-scale identification of disease genes involved in acute myeloid leukemia. *J Virol* 78(4): 1971-80.

31. Estrov Z, Grunberger T (1986). Juvenile chronic myelogenous leukemia: characterization of the disease using cell cultures. *Blood* 67(5): 1382-7.

32. Eto M, Elliot E, Prickett TD, Brautiger DL (2002). Inhibitor-2 regulates protein phosphatase-1 complexed Nim-A related kinase to induce centrosome separation. *J. Biol. Chem*. 277: 44013-44020.

33. Feng Z, Hu W, Rajagopal G, Levine AJ (2008). The tumor suppressor p53: Cancer, and aging. *Cell cycle* 7(7): 842-7.

34. Fountain JW, Wallace MR, Brereton AM, O'Connell P, White RL, Rich DC, Ledbetter DH, Leach RJ, Fournier RE, Menon AG, et al. (1989). Physical mapping of the von Recklinghausen neurofibromatosis region on chromosome 17. *Am J Hum Genet* 44(1): 58-67.

35. Geist RT, Gutmann DH (1996). Expression of a developmentally-regulated neuron-specific isoform of the neurofibromatosis 1 (NF1) gene. *Neurosci Lett.* 211(2): 85-8.

36. Gutmann DH, Wright DE, Geist RT, Snider WD (1995). Expression of the neurofibromatosis 2 (NF2) gene isoforms during rat embryonic development. *Hum. Mol. Genet*. 4(3): 471-8.

37. Hansen J, Floss T, Van Sloun P, Fuchtbauer EM, Vauti F, Arnold HH, Schutgen F, Wurst W, von Melchner H, Ruiz P (2003). A large-scale, gene-driven mutagenesis approach for the functional analysis of the mouse genome. *Proc Natl Acad Sci U S A* 100(17): 9918-22.

38. Ingram, DA, Wenning MJ, Shannon K, Clapp DW (2003). Leukemic potential of doubly mutant Nf1 and Wv hematopoietic cells. *Blood* 101(5): 1984-6.

39. Inoue S, Shibata T, Ravindranath Y, Cyohle N (1987). Clonal origin of erythroid cells in juvenile chronic myelogenous leukemia. *Blood* 69(3): 975-6.

40. Jacks T, Shih TS, Schmitt EM, Bronson RT, Bernards A, Weinberg RA (1994). Tumour predisposition in mice heterozygous for a targeted mutation in Nf1. *Nat Genet* **7**(3): 353-61.

41. Jacks T, Fazeli A, Schmitt EM, Bronson RT, Goodell MA, Weinberg RA (1992). Effects of an Rb mutation in the mouse. Nature 359: 295-300.

42. Joosten M, Vankan-Berkhoudt Y, Tas M, Lunghi M, Jenniskens Y, Parganas E, Valk PJ, Lowenerg B, van den Akker E, Delwel R (2002). Large-scale identification of novel potential disease loci in mouse leukemia applying an improved strategy for cloning common virus integration sites. *Oncogene* 21(47): 7247-55.

43. Kalra R, Paderanga DC, Olson K, Shannon KM (1994). Genetic analysis is consistent with the hypothesis that NF1 limits myeloid cell growth through p21ras. *Blood* 84(10): 3435-9.

44. Kamimura K, Ohi H, Kubota J, Okazuka K, Yoshikai Y, Wakabayashi Y, Aoyagi Y, Mishima Y, Kominami R (2007). Haploinsufficiency of Bcl11b for suppression of lymphogenesis and thymocyte development. *Biochem Biophys. Res. Commun*. 355(2): 538-42.

45. Kelly LM, Liu Q, Kulok JL, Williams IR, Boulton CL, Gilliland DG (2002). FLT3 internal tandem duplication mutations associated with human acute myeloid leukemias induce myeloproliferative disease in a murine bone marrow transplant model. *Blood* 99, 310-318.

46. Kelly L, Clark J, Gilliland DG (2002). Comprehensive genotypic analysis of leukemia: clinical and therapeutic implications. *Curr Opin Oncol* 14: 10-18.

47. Kim HG, Kojima K, Swindle CS, Cotta CV, Huo Y, Reddy V, Klug CA (2008). FLT3-ITD cooperates with inv(16) to promote progression to acute myeloid leukemia. Blood 11(3): 1567-1574.

48. Kim YM, Watanabe T, Allen PB, Kim YM, Lee SJ, Greengard P, Nairn AC, Kwon YG (2003). PNUTS, a protein phosphatase 1 (PP1) nuclear targeting subunit. Characterization of its PP1- and RNA-binding domains and regulation by phosphorylation. *J Biol Chem* 278(16): 13819-28.

49. Kisanuki YY, Hammer RE, Miyazaki J, Williams SC, Richardson JA, Yanagisawa M (2001). Tie2-Cre transgenic mice: a new model for endothelial cell-lineage analysis in vivo. Dev. Biol. 230(2): 230-42.

50. Klumpp S, and Krieglstein J (2002). Serine/threonine protein phosphatases in apoptosis. *Curr Opin Pharmacol* 2(4): 458-62.

51. Knudson Jr AG **(**1971). Mutation and cancer: statistical study of retinoblastoma. *Proc Natl Acad Sci* USA 68:820–823.

52. Kondo M, Weissman IL, Akashi K (1997). Identification of clonogenic common lymphoid progenitors in mouse bone marrow. *Cell* 91(5): 661-72.

53. Krucher NA, Rubin E, Tedesco VC, Roberts MH, Sherry TC, Delong G (2006). Dephosphorylation of Rb (Thr 821) in response to cell stress. *Experimental Research* 12(15): 2757-63.

54. Krutzik PO, Hale MD, Nolan GP (2005). Characterization of the murine immunological signaling network with phosphospecific flow cytometry. *J. Immunology* 175(4): 2366-73.

55. Kuhn R, Schwenk F, August M, Rajewsky K (1995). Inducible gene targeting in mice. *Science* 269: 1427-1429.

56. Largaespada DA (2000). Genetic heterogeneity in acute myeloid leukemia: maximizing information flow from MuLV mutagenesis studies. *Leukemia* 14(7): 1174-84.

57. Largaespada, DA, Brannan CI, Shaughnessy JD, Jenkins NA, Copeland NG (1996). Nf1 deficiency causes Ras-mediated granulocyte/macrophage colony stimulating factor hypersensitivity and chronic myeloid leukaemia. *Nat Genet* 12(2): 137-43.

58. Largaespada, DA, Brannan CI (1996). The neurofibromatosis type 1 (NF1) tumor suppressor gene and myeloid leukemia. *Curr Top Microbiol Immunol* 211: 233-9.

59. Le DT, Kong N, Zhu Y, Lauchle JO, Aiyigari A, Braun BS, Wong E, Kogan SC, Le Beau MM, Parada L, Shannon KM (2004). Somatic inactivation of Nf1 in hematopoietic cells results in a progressive myeloproliferative disorder. *Blood* 103(11): 4243-50.

60. Lee SJ, Lin CJ, Min JK, Lee JK, Kim YM, Lee JY, Won MH, Kwon YG (2007). Protein phosphatase 1 nuclear targeting subunit is a hypoxia inducible gene: its role in post-translational modification of p53 and Mdm2. *Cell Death and Differentiation* (16): 1106-16.

61. Lee EY, Chang CY, Hu N, Wang YC, Lai CC, Herrup K, Lee WH, Bradley A (1992). Mice deficient for RB are nonviable and show defects in neurogenesis and hematopoeisis. *Nature* 359(6393): 288-94.

62. Lesage B, Beullens M, Nuyhen M, Von Eynde A, Keppens S, Himpens B, Bollen M (2004). Interactor-mediated nuclear translocation and retention of protein phosphatase-1. *J Biol Chem* 279(53): 55978-84.

63. Li J, Shen H, Himmel KL, Dupay AJ, Largaespada DA, Nakamura T, Shaughnessy JD Jr, Jenkins NA, Copeland NG (1999). Leukaemia disease genes: large-scale cloning and pathway predictions. *Nat Genet* 23(3): 348-53.

64. Li DW, Liu JP, Schmid PC, Schlosser R, Feng H, Liu WB, Yan Q, Gong L, Sun SM, Deng M, Liu Y (2006). Protein serine/threonine phosphatase-1 dephosphorylates p53 at Serine-15 and Serine-37 to modulate its transcriptional and apoptotic activities. *Oncogene* 28:3006-3022.

65. Look A (1997). Oncogenic transcription factors in the human acute leukemias. *Science 278*, 1059-1064.

66. Loh ML, Vattikuti S, Schubbert S, Reynolds MG, Carlson E, Lieuw KH, Cheng JW, Lee CM, Shokoe D, Bonifas JM et al. (2004). Mutations in PTPN11 implicate the SHP-2 phosphatase in leukemogenesis. *Blood* 103: 2325-2331.

67. Ludlow JW and Nelson DA (1995). Control and activity of type-1 serine/threonine protein phosphatase during the cell cycle. *Semin Cancer Biol* 6(4): 195-202.

68. Malumbres M and Barbacid, M (2003). RAS oncogenes: the first 30 years. *Nat Rev Cancer* **3**, 459-465.

69. McCormack E, Bruserud O, Gjertsen BT (2005). Animal models of acute myelogenous leukaemia - development, application and future perspectives. *Leukemia* 19(5): 687-706.

70. McCormick F, Martin GA, Clarke R, Bollag G, Polakis P (1991). "Regulation of ras p21 by GTPase activating proteins. *Cold Spring Harb Symp Quant Biol* 56: 237-41.

71. McKenzie SB (2005). Advances in understanding the biology and genetics of acute myelocytic leukemia. *Clin Lab Sci* 18(1): 28-37.

72. Miyauchi J, Asada M, Sasaki M, Tsunematsu Y, Kojima S, Mizuteni S (1994). Mutations of the N-ras gene in juvenile chronic myelogenous leukemia. *Blood* 83(8): 2248-54.

73. Moreno-Miralles I, Pan L, Keates-Baleeiro J, Durst-Goodwin K, Yang C, Kim HG, Thompson MA, Klug CA, Cleveland JL, Hiebert SW (2005). The inv(16) cooperates with ARF haploinsuffiency to induce acute myeloid leukemia." *J. Biol. Chem*. 280(48): 40097-103.

74. Mucenski, ML, Taylor BA, Ihle JN, Hartley JW, Morse HC, Jenkins NA, Copeland NG (1988). Identification of a common ecotropic viral integration site, Evi-1, in the DNA of AKXD murine myeloid tumors. *Mol Cell Biol* 8: 301-308.

75. Nakamura T, Largaespada DA, Lee MP, Johnson LA, Ohyashiki K, Toyama K, Chen SJ, William CL, Chen IM, Feinberg AP, Jenkins NA, et al. (1996). Fusion of the nucleoporin gene NUP98 to HOXA9 by the chromosome translocation t(7;11)(p15;p15) in human myeloid leukaemia. *Nat Genet* 12(2): 154-8.

76. Nakamura T, Largaespada DA, Shaughnessy JD, Jenkins NA, Copeland NG (1996). Cooperative activation of Hoxa and Pbx1-related genes in murine myeloid leukaemias. *Nat Genet* 12(2): 149-53.

77. Nelson DA, Krucher NA, Ludlow JW (1997). High molecular weight protein phosphatase type 1 dephosphorylated the retinoblastoma protein. *J. Biol. Chem* 272: 4528-4535.

78. Niemeyer CM, Arico M, Basso G, Biondi A, Cantu Rajnoldi A, Creutzig U, Haas O, Hanbolt J, Hassle H, Kendrup G, et al. (1997). Chronic myelomonocytic leukemia in childhood: a retrospective analysis of 110 cases. European Working Group on Myelodysplastic Syndromes in Childhood (EWOG-MDS). *Blood* 89(10): 3534-43.

79. O'Connell P, Viskochil D, Buchberg AM, Fountain J, Cawthon RM, Culver M, Stevens J, Rich DC, Ledbetter DH, Wallace M, et al. (1990). The human homolog of murine Evi-2 lies between two von Recklinghausen neurofibromatosis translocations. *Genomics* **7**(4): 547-54.

80. Onida F, Kantarjian HM, Smith TL, Ball G, Keating MJ, Estey EH, Glassman AB, Albitar M, Kwari MI, Beran M (2002). Prognostic factors and scoring systems in chronic myelomonocytic leukemia: a retrospective analysis of 213 patients. *Blood* 99, 840-849.

81. Orkin SH (2000). Diversification of haematopoietic stem cells to specific lineages. *Nat Rev Genet* 1(1): 57-64.

82. Passegue E, Wagner EF, Weisman IL (2004). JunB deficiency leads to a myeloproliferative disorder arising from hematopoietic stem cells. *Cell* 119(3): 431-43.

83. Pfaffl MW (2001). A new mathematical model for relative quantification in real time RT-PCR. Nucleic Acids Research 29(9): e45.

84. Pinkel D (1998). Differentiating juvenile myelomonocytic leukemia from infectious diseases. *Blood* 91: 365-367.

85. Qiu RG, Chen J, McCormick F, Symons M (1995). A role for Rho in Ras transformation. *Proc Natl Acad Sci U S A* 92(25): 11781-5.

86. Reeder JE, Sowden MP, Messing EM, Kloven P, Villa-Moruzzi E, Ludlow JW (2003). Inducible expression of catalytically active type 1 serine/threonine protein phosphatase in a human carcinoma cell line. *Cancer Cell Int* 3(1): 12.

87. Roux P, Gauthier-Rouviere C, Doucet-Brutin S, Fort P (1997). The small GTPases Cdc42Hs, Rac1 and RhoG delineate Raf-independent pathways that cooperate to transform NIH3T3 cells. *Curr Biol* **7**(9): 629-37.

88. Shannon KM, Le Beau MM, Largaespada DA, Killen N (2001). Modeling myeloid leukemia tumor suppressor gene inactivation in the mouse. *Semin Cancer Biol* 11(3): 191-200.

89. Shannon KM, O'Connell P, Martin GA, Paderanga D, Olson K, Dinndorf P, McCormick F (1994). Loss of the normal NF1 allele from the bone marrow of children with type 1 neurofibromatosis and malignant myeloid disorders. *N Engl J Med* 330: 597-601.

90. Side L, Taylor B, Cayouette M, Connoer E, Thompson P, Luce M, Shannon K (1997). Homozygous inactivation of the NF1 gene in bone marrow cells from children with neurofibromatosis type 1 and malignant myeloid disorders. *N Engl J Med* 336(24): 1713-20.

91. Side LE, Emanuel PD, Franklin J, Thompson P, Castleberry RP, Shannon KM (1998). Mutations of the NF1 gene in children with juvenile myelomonocytic leukemia without clinical evidence of neurofibromatosis, type 1. *Blood* 92(1): 267-72.

92. Stevenson DA, Zhou H, Ashrafi S, Messiaen LM, Carey JC, D' Astous JL, Santora SD, Viskochil DH (2006). Double Inactivation of NF1 in tibial pseudoarthrosis. *American Journal of Human Genetics* 79(1): 143-148.

93. Stumpf DA, Alksne JF, Annegers, JF (1988). Neurofibromatosis. *Archives Neurol*. 45, 575-578.

94. Suzuki T, Shen H, Akagi, Morse HC, Malley JD, Naiman DQ, Jenkins NA, Copeland NG (2002). New genes involved in cancer identified by retroviral tagging. *Nat Genet* 32(1): 166-74.

95. Tartaglia M, Niemeyer CM, Fragale A, Song X, Buechner J, Jung A, Hahlen K, Hasle H, Lict JD, Gelb BD (2003). Somatic mutations in PTPN11 in juvenile myelomonocytic leukemia, myelodysplastic syndromes and acute myeloid leukemia. *Nat Genet* 34: 148-150.

96. Udho E, Tedesco VC, Zygmunt A, Krucher NA (2002). PNUTS (phosphatase nuclear targeting subunit) inhibits retinoblastoma-directed PP1 activity. *Biochem Biophys Res Commun* 297(3): 463-7.

97. Upadhyaya MC, Cheryson A, Broadhead W,, Fryer A, Shaw DJ, Huson S, Wallace MR, Andersen LB, Marchuk DA, Viskochil D, et al. (1990). A 90 kb DNA deletion associated with neurofibromatosis type 1. *J Med Genet* 27(12): 738-41.

98. Upadhyaya MC, David N. (1998). Neurofibromatosis type 1: from genotype to phenotype. Washington DC, Bios Scientific.

99. Vereecque R, Saudemont A, Quenel B. (2004). Short-term culture of myeloid leukemic cells allows efficient transduction by adenoviral vectors. *J Gene Med* 6(7): 751-9.

100. Vetter IR, and Wittinghofer A (2001). The guanine nucleotide-binding switch in three dimensions. *Science* 294: 1299-1304.

101. von Bergh, AR, Wijers PM, Groot AJ, von Zelderen-Bhola S, Falkenburg JH, Kluin PM, Schurring E (2004). Identification of a novel RAS GTPase-activating protein (RASGAP) gene at 9q34 as an MLL fusion partner in a patient with de novo acute myeloid leukemia. *Genes Chromosomes Cancer* 39(4): 324-34.

102. Vives V, Su J, Zhong S, Ratnayaka I, Slee E, Goldin R, Lu X (2006). ASPP2 is a haploinsuffiency tumor suppressor that cooperates with p53 to suppress tumor growth. *Genes Developent* 20 (10): 1262-7.

103. Wallace MR, Andersen LB, Saulino AM, Gregory PE, Glover TW, Collins FS (1991). A de novo Alu insertion results in neurofibromatosis type 1. *Nature* 353(6347): 864-6.

104. Wallace MR, Marchuk DA, Andersen LB, Letcher R, Odeh HM, Saulino AM, Fountain JW, Brereton A, Wicholson J, Mitchell AL, et al. (1990). Type 1 neurofibromatosis gene: identification of a large transcript disrupted in three NF1 patients. *Science* 249(4965): 181-6.

105. Watanabe T, Huang HB, Horiuchi A, da Cruze Silva EF, Hsieh-Wilson L, Allen PB, Shenolikan S, Greengard P, Nairn AC (2001). Protein phosphatase 1 regulation by inhibitors and targeting subunits. *Proc Natl Acad Sci U S A* 98(6): 3080-5.

106. Zindy F, Nilsson LM, Nguyen L, Meunier C, Smeyne RJ, Rehg JE, Enhert C, Sherr CJ, Roossel MF (2003). Hemangiosarcomas, medulloblastomas and other tumors in Ink4C/p53 null mice. *Cancer Research* 63(17): 5420-7.

# BIOGRAPHICAL SKETCH

Angela Hadjipanayis was born in Winnipeg, Manitoba, Canada, in 1975. She is the daughter of George and Paraskevi Hadjipanayis. Her father is from Cyprus and is a Professor of physics at the University of Delaware in Newark, Delaware. Her mother is from Patras, Greece and is the head librarian at St. Marks High School in Wilmington, Delaware. She has one sibling, Costas Hadjipanayis who is a neurosurgeon in the Department of Neurosurgery at Emory University in Atlanta, Georgia. Angela is also married to Joseph Phillips, who has a Ph.D. in physics and holds a postdoctoral position at the University of Florida with Dr. Weihong Tan.